DOT/FAA/AR-95/80

Office of Aviation Research
Washington, D.C. 20591

Effectiveness of Load Transfer Devices

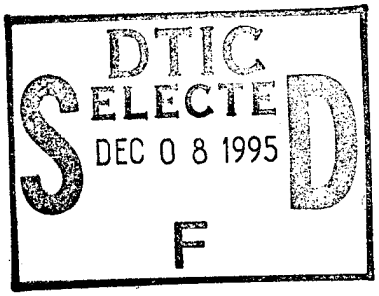

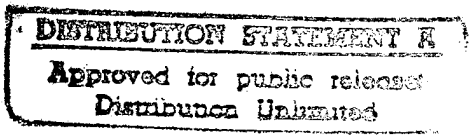

September 1995

Final Report

This document is available to the U.S. public through the National Technical Information Service, Springfield, Virginia 22161.

U.S. Department of Transportation
Federal Aviation Administration

NOTICE

Technical Report Documentation Page

1. Report No.	2. Government Accession No.	3. Recipient's Catalog No.
DOT/FAA/AR-95/80		

4. Title and Subtitle	5. Report Date
EFFECTIVENESS OF LOAD TRANSFER DEVICES	September 1995
	6. Performing Organization Code

7. Author(s)	8. Performing Organization Report No.
Michael I. Hammons, David W. Pittman, Dan D. Mathews	

9. Performing Organization Name and Address	10. Work Unit No. (TRAIS)
U.S. Army Engineer Waterways Experiment Station 3909 Halls Ferry Road Vicksburg, MS 39180-6199	DTFA01-89-Z-02028
	11. Contract or Grant No.

12. Sponsoring Agency Name and Address	13. Type of Report and Period Covered
U.S. Department of Transportation Federal Aviation Administration Office of Aviation Research Washington, D.C. 20591	Final Report
	14. Sponsoring Agency Code AAR-410

15. Supplementary Notes

The U.S. Army Engineer Waterways Experiment Station conducted this study jointly sponsored by the U.S. Army Corps of Engineers and the Federal Aviation Administration under Inter-Agency Agreement No. DTFA01-83-Y-30606.

16. Abstract

Load transfer at rigid pavement joints is a complex mechanism that can vary with concrete pavement temperature, age, moisture content, construction quality, magnitude and repetition of load, and type of joint. The FAA design procedure assumes 25 percent of the load applied to an edge of a slab is transferred at the joint to an adjacent unloaded slab. This effectively reduces the edge stress in the loaded slab by 25 percent compared to a free edge condition allowing for a reduced slab thickness. If the load transfer assumption is violated through a degradation of the joint system, the pavement life can be significantly reduced. The purpose of this study was to evaluate the load transfer effectiveness of several concrete pavement joint types by using nondestructive testing techniques. Several joint types and conditions that affect the efficiency of the joints were considered. Nondestructive field testing was conducted at four U.S. airports with a heavyweight deflectometer (HWD). Joint load transfer was found to be stochastic and not be adequately described by a single deterministic value. Probability distributions for the joint types and conditions were proposed. Based upon these probability distribution functions, the likelihood of observing mean values of load transfer less than 25 percent ranges from 60 to 100 percent, depending on the joint type and conditions.

17. Key Words	18. Distribution Statement
Deflections, Load transfer Design, Portland cement Durability, Concrete pavement Joints, Rigid pavements	This document is available to the public through the National Technical Information Service, Springfield, VA 22161

19. Security Classif. (of this report)	20. Security Classif. (of this page)	21. No. of Pages	22. Price
Unclassified	Unclassified	97	

Form DOT F 1700.7

PREFACE

The investigation reported in this report was sponsored by the Federal Aviation Administration. Mr. H. Tomita was the Technical Monitor.

The research was performed at the U.S. Army Engineer Waterways Experiment Station (WES), Geotechnical Laboratory (GL), under the general supervision of Dr. William F. Marcuson III, Director, GL, and Dr. George M. Hammitt II, Chief, Pavement Systems Division (PSD), GL. Direct supervision was provided by Mr. Jim W. Hall, Jr., Chief, Systems Analysis Branch (SAB), PSD. The Principal Investigators were Messrs. David W. Pittman and Michael I. Hammons, SAB. Mr. Dan D. Mathews, SAB, provided support in the field and laboratory for this investigation. Dr. Walter Barker, SAB, provided valuable technical assistance during the planning, execution, and reporting of this research.

Dr. Robert W. Whalin is the Director of WES. COL Bruce K. Howard, EN, is the Commander.

TABLE OF CONTENTS

LIST OF ILLUSTRATIONS

LIST OF TABLES

EXECUTIVE SUMMARY

The concept of load transfer at concrete pavement joints is fundamental to the Federal Aviation Administration (FAA) rigid pavement design procedure. The FAA procedure assumes 25 percent of the load applied to an edge is transferred at the joint to an adjacent unloaded slab. This effectively reduces the edge stress in the loaded slab by 25 percent compared to a free edge condition allowing for a reduced slab thickness. If the load transfer assumption is violated through a degradation of the joint system, the pavement life can be significantly reduced. The purpose of this study was to evaluate the load transfer effectiveness of several concrete pavement joint types by using nondestructive testing techniques.

Nondestructive field tests using the heavyweight deflectometer (HWD) were conducted at four selected airports representing a wide geographic and climatic range. A variety of joint types and conditions that affect the efficiency of the joints was considered. From joint efficiency data, joint load transfer values were estimated based upon the radius of relative stiffness of the pavement.

The results indicate that the assumption of load transfer as a constant value of 25 percent may be nonconservative, especially during the winter months. Based upon the proposed probability distribution functions, it can be shown that the probability of observing mean values of load transfer less than 25 percent ranges from 60 to 100 percent, depending on the joint type and conditions. Also, it appears that nonstabilized bases tend to increase load transfer as compared to identical joints in pavements on stabilized bases.

The mechanism of load transfer at joints is not well understood. The state-of-the-art in computational techniques and computing power has advanced to the point that explicit, three-dimensional modeling of the joint-slab-foundation system is now practical. These types of analyses, along with experimental verification, can be used to develop a more fundamental, mechanistic understanding of the mechanism of load transfer. Therefore, it is recommended that additional research of this type be conducted before changes in design guidance are implemented.

METRIC CONVERSION FACTORS

Approximate Conversions to Metric Measures

Symbol	When You Know	Multiply by	To Find	Symbol
	LENGTH			
in	inches	* 2.5	centimeters	cm
ft	feet	30	centimeters	cm
yd	yards	0.9	meters	m
mi	miles	1.6	kilometers	km
	AREA			
in^2	square inches	6.5	square centimeters	cm^2
ft^2	square feet	0.09	square meters	m^2
yd^2	square yards	0.8	square meters	m^2
mi^2	square miles	2.6	square kilometers	km^2
	acres	0.4	hectares	ha
	MASS (weight)			
oz	ounces	28	grams	g
lb	pounds	0.45	kilograms	kg
	short tons (2000 lb)	0.9	tonnes	t
	VOLUME			
tsp	teaspoons	5	milliliters	ml
Tbsp	tablespoons	15	milliliters	ml
fl oz	fluid ounces	30	milliliters	ml
c	cups	0.24	liters	l
pt	pints	0.47	liters	l
qt	quarts	0.95	liters	l
gal	gallons	3.8	liters	l
ft^3	cubic feet	0.03	cubic meters	m^3
yd^3	cubic yards	0.76	cubic meters	m^3
	TEMPERATURE (exact)			
°F	Fahrenheit temperature	5/9 (after subtracting 32)	Celsius temperature	°C

* 1 in. = 2.54 (exactly). For other exact conversions and more detailed tables, see NBC Misc. Publ. 286, Units of Weights and Measures, Price $2.25, SD Catalog No. C13.10:286.

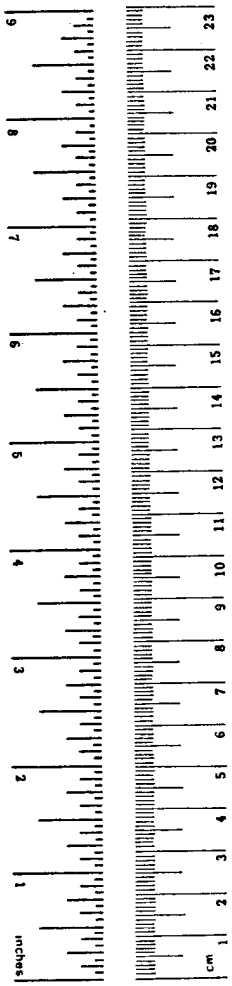

Approximate Conversions to Metric Measures

Symbol	When You Know	Multiply by	To Find	Symbol
	LENGTH			
mm	millimeters	0.04	inches	in
cm	centimeters	0.4	inches	in
m	meters	3.3	feet	ft
m	meters	1.1	yards	yd
km	kilometers	0.6	miles	mi
	AREA			
cm^2	square centimeters	0.16	square inches	in^2
m^2	square meters	1.2	square yards	yd^2
km^2	square kilometers	0.4	square miles	mi^2
ha	hectares (10,000 m^2)	2.5	acres	
	MASS (weight)			
g	grams	0.035	ounces	oz
kg	kilograms	2.2	pounds	lb
t	tonnes (1000 kg)	1.1	short tons	
	VOLUME			
ml	milliliters	0.03	fluid ounces	fl oz
l	liters	2.1	pints	pt
l	liters	1.06	quarts	qt
l	liters	0.26	gallons	gal
m^3	cubic meters	35	cubic feet	ft^3
m^3	cubic meters	1.3	cubic yards	yd^3
	TEMPERATURE (exact)			
°C	Celsius temperature	9/5 (then add 32)	Fahrenheit temperature	°F

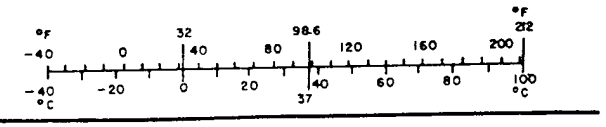

INTRODUCTION

BACKGROUND.

The concept of load transfer at concrete pavement joints is very important and fundamental to the Federal Aviation Administration (FAA) rigid pavement design procedure. The FAA procedure assumes 25 percent of the load applied to an edge is transferred at the joint to an adjacent unloaded slab. This effectively reduces the edge stress in the loaded slab by 25 percent compared to a free edge condition allowing for a reduced slab thickness. If the load transfer assumption is violated through a degradation of the joint system, the pavement life can be significantly reduced. Load transfer is a complex mechanism that can vary with concrete pavement temperature, age, moisture content, construction quality, magnitude and repetition of load, and type of joint. Thus, the assumed 25 percent load transfer in the FAA design procedure is a simplifying assumption.

Load transfer is difficult to measure directly in concrete slabs because stresses in slabs on grade are difficult to measure. Load transfer can be calculated directly from measurements taken from strain gages embedded in the slabs at the joint or estimated from deflection measurements of the slabs as one slab is loaded (figure 2). From the deflection measurements, an analytical model can be used to estimate the amount of load transferred by shear and/or moment across the joint. This model will be described elsewhere in this report.

Various concrete pavement joints are used in the field to serve different purposes of joint load transfers. The following paragraphs provide brief descriptions on these concrete airport pavement joints and methods currently being used to measure joint load transfers.

Aggregate Interlock — A load transfer mechanism that relies on the shear force developed at the rough vertical interface of a concrete pavement joint. This shear force is due solely to friction.

Joints — Discontinuities in a concrete pavement which divide a pavement into slabs. There are three basic types of joints: expansion, contraction, and construction (figure 1).

Contraction Joint — A joint in a concrete pavement designed to relieve tensile stresses caused by shrinkage of the slab due to moisture and temperature changes. Typically, a groove is sawn in the concrete in the early stages of construction inducing a crack in the concrete. Contraction joints may be plain (often called dummy joints), doweled, or tied (often called hinged joints) (figure 1).

Construction Joint — Joints that separate areas of pavement that are placed at different times. They are usually formed at the end of a paving day or at the boundary of a section of paved area. Construction joints may be keyed, doweled, or hinged (figure 1).

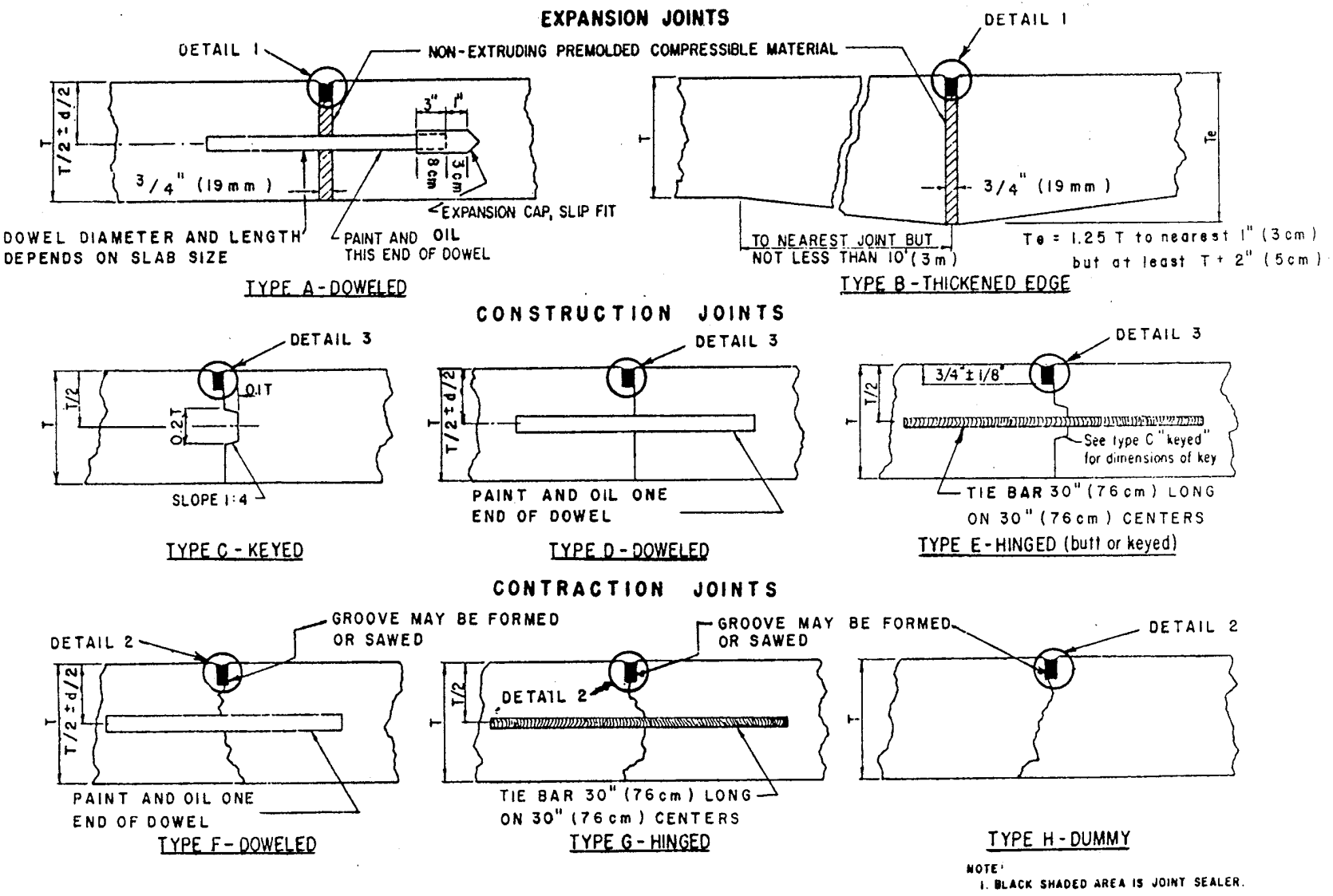

FIGURE 1. TYPES OF JOINTS (FAA 1978)

Expansion Joint — Joints constructed in a concrete pavement to relieve compressive stresses induced by expansion of the concrete caused by temperature and moisture changes. Expansion joints may be doweled or thickened edge (figure 1).

Retrofitted Joint — A joint that has been equipped with a device designed to transfer load across the joint with the installation occurring after the joint has been constructed.

Falling Weight Deflectometer (FWD) — A trailer-mounted device capable of producing impulsive loads (typically 8,000 to 50,000 lb) on a pavement surface while simultaneously measuring the deflected shape of the surface. A type of FWD capable of producing impulsive loads of 25,000 to 50,000 lb is referred to as a heavy-weight deflectometer (HWD).

Load Transfer — That portion of load (in percent of applied load) that is carried by an unloaded concrete slab due to loading applied to the adjacent slab. Alternatively, the load transfer may be defined as the difference in the percent maximum edge stress condition for a free edge loading condition (load applied at the slab edge with no adjacent slab) and with an adjacent unloaded slab at the joint (figure 2). It is assumed that

$$\sigma_L + \sigma_U = \sigma_E$$

where

σ_L = maximum tensile stress at the bottom of a loaded slab (where an adjacent, nonloaded slab is present)

σ_U = maximum tensile stress at the bottom of a nonloaded slab (where an adjacent loaded slab is present)

σ_E = maximum tensile stress at the bottom of an edge-loaded slab (where no adjacent slab is present)

The load transfer can then be expressed as

$$\textit{Load Transfer (\%)} = \left(\frac{\sigma_U}{\sigma_E}\right) x\ 100 = \left(\frac{\sigma_E - \sigma_L}{\sigma_E}\right) x\ 100$$

$$= \left(1 - \frac{\sigma_L}{\sigma_E}\right) x\ 100 \qquad (1)$$

Load Transfer Efficiency — The ratio of the deflection of the slab surface of a nonloaded slab (D_U) to the deflection of a loaded slab (D_L) in percent (also joint efficiency) as follows

$$Joint\ Efficiency = \frac{\Delta_U}{\Delta_L} \quad (2)$$

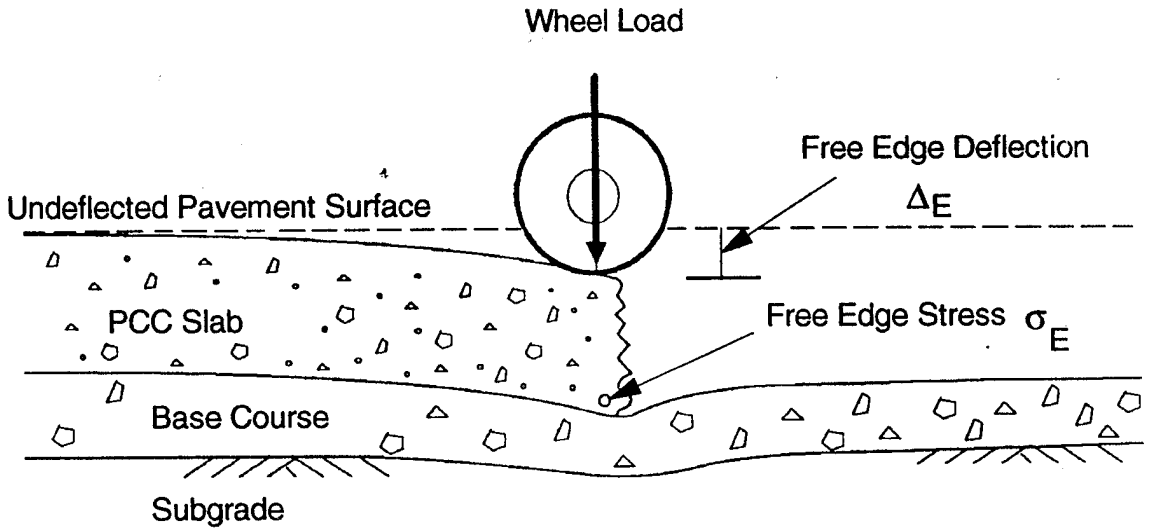

Free Edge Condition

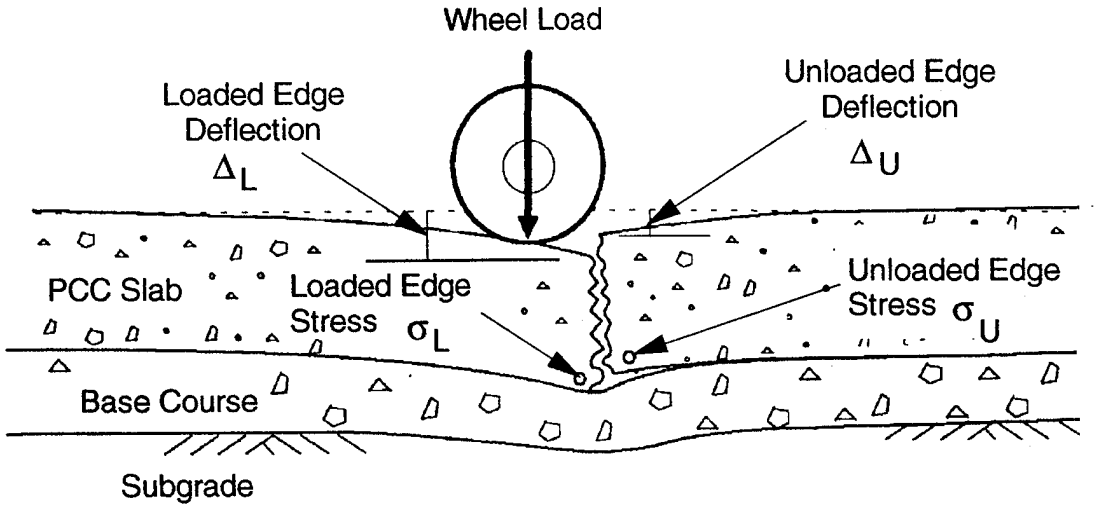

Load Transfer From Adjacent Slab

FIGURE 2. CONCEPT OF LOAD TRANSFER

PURPOSE.

The purpose of this study was to evaluate the load transfer effectiveness of several concrete pavement joint types by using nondestructive testing techniques. A variety of joint types and conditions that affect the efficiency of the joints were considered.

SCOPE.

The literature was reviewed to identify variables crucial to the study of load transfer performance of concrete pavement joints. Included in this review was a previous FAA study (Tabatabaie, Barenburg, and Smith 1979) in which visual inspection and finite element analysis of slip-formed concrete pavement joints were conducted. A matrix of independent variables (type of joint, joint spacing, type of base, etc.) which influence load transfer was identified. A survey of airports was conducted to identify airports for testing which would allow incorporation of as many variables in the test matrix as possible within the constraints of the project schedule and funding. Based upon this survey four U.S. airports were selected for testing with an HWD device. Nondestructive field testing was conducted according to the plan of test at the four selected airports. The data from these were summarized and analyzed. Probability distributions for the joint types and conditions are proposed. Conclusions and recommendations were made based upon the findings of the study.

LITERATURE REVIEW

LONGITUDINAL JOINT SYSTEMS IN SLIP-FORMED RIGID PAVEMENTS.

In an FAA-sponsored study on the analysis of longitudinal jointing systems for slip-formed rigid pavements, Tabatabaie, Barenburg, and Smith (1979) presented an extensive literature review of various joint types and load transfer systems. They recommended that several joint types be evaluated in the field for both short- and long-term performance. This previous research may be regarded as a precursor to the current study. The pertinent conclusions and recommendations will be presented here.

Load transfer systems provide two essential and distinct functions in a rigid pavement — to reduce the level of stress and deflection at a pavement edge and to maintain slab alignment. Load transfer systems translate the load across a joint principally by shear. Some moment may also be transferred across the joint, but its magnitude is small enough to be ignored in design calculations.

Conventional load transfer systems typically rely on aggregate interlock, dowel bars, or keyways to transfer part of the applied load across a joint. Joints that depend on aggregate interlock for load transfer are very sensitive to crack width opening to develop shear transfer across the roughened faces of the joint and therefore perform better with short joint spacings. Tie bars may be used to ensure a small joint opening, and a stabilized base will help maintain slab alignment and reduce the stresses due to edge loading. Doweled joints depend primarily on the shear and bending strength of the dowel and the bearing stress of the concrete to transfer the load across a joint. Their design is usually limited by the bearing strength of the concrete, which will govern

how loose the dowel becomes after repeated heavy loads. Keyed joints use the geometry of the key shape to transfer the load across a joint by producing bearing and shear stresses in the male and female portions of the key. A keyed joint may also contain tie bars to keep the joint opening small (and therefore improve the effectiveness of the joint) or dowels to help transfer shear across the joint.

A two-dimensional linear-elastic finite element-based analysis was conducted on models of these three basic joint types to compare their effectiveness in reducing the stresses due to an edge loading condition, as compared to the stresses due to an interior loading condition. These analyses indicated that the keyed and doweled joints were almost identically effective in reducing the edge stress to a level below that produced from an interior loading condition (figure 3). The aggregate interlock joint, which used a reduced spring stiffness element in the finite element model to characterize the behavior of the joint, produced a reduced edge stress of a magnitude midway between the free edge condition and the interior loading condition. The addition of a 4-inch-thick stabilized base reduced the stress even more, to a magnitude approaching that of the interior loading condition.

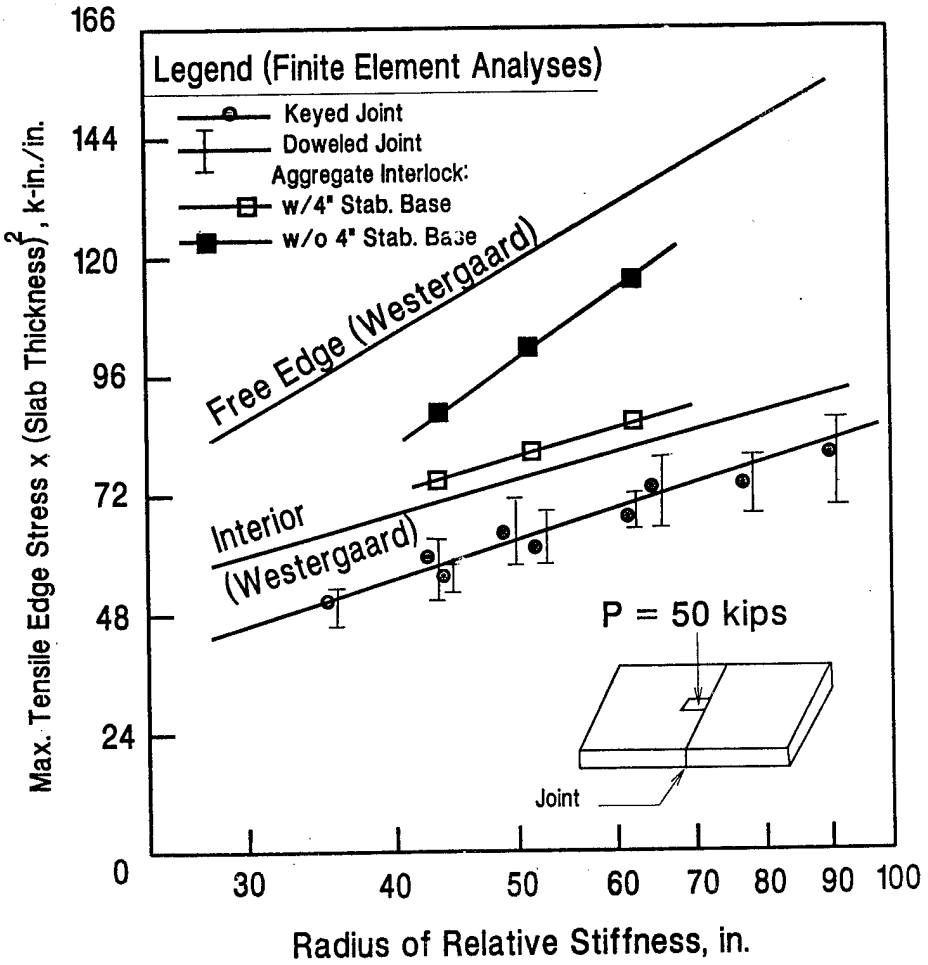

FIGURE 3. EFFECT OF JOINT TYPE ON EDGE STRESS
(Tabatabaie, Barenberg, and Smith 1979)

A visual condition survey of in-service joints suggested that the keyed joints were particularly susceptible to failure under heavy loads and/or low-strength subgrades, i.e., any combination which produces large deflections.

The larger deflections result in stress concentrations in the male and female portions of the key, which can cause premature fracture of those portions of the joint. The joint becomes ineffective in transferring load and is very difficult to repair. However, short-term performance records of doweled or tied contraction joints indicated that these designs should give good performance over a 20-year life.

The report recommended that the performance of doweled and tied joints with aggregate interlock be validated under field conditions. It also suggested that the finite element analysis be verified by instrumenting full-scale pavements in the field to measure strains and deflections under a variety of loading conditions.

NONDESTRUCTIVE TESTING AND EVALUATION OF RIGID AIRFIELD PAVEMENTS.

Foxworthy (1985) investigated the use of the Dynatest Model 8000 FWD to measure pavement response to simulated aircraft movement at the center and along the joints of airfield concrete pavement slabs. The deflection measurements obtained from the FWD testing were input to the ILLI-SLAB finite element-based program to calculate stresses in the concrete slab at the joints and at midslab due to applied loads. Modulus values for the concrete slab and subgrade were also backcalculated. The Dynatest FWD and the ILLI-SLAB program were selected as the most versatile choices after an extensive review of nondestructive testing devices and mechanistic models.

The study showed that the load transfer efficiencies obtained from FWD deflection measurements were independent of load magnitude ranging from 7,000 to 25,000 lb. This provides some validity to the notion that the efficiencies obtained with the FWD measurements can be extrapolated with some confidence to include loads of the magnitude applied by heavy aircraft gear. Load transfer was shown to change with significant changes in air and pavement temperature in a characteristic S-shaped curve as the load transfer efficiencies varied from 25 to 100 percent (figure 4). The study also showed that the load transfer efficiency is not significantly influenced by the direction of traffic and that aircraft wander is sufficient to minimize the effects of varying load efficiencies along the edge of a slab.

AGGREGATE INTERLOCK AT JOINTS.

Colley and Humphrey (1967) performed a laboratory simulation of a slab on grade being repeatedly loaded by truck traffic to determine the performance of concrete pavement joints that depend primarily on aggregate interlock. Five independent variables were selected for the study: width of joint opening, thickness of concrete slab, magnitude of load, foundation support, and shape of aggregate (maximum size of aggregate maintained constant).

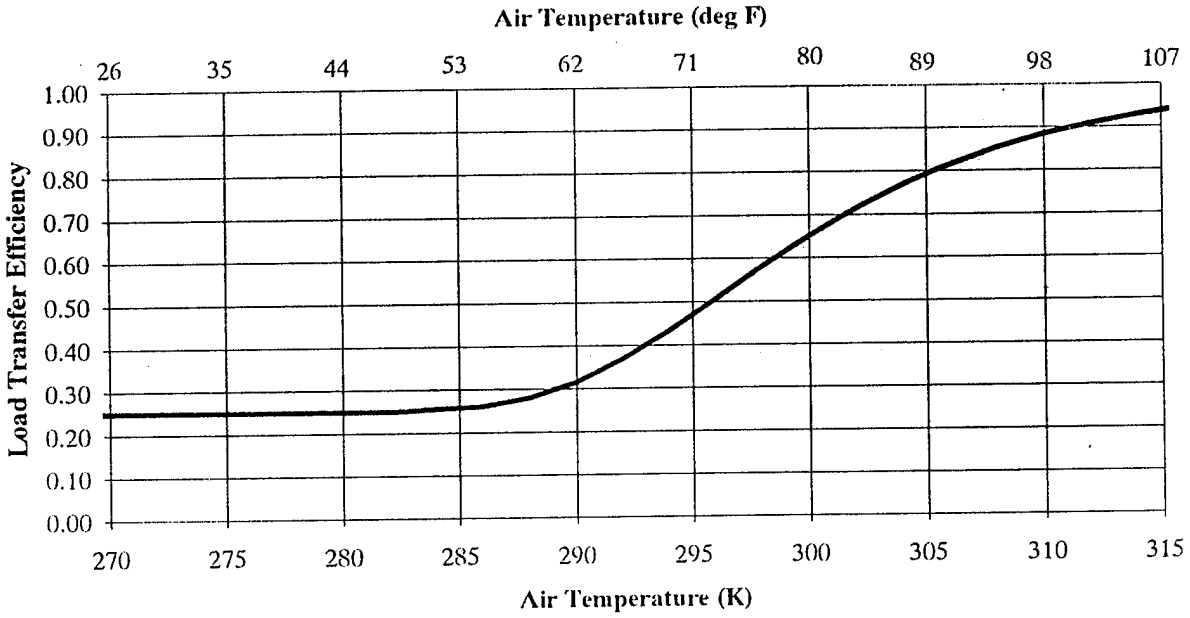

FIGURE 4. FOXWORTHY'S (1985) CHARACTERISTIC "S-CURVE" RELATING LOAD TRANSFER TO TEMPERATURE CHANGE

The laboratory model pavement consisted of an 18- by 4-ft slab with a transverse crack induced at the midpoint (figure 5). The slab was constructed at thicknesses of 7 and 9 in. in separate tests. The slabs were mounted on a boxed-in subgrade consisting of a silty clay material 2.5 ft deep with a modulus of subgrade reaction (k) of 89 psi/in. Two subbase types were used, a sand-gravel and a cement-treated material. Repetitive loads were applied to the slabs on either side of the joint at a rate and lag time to simulate a vehicle tire passing over the joint. An electrically operated air-hydraulic system applied loads up to a maximum of 12,000 lb joint openings were varied from tight to 0.10 in. to a precision of 0.001 in. by using threaded steel rods anchored in the concrete slabs. Deflections on both sides of the joint were measured for regular intervals of load cycles after applying a static load of 9,000 lb on one side of the joint. The effectiveness (E) was then calculated using the formula:

$$E\,(\%) = \frac{2\,\Delta_U}{\Delta_L + \Delta_U} \_ 100 \qquad (3)$$

The results of the testing indicated that the effectiveness of the joint reduced dramatically as a large number of load applications were applied (figure 6). The effectiveness lowered at a faster rate for greater joint opening widths and the thinner slab thickness.

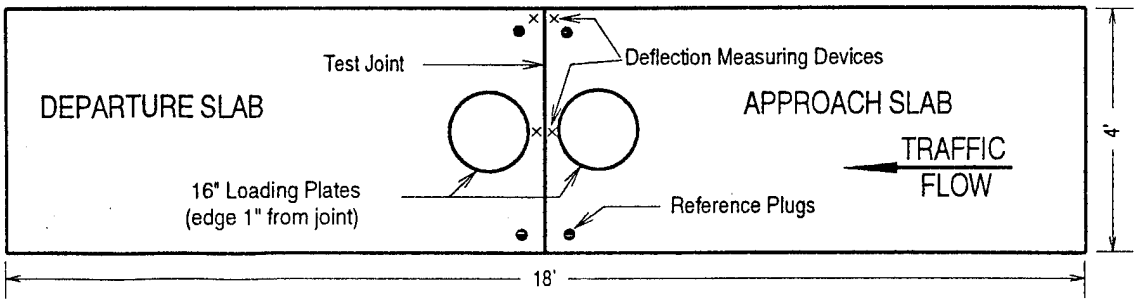

FIGURE 5. PLAN OF TEST SLAB AND INSTRUMENTATION
(Colley and Humphrey 1967)

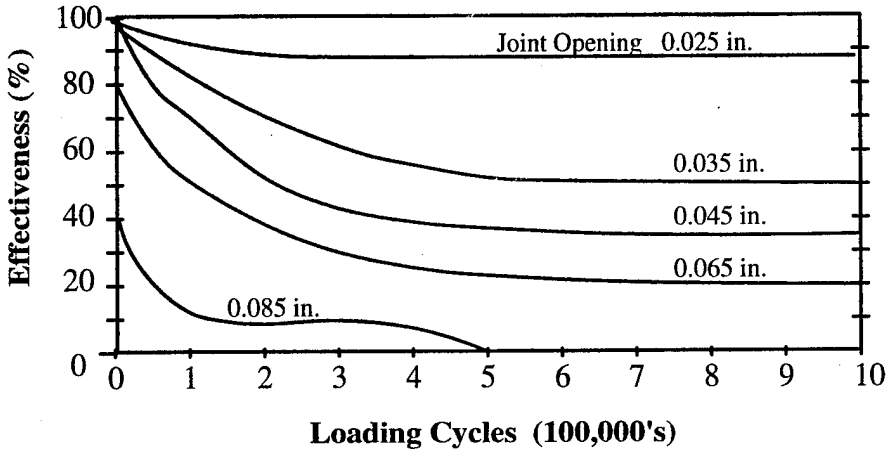

FIGURE 6. INFLUENCE OF JOINT OPENING ON EFFECTIVENESS OF AGGREGATE INTERLOCK JOINTS
(Colley and Humphrey 1967)

To characterize the performance of the joint effectiveness after many repetitions of load, a statistic called the endurance index (EI) was developed. The EI was defined as the ratio of the area under the curve of effectiveness versus load cycles to the same area had the joint maintained an effectiveness of 100 percent for one million load cycles. The EI generally decreased with increasing joint opening width and decreasing slab thickness (figure 7a). The EI generally increased with increasing foundation strength (figure 7b) and decreased with magnitude of applied load (figure 7c). These relative effects on the EI were expressed in a single equation:

$$EI = 230\frac{h}{Pw}k \tag{4}$$

where

h = slab thickness (in.)
k = modulus of subgrade reaction (psi/in.)
P = wheel load (lb)
w = joint opening (in.)

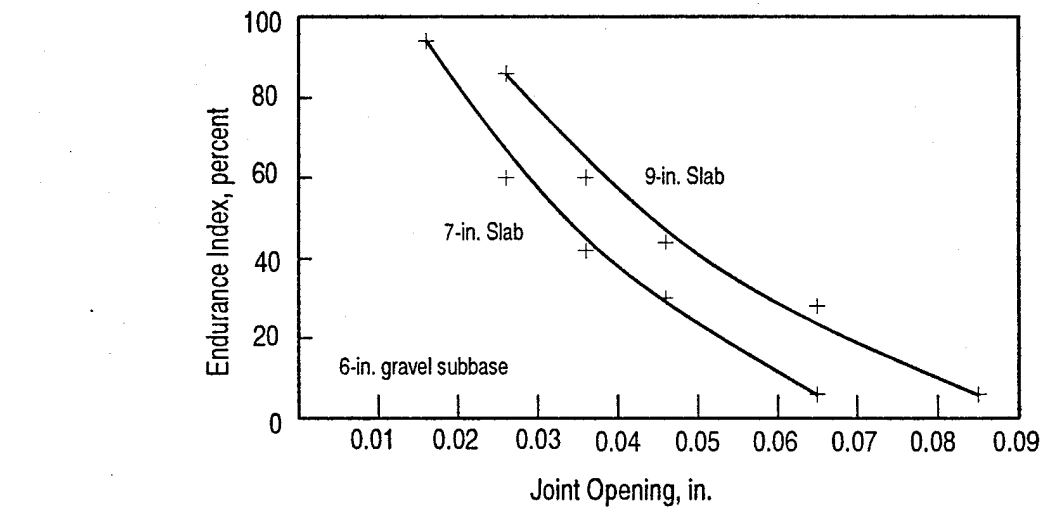

(a)

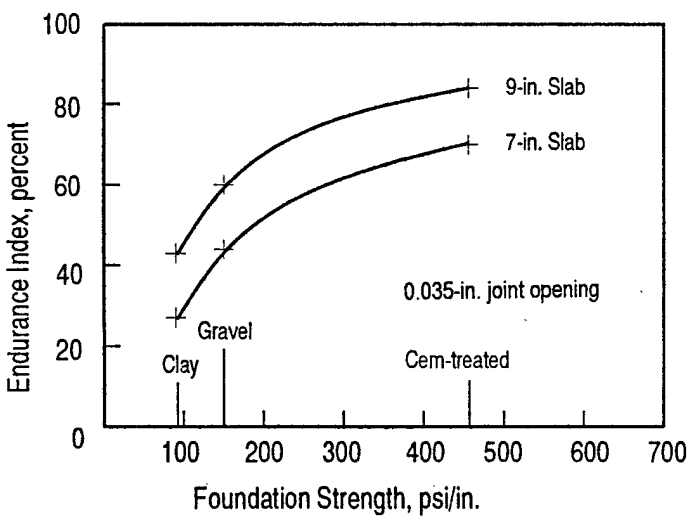

(b)

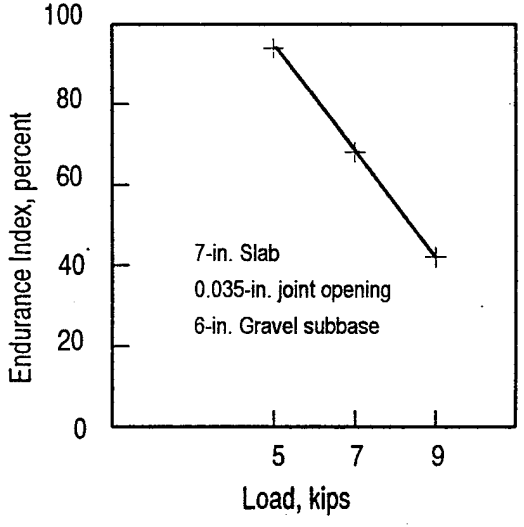

(c)

FIGURE 7. INFLUENCE OF JOINT OPENING (A), FOUNDATION STRENGTH (B), LOAD ON ENDURANCE INDEX (C)

EXPERIMENTAL PARAMETERS

GENERAL.

This chapter includes a discussion of the experimental parameters found from the literature review to influence load transfer. It was the intention from the outset of the project to include as many of these parameters as practically possible within the schedule and budget. Drawing upon the identified parameters, a plan of test is given. Also, the selection of airport sites for testing is discussed.

INDEPENDENT VARIABLES.

From a review of the literature, several independent variables considered to have potential of significant influence on the dependent variable (load transfer) were identified: type of joint, type of subbase, magnitude of load, number of load repetitions, slab thickness, width of joint opening, joint spacing, air/slab temperature, and joint face skewing.

One should note that some independent variables are dependent upon each other, i.e., width of joint opening and joint spacing. The expected influence of the individual independent variables and a strategy for accounting for them is described in this section.

TYPE OF JOINT. Joint type was shown by Tabatabaie, Barenberg, and Smith (1979) and by Rollings (1987), and others to influence the amount of load transfer expected at the joint. Tabatabaie, Barenberg, and Smith analysis (1979) showed that the doweled or keyed contraction joints were more effective in reducing the edge loading stress condition than the joint depending on aggregate interlock. In a test-section study to evaluate the effects of multiple-wheel heavy gear loads (MWHGL) on pavements, Brown and Rice (1971) concluded that keyed longitudinal construction joints perform poorly in pavements subjected to MWGHL traffic. Rollings (1987) showed variable load transfer values for different joint types (table 1).

The following joint types represent the three major types of joints used in airport pavements (aggregate interlock, doweled, and keyed) and a retrofitted joint: sawed contraction joint (dummy joint), tied contraction joint (hinged), doweled construction joint, keyed construction joint, and retrofitted joint. It was attempted to test as many as possible of these types of joints; however, retrofitted joints were rare at the airports tests and limited data were obtained.

TYPE OF SUBBASE. The type of subbase, another unquantifiable variable, can also have a significant influence on the performance of a joint over time. A finite element analysis conducted by Tabatabaie, Barenberg, and Smith (1979) of aggregate-interlock joints with and without a stabilized base indicated that the free edge stress can be reduced to a magnitude almost equal to that caused by an interior loading condition if a stabilized base is used. Ball and Childs (1975) showed in laboratory tests of concrete beams containing different joint types that the performance of the joints was improved when a stabilized subbase was used. For purposes of this study, the subbase types were categorized into two types: stabilized and nonstabilized. A subbase was considered to be nonstabilized if the first layer underneath the PCC was a granular layer.

TABLE 1. TYPICAL LOAD TRANSFER VALUES
(Rollings 1987)

Type of Joint	Number of Data Points	Load Transfer		
		Range	Mean	Coefficient of Variation
Doweled Construction Joint	195	0.0 - 50.0	30.6	38.0
Doweled Expansion Joint	15	15.4 - 42.6	30.5	24.4
Contraction Joint with Aggregate Interlock	46	15.6 - 50.0	37.2	19.2
Keyed Joint	61	5.6 - 49.0	25.4	41.4
Lockbourne "Free" Joint	8	5.8 - 24.5	15.5	40.9

MAGNITUDE OF LOAD. The joint efficiency studies conducted by Colley and Humphrey (1967), suggested that the efficiency of an aggregate-interlock joint (with no dowels or tie-bars) deteriorates much more rapidly under many load repetitions when greater magnitudes of load are applied. This is in contrast to and should be distinguished from a conclusion by Foxworthy (1985) that the load transfer values obtained from analysis of the FWD deflections was virtually independent of the magnitude of the load applied to obtain the deflections.

While it is impossible to have controlled conditions of magnitude and frequency of loading on various features (taxiways, runways, ramps, etc.) of an active airport pavement, certain patterns of traffic type and paths may develop such that one feature of an airport obtains a greater frequency of higher load magnitudes than other features of the same airport. Testing conducted at different airports provides some variability in traffic loads and frequency.

NUMBER OF LOAD REPETITIONS. Colley and Humphrey (1967) showed that the load transfer at a joint due solely to aggregate interlock decreased with an increasing number of load repetitions regardless of load magnitude, slab thickness, foundation support, or width of joint opening (these factors influenced only the rate of deterioration). Ball and Childs (1975) also demonstrated a reduction in joint efficiencies with increasing number of load repetitions for a variety of joint types. As discussed previously in the section on magnitude of load, it would be quite impossible to control the number of load repetitions of a particular aircraft to determine specifically the rate of deterioration for a particular aircraft, thickness of slab, etc. Probably the best control of this variable in this study is to test within sufficiently different airport features to obtain a wide range of traffic frequencies.

SLAB THICKNESS. Colley and Humphrey (1967) and Ball and Childs (1975) demonstrated in laboratory studies that thicker slabs are more effective in transferring load when aggregate interlock is a factor (with or without ties); however, the effect of a thicker slab on the performance of a doweled or keyed joint was inconclusive (Ball and Childs 1975). Tests conducted at different airports and on different features within those airports provided a range of slab thicknesses. For purposes of this study a thin pavement was defined as one in which the PCC was 15 in. or less in thickness.

WIDTH OF JOINT OPENING. Colley and Humphrey (1967) showed with a laboratory model that the load transfer due to aggregate interlock is inversely proportional to the joint opening (or crack width). As the joint opening increased from 0.02 to 0.09 in., the EI reduced from more than 90 percent to less than 20 percent. Ball and Childs (1975) demonstrated the effect of the joint opening increasing from 0.125 to 0.5 in. for a doweled joint, with the joint efficiency decreasing about 2 to 5 percent. Owusu-Antwi, Meyer, and Hudson (1989) demonstrated from FWD testing on a full-scale test slab that the efficiency of a doweled joint decreased from about 60 percent to about 30 percent as the joint opening increased from 0 to 1 in.

In actual field conditions, the joint opening is controlled primarily by the joint spacing (slab size) and the pavement temperature. As the joint spacing increases, the joint opening increases with changes in temperature, the larger joint openings occurring for cooler slab temperatures as the slab contracts. Therefore, instead of controlling the joint opening per se as an independent variable, the joint opening may be more practically varied by testing various combinations of joint spacing (small to large) and slab temperature (cool to hot). The more extreme combinations would be a small joint spacing coupled with a hot slab temperature for a small joint opening and a large joint spacing coupled with a cool slab temperature for a large joint opening. In this study joint opening per se was not measured as a variable, but a range of joint spacing was tested to ensure that the effects of variable joint opening were considered.

JOINT SPACING. The effects of joint spacing on joint opening and the subsequent effect on the load transfer have been discussed in the previous paragraph. Joint spacing of 12.5 to 25 ft. are allowed in the current FAA design guidance (FAA 1978) depending on slab thickness and orientation of the joint to traffic (longitudinal or transverse). Therefore, spacing of 12.5 and 25 ft would allow the greatest possible range of load transfer values to be obtained for a given jointing system. For purposes of this study, a short joint spacing was defined as any spacing less than or equal to 15 ft.

AIR/SLAB TEMPERATURE. The effects of temperature changes in the slab on the load transfer of joints that depend on aggregate interlock to transfer the load have been discussed in a previous paragraph, i.e., cooler temperatures cause a larger joint opening and consequently a reduced load transfer, and the converse is also true. Foxworthy (1985) suggested a characteristic S-shaped load transfer efficiency function for dummy and keyed joints that is based upon the air temperature. This function allows the determination of the load transfer efficiency over a wide range of temperatures for any given joint if only one combination of air temperature and joint efficiency is known.

The temperature of a slab is controlled by two sources of heat: the air above the slab and the ground below the slab. Not often is the temperature of these sources the same, especially within a daily cycle; therefore, temperature gradients often develop in the slab. Owusu-Antwi, Meyer, and Hudson (1989) and Poblette, Valenzuela, and Salsilli (1989) have measured differences in the bottom and surface temperature ranging from 0 to 15°F for slab thicknesses of 9 to 10 in. The temperature differentials have been shown to have an effect on the load transfer efficiency of doweled and undoweled joints. The effects are the result of the slab curling and warping; the

rotation of the vertical edges as the slabs curl or warp compresses either the top or bottom portions of the slab together (figure 8) resulting in an improved load transfer mechanism.

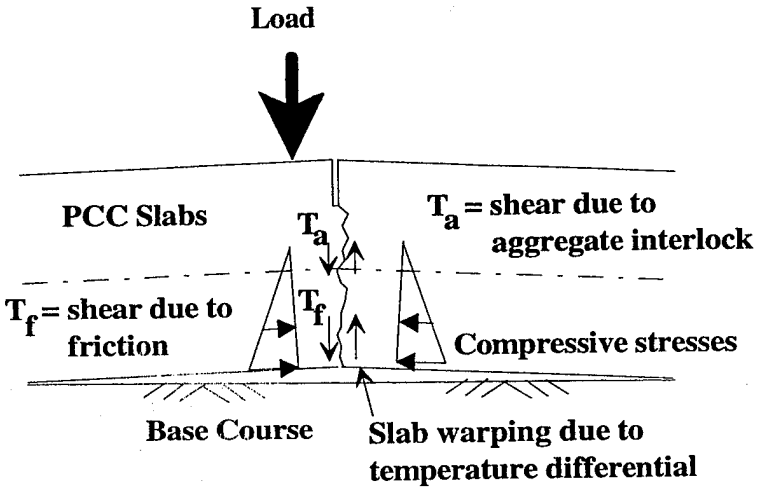

FIGURE 8. EFFECT OF WARPING ON LOAD TRANSFER
(Poblette, Valenzuela, and Sasilli 1989)

This phenomenon of variable load transfer with slab temperature differentials will require that the FWD tests for a common group of independent variables be conducted within a short time frame, as the load transfer can vary greatly throughout the day. The effects of changing temperature and thermal gradients can perhaps be most effectively addressed by testing at the extreme conditions, i.e., in the summer and winter and in the day and night.

JOINT FACE SKEWING. For joints that form as the result of an induced crack, the alignment of the crack will often be skewed from a line perpendicular to the surface of the pavement. If the skewness exceeds a certain degree, the joint efficiency will be different depending on the direction of test. One slab can bear upon the other as the load is applied to it, but if the load is applied to the opposing slab, this bearing force is totally lost resulting in a completely different transfer of load (figure 9). Poblette, Valenzuela, and Salsilli (1989) found differences of up to 60 percent joint efficiency between testing the same joint in different directions. Foxworthy (1985) also detected this phenomenon in loading opposite sides of a joint and measuring deflection. Differences of over 40 percent efficiency were shown at some of the slabs. This effect can be countered by testing in both directions across each joint within a short time frame to minimize effects of temperature change.

SITE SELECTION.

After the experimental parameters were established, specific airport sites were required to execute the experimental program. Four airport sites were chosen for this phase of the project. The selection criteria and airports selected are described below.

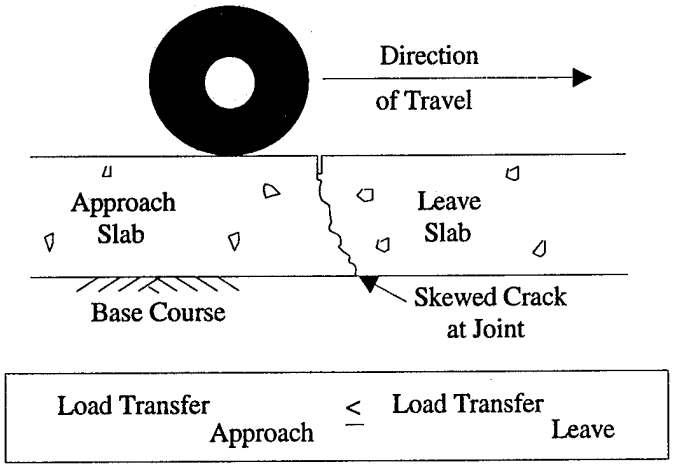

FIGURE 9. EFFECT OF SKEWING ON LOAD
(Poblette, Valenzuela, and Sasilli 1989)

CRITERIA FOR SELECTION. The selection of airports for this study was based upon several criteria. A suitable airport would preferably be located within the United States, would handle large commercial and/or passenger aircraft, and would, of course, use Portland cement concrete for some of the pavements. The following criteria were also deemed important for this study. Existing load transfer data allowed a determination of the performance of the joint (in terms of load transfer) with time or load repetitions by comparing the new data to the old. This criterion is one of the most restrictive; not only does FWD test data from previous testing need to exist for the airport, but also the data needs to be associated with the particular joint from whence it came. Since the purpose of this study was to evaluate the effectiveness of several joint types, the existence of several types at one facility would allow a comparison of the joints for the same climatic temperatures. Most of the larger airports are very busy with aircraft traffic on parts of the airport, and routing traffic around a specific area of the airport to facilitate FWD testing would not be practical. Although most testing could be conducted at night when the aircraft traffic is lightest (and the pavement slab is coolest, resulting in the wider crack spacing), testing during the day would be needed to provide a realistic assessment of load transfer during the day. Daytime testing would also provide a more realistic magnitude of load transfer if it is weighted for the amount of traffic applied to it during the daily cycle of loading. Although smaller airports might have the advantage of lower traffic rates and therefore might be inclined to allow FWD testing on runways or taxiways in addition to aprons during the day, most airports would be equally cautious about allowing any daytime testing that would interrupt aircraft operation. Therefore, this criterion favors smaller airports but does not represent an insurmountable obstacle for larger airports, all other criteria considered.

SELECTION PROCEDURE. To facilitate the selection process, a survey form was sent to 40 airports around the country. Most sites were selected at random, although some were recommended by consultation with pavement evaluation experts around the nation.

Seventeen survey forms (42 percent) were returned. As expected, the prior existence of FWD data severely limited the number of choices that were regarded as highly desirable. After consultation with several firms responsible for FWD testing of civilian airports, the following sites were chosen as the best candidates for possible testing (table 2): Atlanta-Hartsfield International Airport, Georgia, Dallas/Fort Worth International Airport, Texas, Dane County Regional Airport, Madison, Wisconsin, Denver International Airport, Colorado.

Although the Denver International Airport was not a part of the survey, this site was selected for testing because of other research being conducted at the site before the airport opened and because the joints could be tested before any aircraft loadings were placed on the pavement.

TABLE 2. FIELD TEST SITES

Year	Season	Time of Day
	Atlanta-Hartsfield International Airport, Georgia	
1984	Summer	Night
1987	Winter	Night
1990	Summer	Day
1990	Summer	Night
1992	Winter	Day
1992	Winter	Night
	Dallas-Ft. Worth International Airport, Texas	
1992	Winter	Night
	Denver International Airport, Colorado	
1993	Winter	Day
	Dane County Regional Airport, Madison, Wisconsin	
1993	Winter	Day

TEST MATRIX.

Unfortunately, all of the possible combinations of experimental parameters could not be tested within the allotted project funding and schedule. Also, because the conditions at the airports tested could not be controlled, tests comprising a complete statistical experimental design could not be conducted. Thus, the objective of the testing was to test as many joint types and conditions as possible. Figure 10 is a summary of the combinations of parameters tested during summer conditions at the four selected airports. Likewise, figure 11 summarizes the combinations of parameters tested during the winter.

	Summer					
	Thick PCC (> 15 in.)				Thin PCC (≤ 15 in.)	
	Large Joint Spacing (> 15 ft)		Small Joint Spacing (≤ 15 ft)		Large Joint Spacing (> 15 ft)	
	Stab. Base	Nonstab. Base	Stab. Base	Nonstab. Base	Stab. Base	Nonstab. Base
Dummy						
Tied Dummy						
Doweled Contraction	D, N	N				
Keyed Construction	N					
Doweled Construction	D, N					
Hinged Construction						
Retrofitted						
Doweled Key						
Doweled Expansion						
Tied Key	D, N	N				
Crack with Reinforcement						

D = Day Testing, N = Night Testing

FIGURE 10. TEST MATRIX, SUMMER TESTING

	Winter					
	Thick PCC (> 15 in.)				Thin PCC (≤ 15 in.)	
	Large Joint Spacing (> 15 ft)		Small Joint Spacing (≤ 15 ft)		Large Joint Spacing (> 15 ft)	
	Stab. Base	Nonstab. Base	Stab. Base	Nonstab. Base	Stab. Base	Nonstab. Base
Dummy	D, N					
Tied Dummy	D					
Doweled Contraction	D, N	D, N	N			D
Keyed Construction	N	N				
Doweled Construction	D					
Hinged Construction	D					D
Retrofitted	N					
Doweled Key	N					
Doweled Expansion	D					
Tied Key		N				
Crack with Reinforcement	D	D, N				

D = Day Testing, N = Night Testing

FIGURE 11. TEST MATRIX, WINTER TESTING

ESTIMATION OF LOAD TRANSFER

GENERAL.

Load transfer is difficult to measure directly in concrete slabs because stresses in slabs on grade are difficult to measure. Load transfer can be calculated directly from measurements taken from strain gages embedded in the slabs at the joint. However, this method of measuring load transfer is limited to joints that are strain gaged. This technique, although likely the preferred method, would be costly and impractical on a scale large enough to meet the requirements of a project such as this in which it is desired to include a multitude of test parameters and sites. Therefore, an alternative method of estimating load transfer from deflection measurements was employed for this study. This method involved nondestructively loading a slab at its edge along a joint and measuring the resulting deflections on either side of the joint. The method of measuring the deflections and estimating the load transfer is explained in this chapter.

NONDESTRUCTIVE TESTING EQUIPMENT. The loading mechanism chosen for this study was the HWD. Figure 12 shows two views of the HWD test setup typical for this research. The HWD transmits an impulsive force to the pavement through a loading plate placed on the surface of the pavement. A mass is dropped a prescribed distance creating the impulse force. The magnitude of the force is varied by either changing the mass or by changing the drop height. A hydraulic system is used to raise the mass to the preselected height before release. An array of retractable velocity transducers records the motion of the pavement due to the impulse loading. As shown in figure 12, the velocity transducers are spaced at 1-ft intervals for a total distance of 6 ft from the center of the loading plate. The loading plate also contains a velocity transducer at its center. The resulting velocity measurements are integrated to obtain displacements at each transducer. A load cell as integrated into the loading system is used to measure the magnitude of the impulsive load. The entire system is trailer mounted and can be pulled behind a light van. The van provides electrical power to the trailer and contains a personal computer system to control the system and record the resulting loads and velocities. A photograph of the falling weight system and trailer is shown in figure 13.

For this test program, two load levels were employed: low and high. The mass and drop heights were established to produce a force of approximately 25,000 lb for the low-load level and approximately 50,000 lb for the high-load level.

TEST DESCRIPTION. Two major categories of tests were conducted as a part of the load transfer study. The first type of test was a midslab deflection basin. For each feature (i.e., runway, taxiway, ramp, etc.) of an airport, a series of 12 midslab deflection tests were conducted. The results of these tests were averaged to obtain a characteristic deflection basin (figure 14) for the feature.

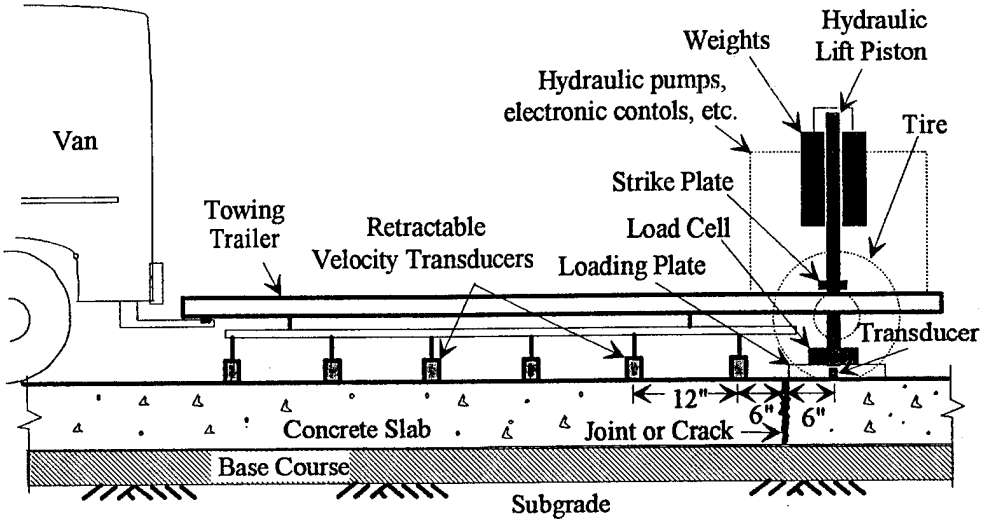

Side View

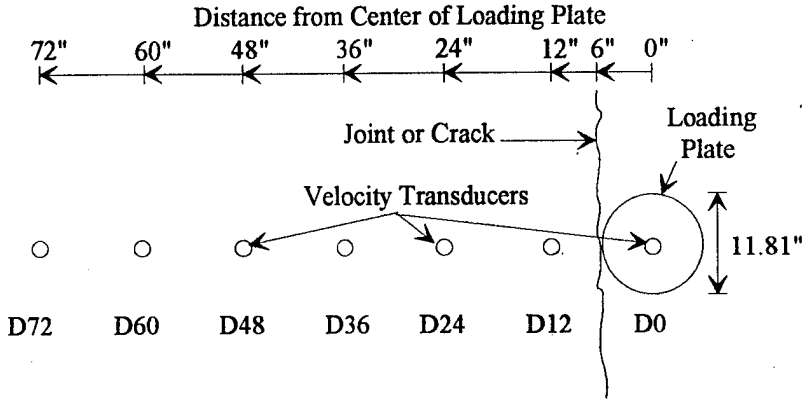

Overhead View

FIGURE 12. HWD TEST SETUP

The second type of test was a joint test. Figure 15 shows the orientation of the HWD for the joint tests. The loading plate was placed next to a joint or crack with the velocity transducers equidistant on either side of the joint (figures 12 and 15). After the test was completed on one side of the joint, the test device was immediately repositioned to load the slab on the other side of the joint, again making displacement measurements equidistant on each side of the joint (referred to in figure 15 as D0 and D12). Although the deflections at each of the velocity transducers were measured, only the transducers at the D0 and D12 positions were required to calculate joint efficiency. The joint tests were categorized using the following system: airport and feature, load level (low or high), joint type (doweled construction, hinged contraction, etc.), orientation of joint (longitudinal or transverse to the direction of paving, figure 15), side of joint loaded (north or south, east or west), and position of loading device (center of slab or corner).

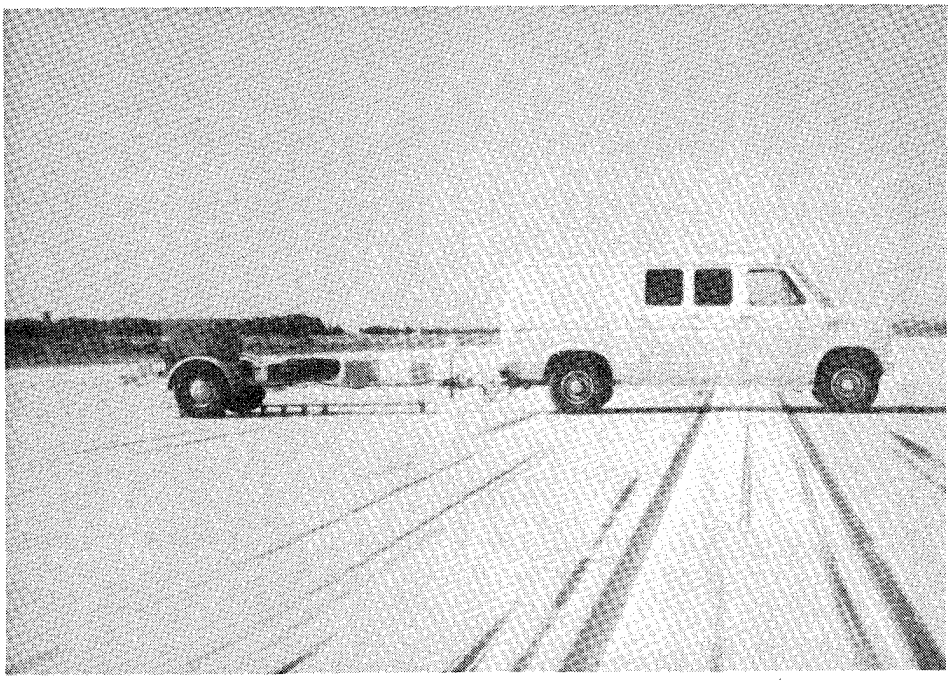

FIGURE 13. PHOTOGRAPH OF HWD TRAILER AND VAN

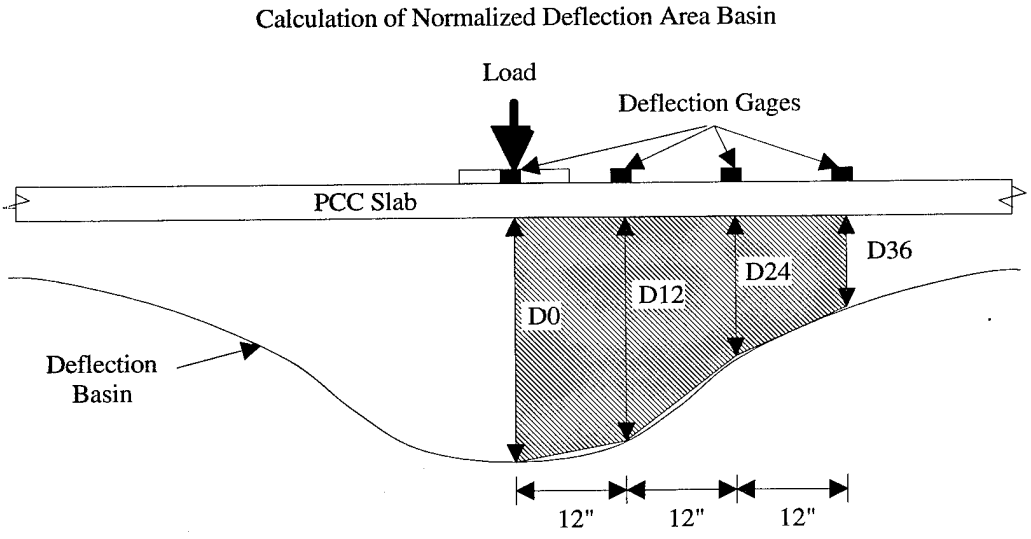

Area = 12{ (D0+D12)/2 + (D12+D24)/2 + (D24+D36)/2}
= 6 { D0 + 2 D12 + 2 D24 + D36 }

Normalized AREA = Area/D0

FIGURE 14. DETERMINATION OF AREA FROM MIDSLAB DEFLECTION BASIN

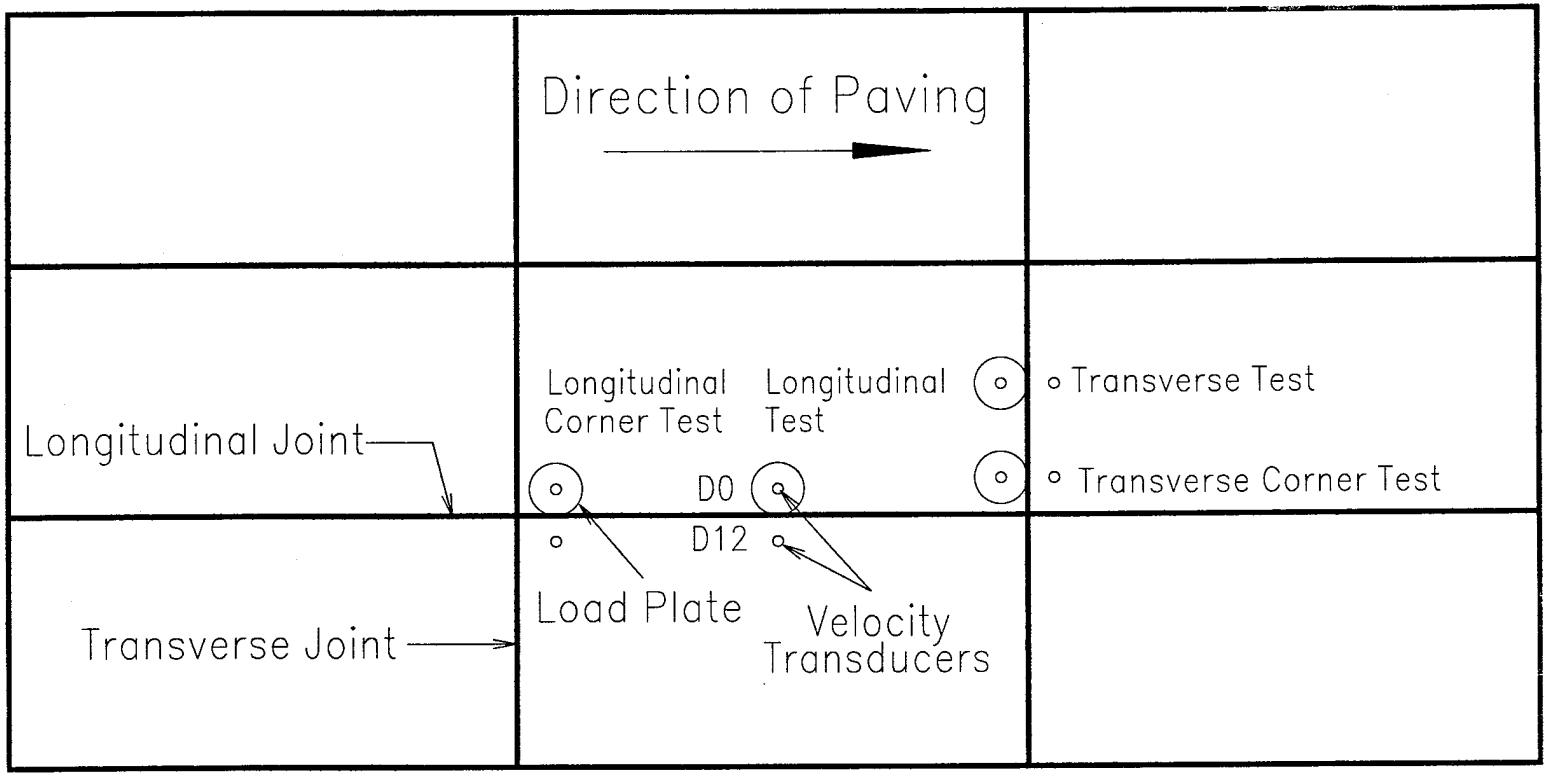

Note: Each symbol is meant to indicate that a test was also conducted with D0 and D12 in reversed positions.

FIGURE 15. ORIENTATION OF HWD FOR JOINT TESTS

CALCULATIONS.

Estimating the load transfer from the nondestructive field test data is a multistep process. First, the normalized area must be calculated from the characteristic deflection basin for the feature. From the normalized area, the radius of relative stiffness of the feature is estimated. Next, the joint efficiency for each joint of the feature is calculated from the deflection measurements made on each side of the joint. Subsequently, the load transfer is estimated for the joint as a function of the radius of relative stiffness of the pavement system and the joint efficiency. This process is described in more detail in this section.

NORMALIZED AREA. Using the average, characteristic deflection basin from the center slab tests for a given airport and feature, a parameter called the "normalized area" (AREA) was calculated from the deflections recorded by the velocity transducers at radii of at 0, 12, 24, and 36 in. from the center of the loading plate. The parameter AREA for a deflection basin was defined by Hoffman and Thompson (1981) as:

$$AREA = \frac{S}{2D_0}[D_0 + 2(D_1 + D_2 + \ldots + D_{n-1}) + D_n]$$

where

AREA = normalized deflection area (in.)
S = constant spacing between sensors (12 in.)
D_i = deflection at sensor i (in.)
n = number of sensors used in calculation, less one.

RADIUS OF RELATIVE STIFFNESS. The radius of relative stiffness (ℓ) was determined by a backcalculation procedure based upon a relationship between the normalized deflection basin area (AREA) and ℓ proposed by Ioannides (1990). Ioannides developed the unique relationship between AREA and ℓ for the radius of loaded area a of 5.9055 in. (the radius of the HWD loading plate). For a center loaded slab on a dense liquid foundation (Westergaard k), the unique relationship is shown in figure 16. To simplify the calculation of ℓ from the AREA, a sixth-order polynomial relationship was developed by linear regression:

$$\ell = 0.5 - 1.25AREA + 1.25\,AREA^2 - 0.1803\,AREA^3 + 0.011098\,AREA^4 - 0.0003075\,AREA^5 + 0.0000003198\,AREA^6 \quad (5)$$

For purposes of analysis, the radius of relative stiffness was normalized by forming the a/l ratio, where a/ℓ is the radius of the loading plate. For each of the tests, the radius of loaded area was simply the radius of the HWD loading plate (about 5.9 in.).

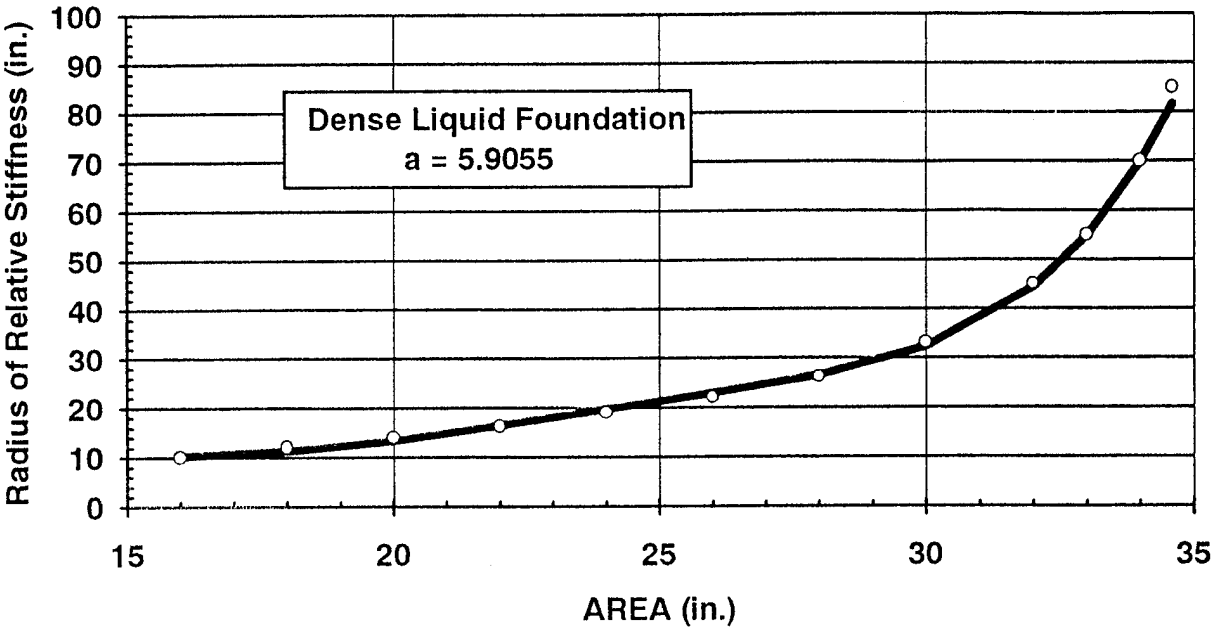

FIGURE 16. RELATIONSHIP BETWEEN AREA AND ℓ FOR A DENSE LIQUID FOUNDATION, a = 5.90655 IN.

JOINT EFFICIENCY. The joint efficiency for each of the test locations was calculated using the formula

$$JE = \frac{\Delta_U}{\Delta_L} \qquad (6)$$

where:

JE = joint efficiency
Δ_U = deflection of unloaded side of joint
Δ_L = deflection of loaded side.

The joint efficiency was calculated for the tests conducted on each side of the joint, and the resultant two efficiencies averaged for that joint. This was done to counter any effects of crack face skewing on the joint efficiency.

LOAD TRANSFER. The average joint efficiency was used to estimate the average load transfer for each joint (figure 17). The average load transfer was determined by using a set of curves relating joint efficiency to load transfer as a function of the a/ℓ ratio developed by Ioannides and Korovesis (1990). The basis for these curves is the two-dimensional finite element code ILLI-SLAB. The underlying assumptions included linear elasticity, plate theory, and a dense liquid

foundation. Load transfer at a joint was modeled by linear elastic spring elements between slabs. ILLI-SLAB runs were made varying a/ℓ between 0.047 and 0.584. The resulting deflection calculations were used to calculate joint efficiencies and stresses were used to calculate load transfer. These results indicated a dependence of load transfer on a/ℓ.

To more accurately determine the load transfer/joint efficiency relationship for the actual a/ℓ values computed for this study, additional a/ℓ curves were approximated by linear interpolation of the original results presented by Ioannides and Korovesis (1990). In addition to the original a/ℓ values of 0.584, 0.312, 0.156, and 0.047, curves were estimated for a/ℓ values of 0.35, 0.27, 0.25, 0.2, and 0.17 (figure 18). Note that the curves are concentrated between a/ℓ values of 0.156 and 0.35, suggesting a uniform set of relative stiffness values considering the range of possible values.

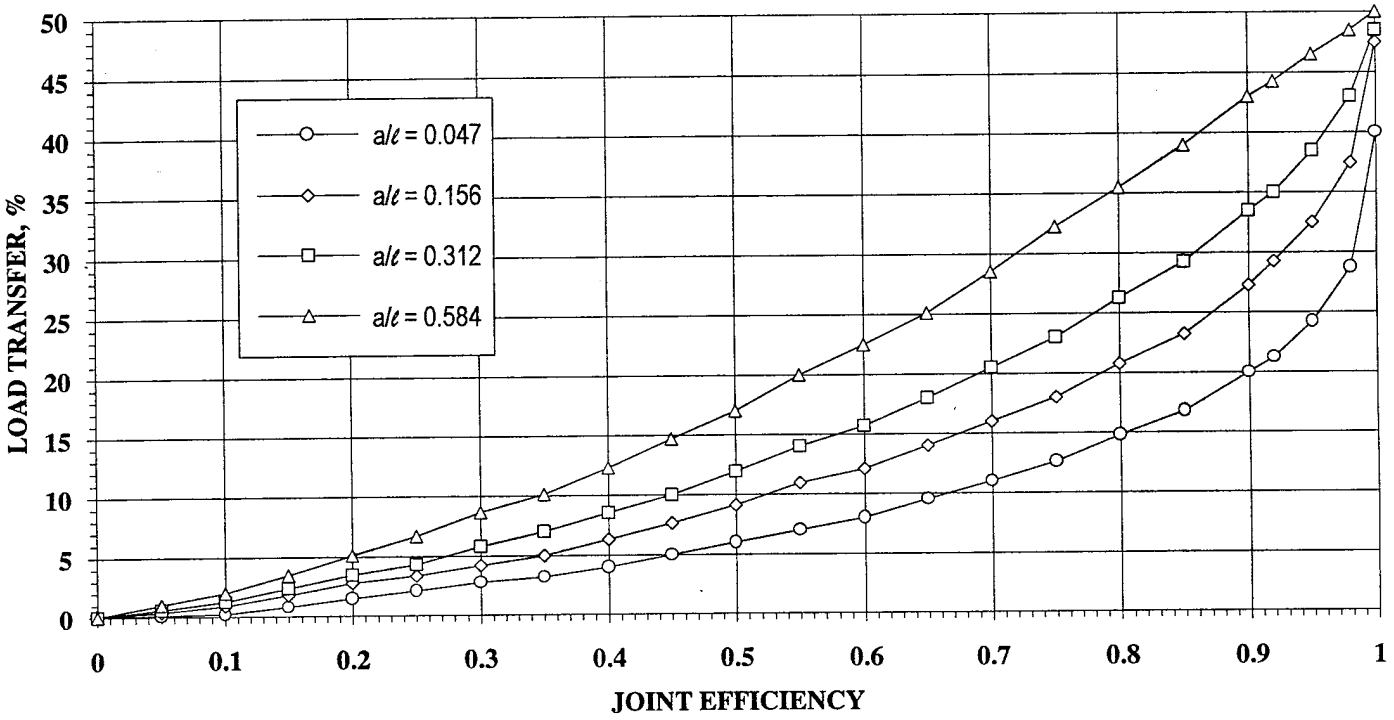

FIGURE 17. RELATIONSHIP BETWEEN JOINT EFFICIENCY AND LOAD TRANSFER AS A FUNCTION OF a/ℓ

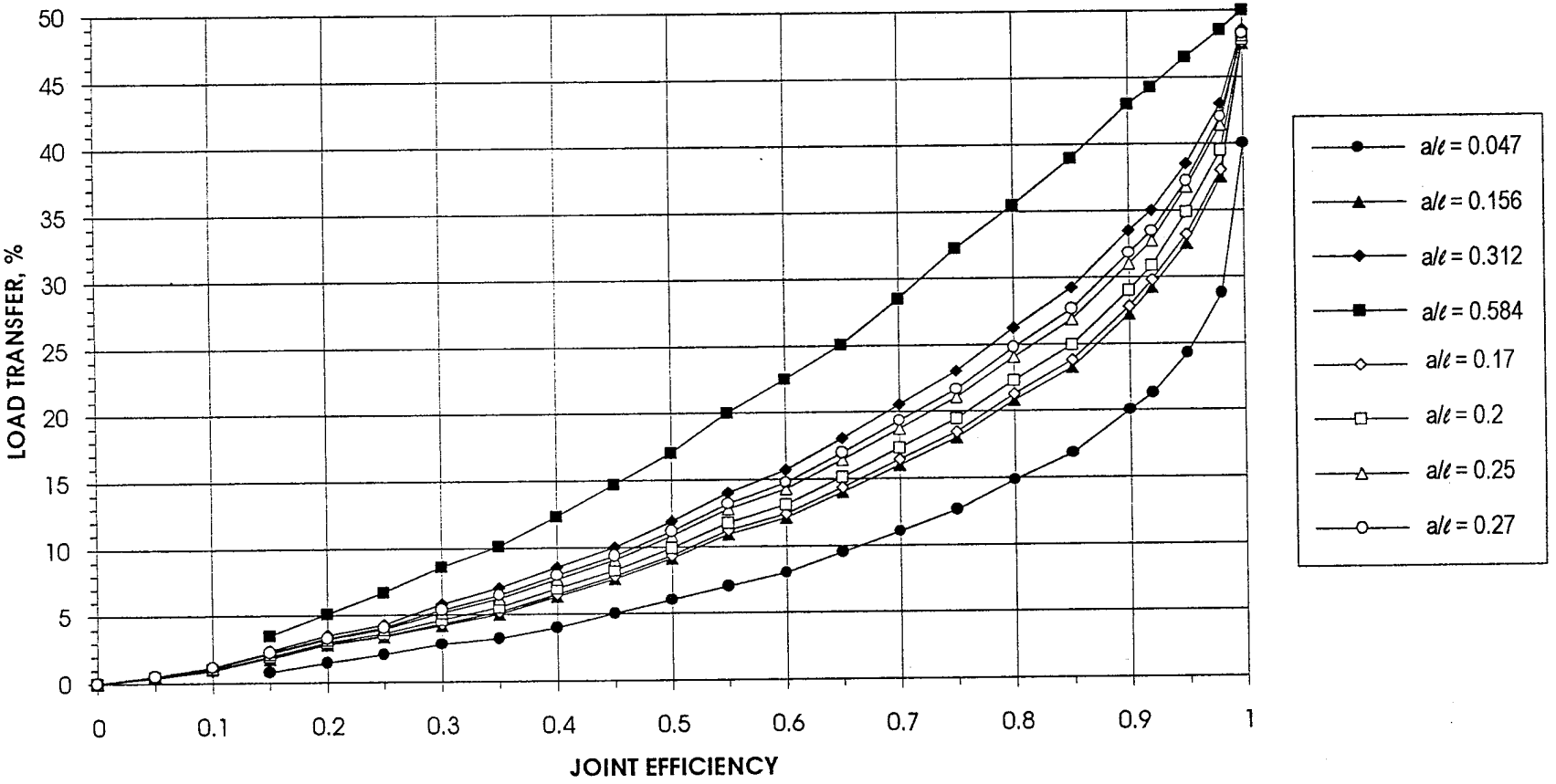

FIGURE 18. INTERPOLATED RELATIONSHIPS BETWEEN JOINT EFFICIENCY AND LOAD TRANSFER AS A FUNCTION OF a/ℓ

FIELD TEST RESULTS

GENERAL.

Table 2 shows the locations and dates of field tested results conducted in support of this research. All field testing conducted as a part of this study took place in calendar years 1992 and 1993. For Atlanta-Hartsfield International Airport, historical joint efficiency data were available from 1984, 1987, and 1990. These data were also included as a part of this report. The locations of the tests and a description of the test data are included in the following paragraphs.

ATLANTA-HARTSFIELD INTERNATIONAL AIRPORT.

Figure 19 shows a plan of the Atlanta-Hartsfield International Airport. Tests were conducted at selected locations on Runways 8R-26L and 9L-27R; Taxiways D, E, and M; and Ramp 5. In figure 19 the locations of features on which joint efficiency tests were conducted have been highlighted.

As shown in figure 20, the joints tested at Atlanta were located in five different rigid pavement systems. The PCC thicknesses were 16 in., with the exception of Taxiway E, which had a 22-in.-thick PCC section. All PCC pavements were supported by a stabilized base except Runway 8R-26L, which rested on a crushed stone base. Joint spacings ranged from 25 to 75 ft. The results of the midslab tests are tabulated in table 3.

As a part of this testing program, data were obtained at Atlanta during the winter of 1992 under both day and night conditions. The pavement surface temperatures for the night tests ranged from 32 to 68°F, while the pavement temperatures for the day tests ranged from 64 to 86°F. The pavement surface temperatures for the historical data were not known.

For each joint type on each feature of the airport, the means and coefficients of variation (COV) were calculated. These data are summarized in tables 4 through 9. The results from the joint efficiency tests at the low load levels are presented graphically in figures 21 and 22. Figures 23 and 24 summarize the results of the 1992 day and night summer testing for all joint types and features. Figures 25 through 28 present bar charts summarizing the 1992 winter tests at Atlanta. Included in these plots are all tested features of the airport at all the times of testing.

DALLAS-FORT WORTH INTERNATIONAL AIRPORT.

Figure 29 highlights the features of the Dallas-Fort Worth International Airport which were tested as a part of this study. Tests were conducted in the winter of 1992 on Runway 31R, Cross-Taxiway 3, and Taxiways K and J.

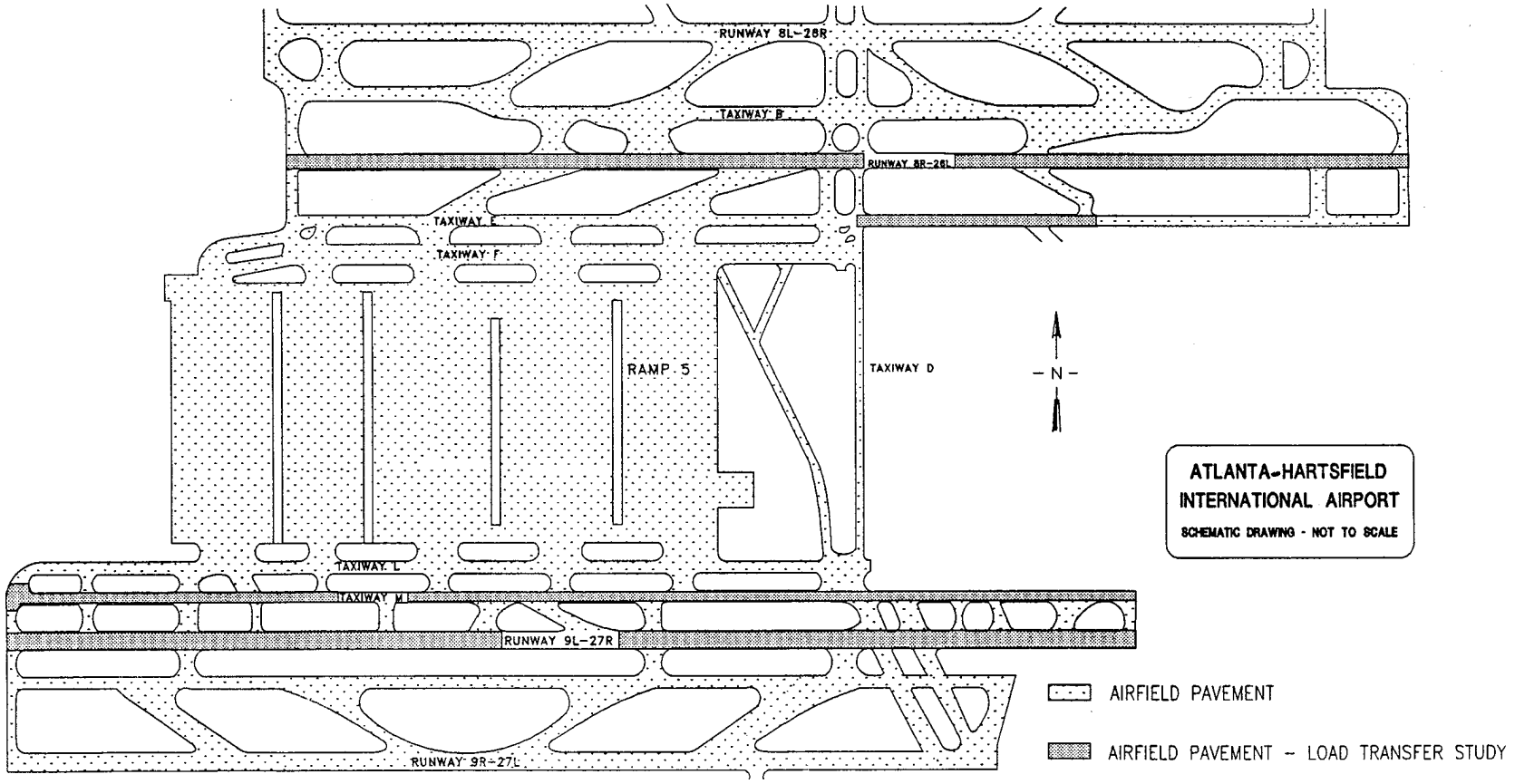

FIGURE 19. PLAN OF ATLANTA-HARTSFIELD INTERNATIONAL AIRPORT SHOWING FEATURES TESTED

Atlanta-Hartsfield International Airport

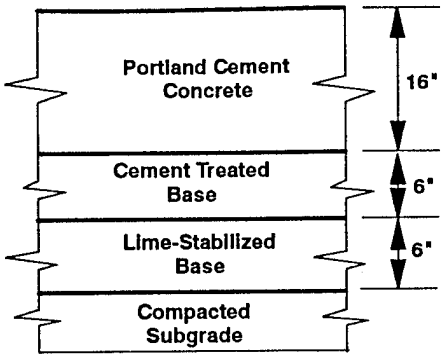

Taxiway D and Ramp 5 (50-ft Joint Spacings)

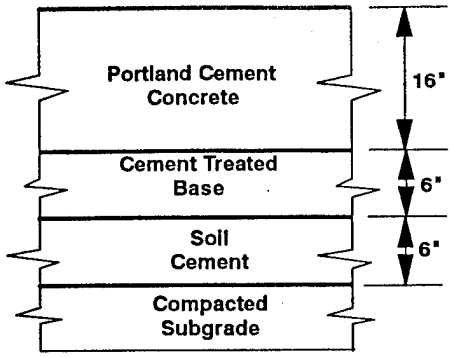

Taxiway M (25- and 75-ft Joint Spacings)

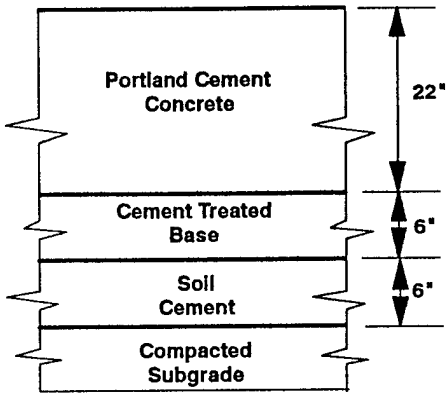

Taxiway E (50-ft Joint Spacings with Cracks)

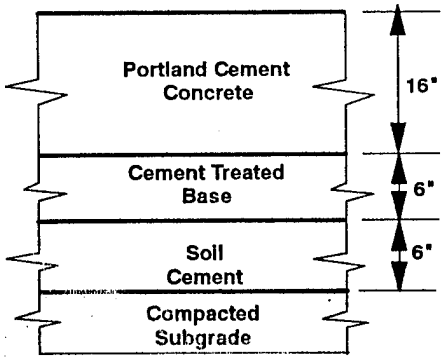

Runway 9L-27R (50- and 75-ft Joint Spacings)

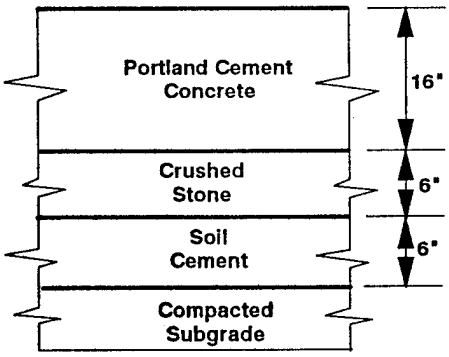

Runway 8R-26L (75-ft Joint Spacings)

FIGURE 20. CROSS SECTIONS OF PAVEMENTS TESTED AT ATLANTA

TABLE 3. RESULTS OF MIDSLAB TESTS, ATLANTA-HARTSFIELD INTERNATIONAL AIRPORT

	Area		ℓ		a/ℓ	
Airport Feature	Mean in.	COV %	Mean in.	COV %	Mean in.	COV %
Taxiway M	32.1	2.5	46.4	15.1	0.130	15.8
Taxiway E	30.2	5.1	34.8	18.2	0.175	18.8
Runway 9L-27R	30.7	4.2	37.0	19.0	0.164	18.2
Runway 8R-26L	30.2	5.1	34.8	18.2	0.175	18.8

TABLE 4. SUMMARY OF RESULTS FROM JOINT EFFICIENCY TESTS, ATLANTA-HARTSFIELD INTERNATIONAL AIRPORT, 1984 SUMMER NIGHT TESTS

			Joint Efficiency		Load Transfer, %	
Joint Type	Load	n	Mean	COV	Mean	COV
Runway 8R-26L						
Transverse Contraction Dowel Corner	Low	9	0.93	4.1	31.3	14.6
Longitudinal Construction Keyed and	Low	10	0.79	27.0	22.1	36.2

TABLE 5. SUMMARY OF RESULTS FROM JOINT EFFICIENCY TESTS, ATLANTA-HARTSFIELD INTERNATIONAL AIRPORT, 1987 WINTER NIGHT TESTS

			Joint Efficiency		Load Transfer, %	
Joint Type	Load	n	Mean	COV	Mean	COV
Runway 8R-26L						
Transverse Contraction Dowel Corner	Low	12	0.49	44.8	10.0	76.1
Longitudinal Construction Keyed and Tied	Low	12	0.61	29.9	13.5	50.6
Runway 9L-27R						
Transverse Contraction Dowel (1974)	Low	11	0.26	48.8	4.1	54.5
Transverse Contraction Dowel Corner (1974)	Low	12	0.25	89.4	5.6	151.3
Transverse Contraction Dowel (1985)	Low	13	0.31	44.3	5.0	56.7
Transverse Contraction Dowel Corner (1985)	Low	4	0.19	46.6	2.9	30.2
Transverse Thick Edge - No Dowel (1985)	Low	3	0.11	19.6	2.2	10.8
Longitudinal Construction Dowel (1985)	Low	12	0.64	9.9	13.8	16.8
Longitudinal Construction Key - No Tie (1974)	Low	12	0.56	32.3	11.5	49.9
Longitudinal Construction Key and Tie (1974)	Low	12	0.85	7.0	24.0	16.9
Taxiway M						
Transverse Contraction Dowel (1978)	Low	1	0.55	*	10.6	*
Transverse Contraction Dowel (1985)	Low	6	0.40	28.9	6.7	37.2

* Only one measurement was taken on this joint type; therefore, the coefficient of variation has no meaning.

TABLE 6. SUMMARY OF RESULTS FROM JOINT EFFICIENCY TESTS, ATLANTA-HARTSFIELD INTERNATIONAL AIRPORT, 1990 SUMMER DAY TESTS

			Joint Efficiency		Load Transfer, %	
Joint Type	Load	n	Mean	COV	Mean	COV
Taxiway M						
Transverse Contraction Dowel (1978)	Low	6	0.88	2.4	25.7	6.9
Transverse Contraction Dowel (1985)	Low	1	0.91	*	28.3	*
Transverse Contraction Dowel Corner (1985)	Low	11	0.93	3.6	30.9	10.8
Longitudinal Construction Tied (1985)	Low	1	0.95	*	33.2	*
Longitudinal Construction Keyed and Tied (1978)	Low	4	0.87	2.4	25.1	6.5

* Only one measurement was taken on this joint type; therefore, the coefficient of variation has no meaning.

TABLE 7. SUMMARY OF RESULTS FROM JOINT EFFICIENCY TESTS, ATLANTA-HARTSFIELD INTERNATIONAL AIRPORT, 1990 SUMMER NIGHT TESTS

			Joint Efficiency		Load Transfer, %	
Joint Type	Load	n	Mean	COV	Mean	COV
Runway 8R-26L						
Transverse Contraction Dowel Corner	Low	12	0.87	7.6	25.8	17.8
Longitudinal Construction Keyed and Tied	Low	12	0.86	9.4	25.6	23.2
Runway 9L-27R						
Transverse Contraction Dowel (1974)	Low	11	0.90	3.2	27.5	10.0
Transverse Contraction Dowel Corner (1974)	Low	12	0.88	13.2	27.9	24.9
Transverse Contraction Dowel (1985)	Low	13	0.88	7.3	26.9	16.6
Transverse Contraction Dowel Corner (1985)	Low	8	0.94	3.2	32.1	11.8
Transverse Thick Edge - No Dowel (1985)	Low	3	0.36	99.0	9.4	109.4
Longitudinal Construction Dowel (1985)	Low	12	0.86	11.0	25.4	23.6
Longitudinal Construction Key - No Tie (1974)	Low	12	0.92	2.2	29.5	7.2
Longitudinal Construction Key and Tie (1974)	Low	12	0.93	3.4	30.9	11.2
Taxiway E - Replaced Slabs						
Transverse Contraction Dowel	Low	7	0.87	8.2	27.4	26.2
Transverse Contraction Dowel Corner	Low	11	0.90	6.8	28.4	22.1
Longitudinal Construction Dowel	Low	12	0.76	6.4	18.4	12.0
Taxiway M						
Transverse Contraction Dowel (1978)	Low	6	0.87	3.7	25.4	10.4
Transverse Contraction Dowel (1985)	Low	6	0.91	1.7	29.0	5.6
Longitudinal Construction Keyed and Tied (1978)	Low	6	0.88	6.0	26.0	1 5.1

TABLE 8. SUMMARY OF RESULTS FROM JOINT EFFICIENCY TESTS, ATLANTA-HARTSFIELD INTERNATIONAL AIRPORT, 1992 WINTER DAY TESTS

			Joint Efficiency		Load Transfer, %	
Joint Type	Load	n	Mean	COV	Mean	COV
Runway 8R-26L						
Transverse Contraction Dowel	Low	12	0.84	8.5	23.6	20.5
	High	12	0.84	8.6	23.2	21.0
Transverse Crack Reinforced	Low	11	0.90	3.2	28.0	9.7
	High	11	0.90	3.0	27.8	9.2
Longitudinal Construction Keyed (No Tie)	Low	6	0.86	1.7	24.5	4.7
	High	6	0.86	2.9	24.5	7.8
Taxiway D						
Expansion Dowel	Low	4	0.54	32.5	16.4	53.6
	High	4	0.55	32.3	16.8	53.4
Taxiway M						
Transverse Contraction Dowel (1978)	Low	6	0.70	23.74	17.1	39.4
	High	6	0.69	21.2	16.3	37.6
Transverse Contraction Dowel (1985)	Low	6	0.62	24.3	14.1	49.2
	High	6	0.61	28.6	13.9	54.5
Transverse Contraction Dowel Corner (1985)	Low	6	0.77	25.6	21.9	41.7
	High	6	0.74	32.9	20.9	48.9
Longitudinal Construction Keyed and Tied (1978)	Low	4	0.82	4.3	21.5	9.4
	High	4	0.82	3.9	21.5	8.3

TABLE 9. SUMMARY OF RESULTS FROM JOINT EFFICIENCY TESTS, ATLANTA-HARTSFIELD INTERNATIONAL AIRPORT, 1992 WINTER NIGHT TESTS (1 OF 2)

			Joint Efficiency		Load Transfer, %	
Joint Type	Load	n	Mean	COV	Mean	COV
Runway 8R-26L						
Transverse Contraction Dowel	Low	11	0.88	7.4	27.0	24.8
	High	11	0.87	6.2	25.3	15.7
Transverse Contraction Dowel Corner	Low	11	0.85	11.3	24.9	24.6
	High	11	0.84	9.3	23.4	20.5
Transverse Crack Reinforced	Low	11	0.90	3.3	28.1	10.0
	High	11	0.91	3.6	28.5	11.6
Runway 9L-27R						
Longitudinal Construction Keyed and Tied	Low	11	0.85	6.5	23.6	15.5
	High	11	0.85	6.5	23.7	16.5
Longitudinal Construction Keyed (No Tie)	Low	11	0.88	3.7	26.1	9.8
	High	11	0.86	11.2	24.9	20.6
Longitudinal Construction Keyed (No Tie) Corner	Low	11	0.79	16.1	21.0	26.6
	High	11	0.78	14.6	20.4	24.3
Transverse Contraction Dowel (1974)	Low	11	0.84	21.2	25.3	28.2
	High	11	0.84	18.8	25.0	26.4
Transverse Contraction Dowel Corner (1974)	Low	12	0.82	15.5	23.5	30.4
	High	12	0.83	12.7	23.1	24.8
Transverse Contraction Dowel (1985)	Low	13	0.47	51.1	10.1	91.9
	High	13	0.47	44.8	9.7	80.6
Transverse Contraction Dowel Corner (1985)	Low	12	0.48	64.6	12.0	96.1
	High	12	0.52	48.1	12.0	82.9
Transverse Thick Edge - No Dowel (1985)	Low	4	0.19	33.4	3.0	23.8
	High	4	0.17	36.5	2.8	21.8
Longitudinal Construction Dowel (1985)	Low	18	0.70	16.9	16.6	35.6
	High	18	0.70	13.6	16.6	28.6
Longitudinal Construction Dowel Corner (1985)	Low	12	0.63	19.9	14.0	37.9
	High	12	0.65	17.4	14.3	32.1
Longitudinal Construction Key - No Tie (1974)	Low	18	0.81	15.2	22.2	27.7
	High	18	0.81	12.5	22.3	24.0
Longitudinal Construction Key Corner - No Tie (1974)	Low	12	0.78	18.6	20.9	32.5
	High	12	0.79	16.9	21.0	30.3
Longitudinal Construction Key and Tie (1974)	Low	12	0.85	7.0	24.0	16.9
	High	12	0.89	7.6	27.7	19.5
Transverse Contraction Dowel	Low	11	0.44	22.0	7.6	34.5
	High	11	0.48	19.4	8.4	31.7

TABLE 9. SUMMARY OF RESULTS FROM JOINT EFFICIENCY TESTS, ATLANTA-HARTSFIELD INTERNATIONAL AIRPORT, 1992 WINTER NIGHT TESTS (2 OF 2)

			Joint Efficiency		Load Transfer, %	
Joint Type	Load	n	Mean	COV	Mean	COV
Runway 9L-247 (Continued)						
Transverse Contraction Dowel Corner	Low	11	0.35	36.7	5.5	50.9
	High	11	0.45	28.3	8.0	44.7
Expansion - Dowel	Low	1	0.51	*	9.4	*
	High	1	0.54	*	10.2	*
Transverse Crack Reinforced	Low	12	0.66	25.4	15.1	38.5
	High	12	0.66	24.4	14.9	36.9
Longitudinal Construction Dowel	Low	12	0.72	7.9	16.6	13.8
	High	12	0.72	7.8	16.9	13.8
Taxiway D						
Expansion - Dowel	Low	4	0.54	32.5	10.9	51.4
	High	4	0.55	32.3	11.2	51.3
Ramp 4						
Stitched	Low	1	0.90	*	27.2	*
	High	1	0.88	*	25.5	*
Taxiway M						
Transverse Contraction Dowel (1978)	Low	6	0.80	15.6	21.9	30.0
	High	6	0.81	9.4	21.3	18.8
Transverse Contraction Dowel (1985)	Low	6	0.61	31.6	14.0	58.4
	High	6	0.74	11.6	17.9	22.6
Transverse Contraction Dowel Corner (1985)	Low	6	0.69	19.6	16.5	35.6
	High	6	0.71	16.0	16.8	29.1
Longitudinal Construction Dowel (1985)	Low	12	0.76	7.7	18.8	15.1
	High	12	0.77	5.2	19.1	9.9
Longitudinal Construction Keyed and Tied (1978))	Low	12	0.61	30.3	13.5	48.0
	High	12	0.62	26.0	13.5	40.7
Longitudinal Construction Keyed and Tied Corner (1985)	Low	12	0.61	17.8	12.9	33.7
	High	12	0.63	15.8	13.4	29.0
Longitudinal Construction Tied	Low	12	0.74	13.1	17.8	22.7
(1985)	High	12	0.75	11.7	18.4	20.2

* Only one measurement was taken on this joint type; therefore, the coefficient of variation has no meaning.

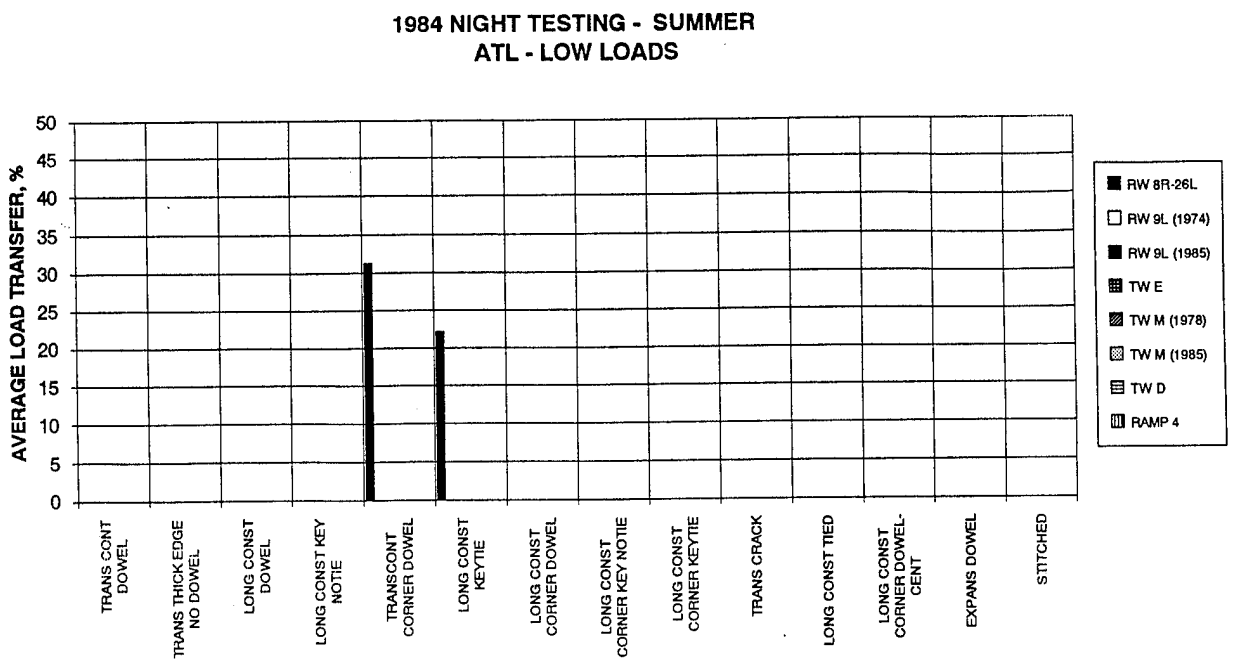

FIGURE 21. SUMMARY OF LOW-LOAD TESTS, 1984 NIGHT TESTING, SUMMER CONDITIONS, ATLANTA

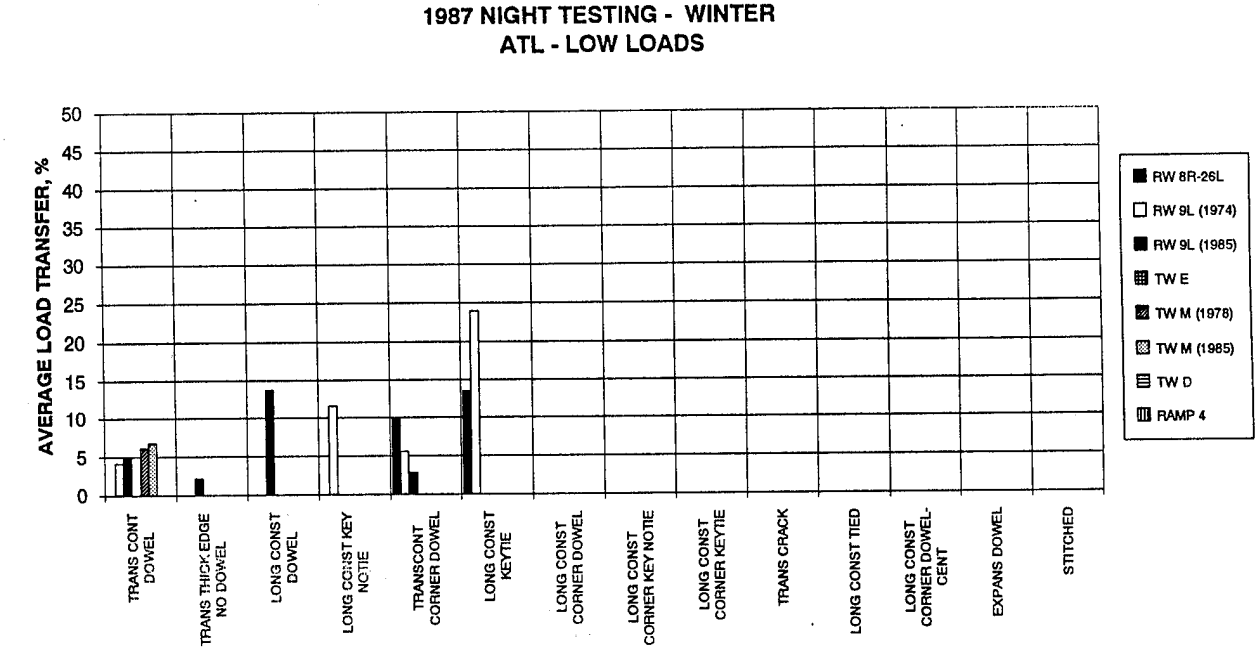

FIGURE 22. SUMMARY OF LOW-LOAD TESTS, 1987 NIGHT TESTING, WINTER CONDITIONS, ATLANTA

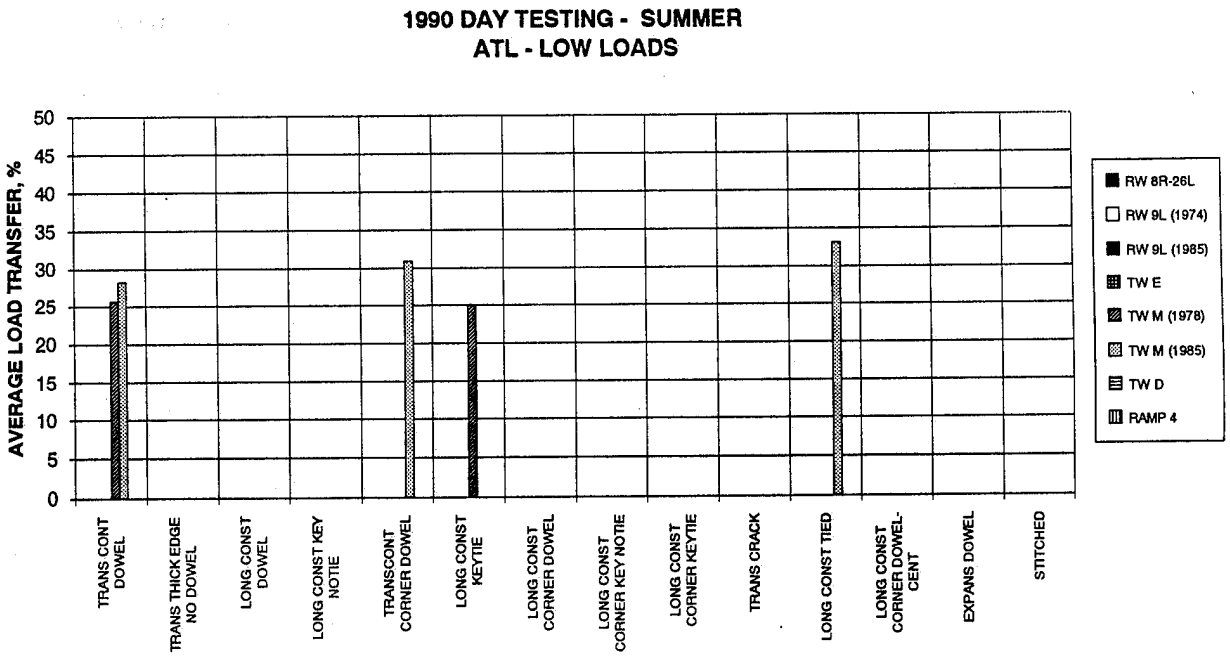

FIGURE 23. SUMMARY OF LOW-LOAD TESTS, 1990 DAY TESTING, SUMMER CONDITIONS, ATLANTA

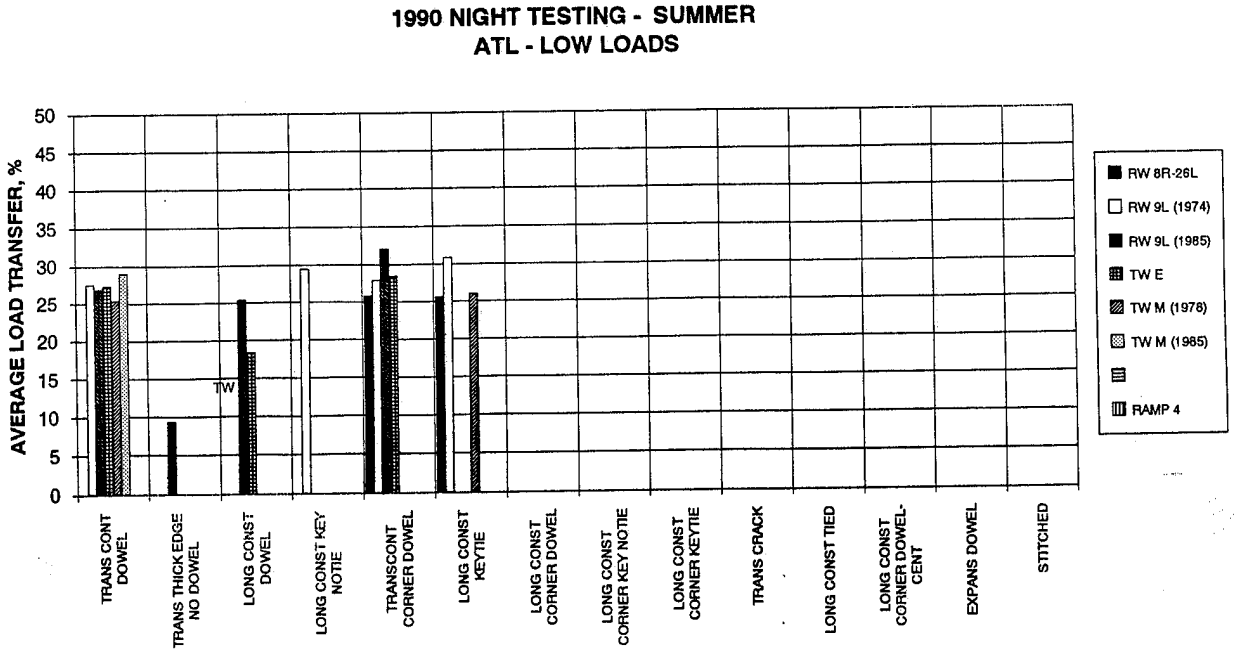

FIGURE 24. SUMMARY OF LOW-LOAD TESTS, 1990 NIGHT TESTING, SUMMER CONDITIONS, ATLANTA

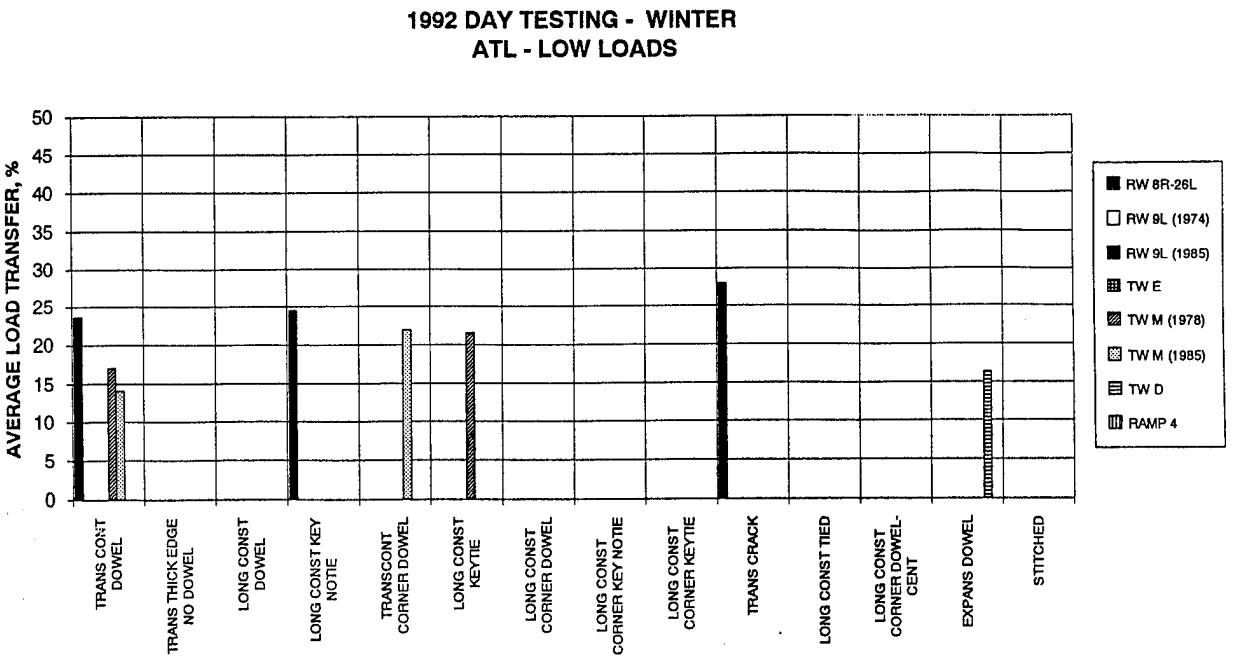

FIGURE 25. SUMMARY OF LOW-LOAD TESTS, 1992 DAY TESTING, WINTER CONDITIONS, ATLANTA

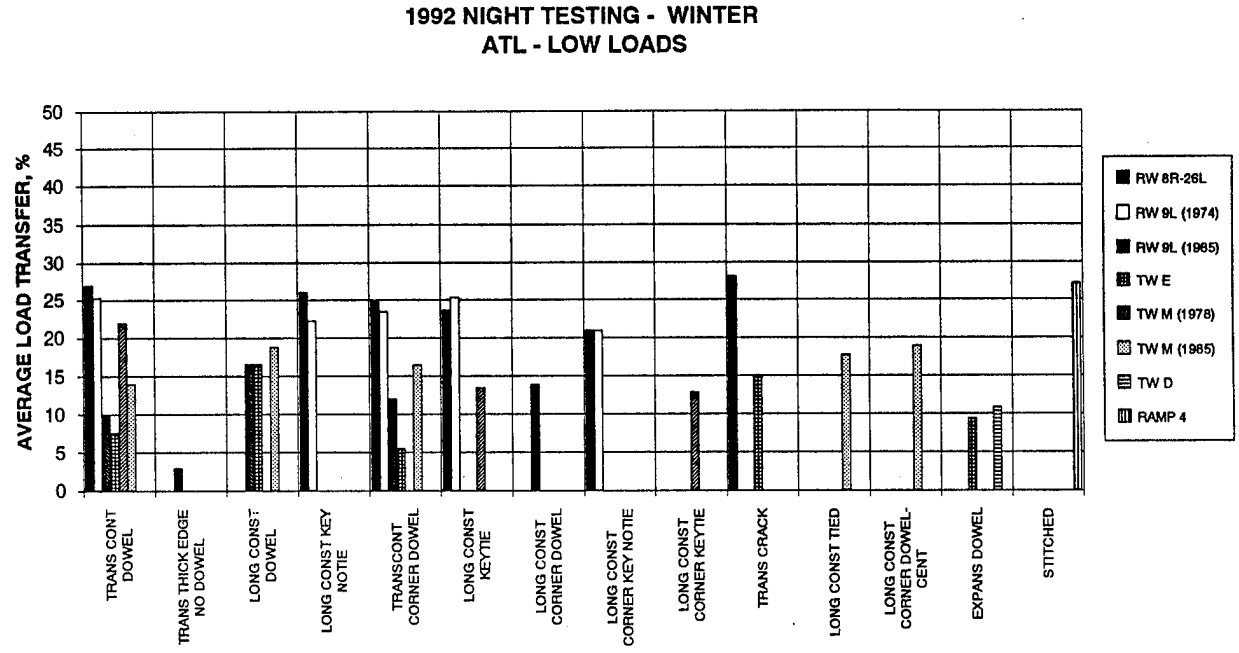

FIGURE 26. SUMMARY OF LOW-LOAD TESTS, 1992 NIGHT TESTING, WINTER CONDITIONS, ATLANTA

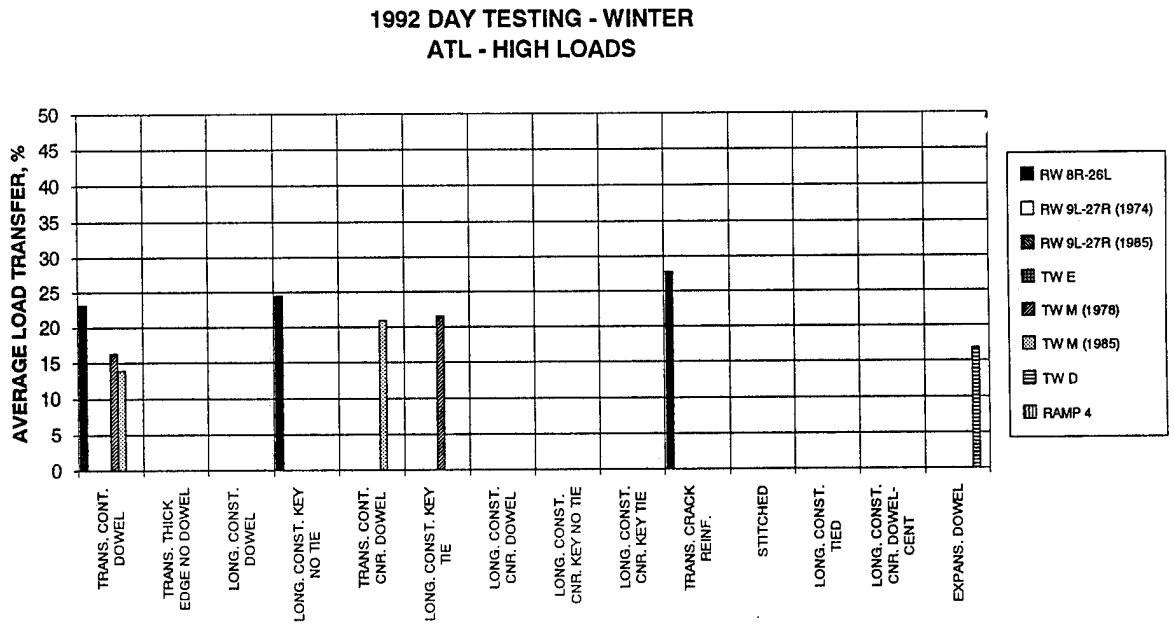

FIGURE 27. SUMMARY OF HIGH-LOAD TESTS, 1992 DAY TESTING, WINTER CONDITIONS, ATLANTA

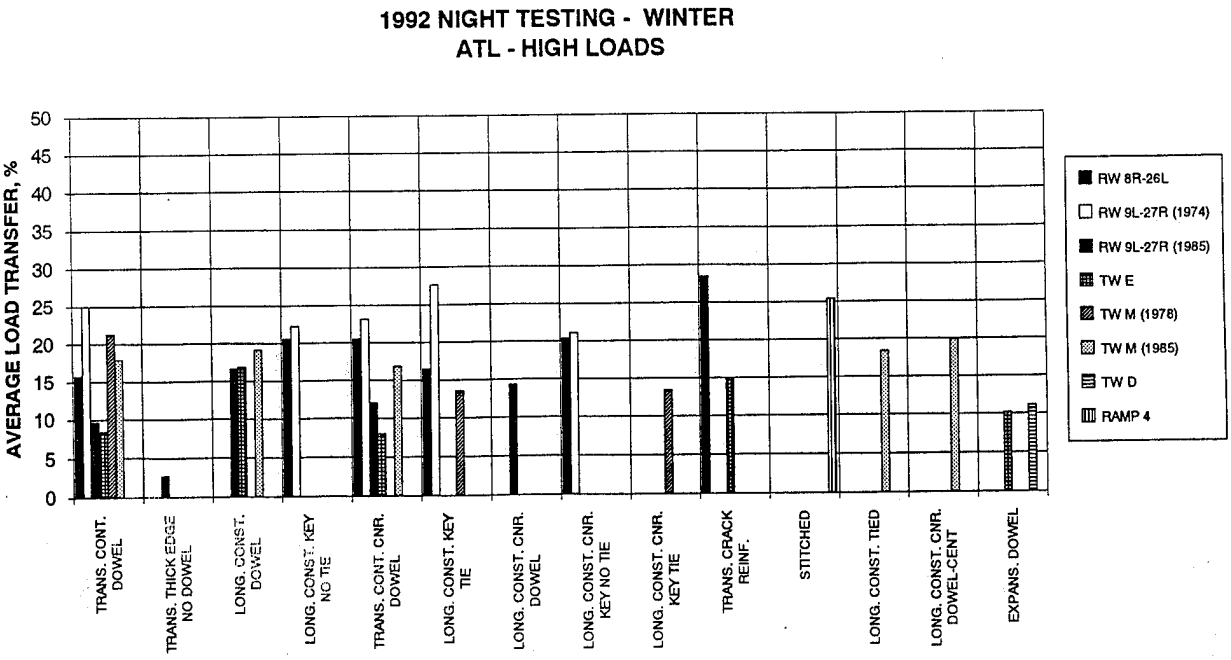

FIGURE 28. SUMMARY OF HIGH-LOAD TESTS, 1992 NIGHT TESTING, WINTER CONDITIONS, ATLANTA

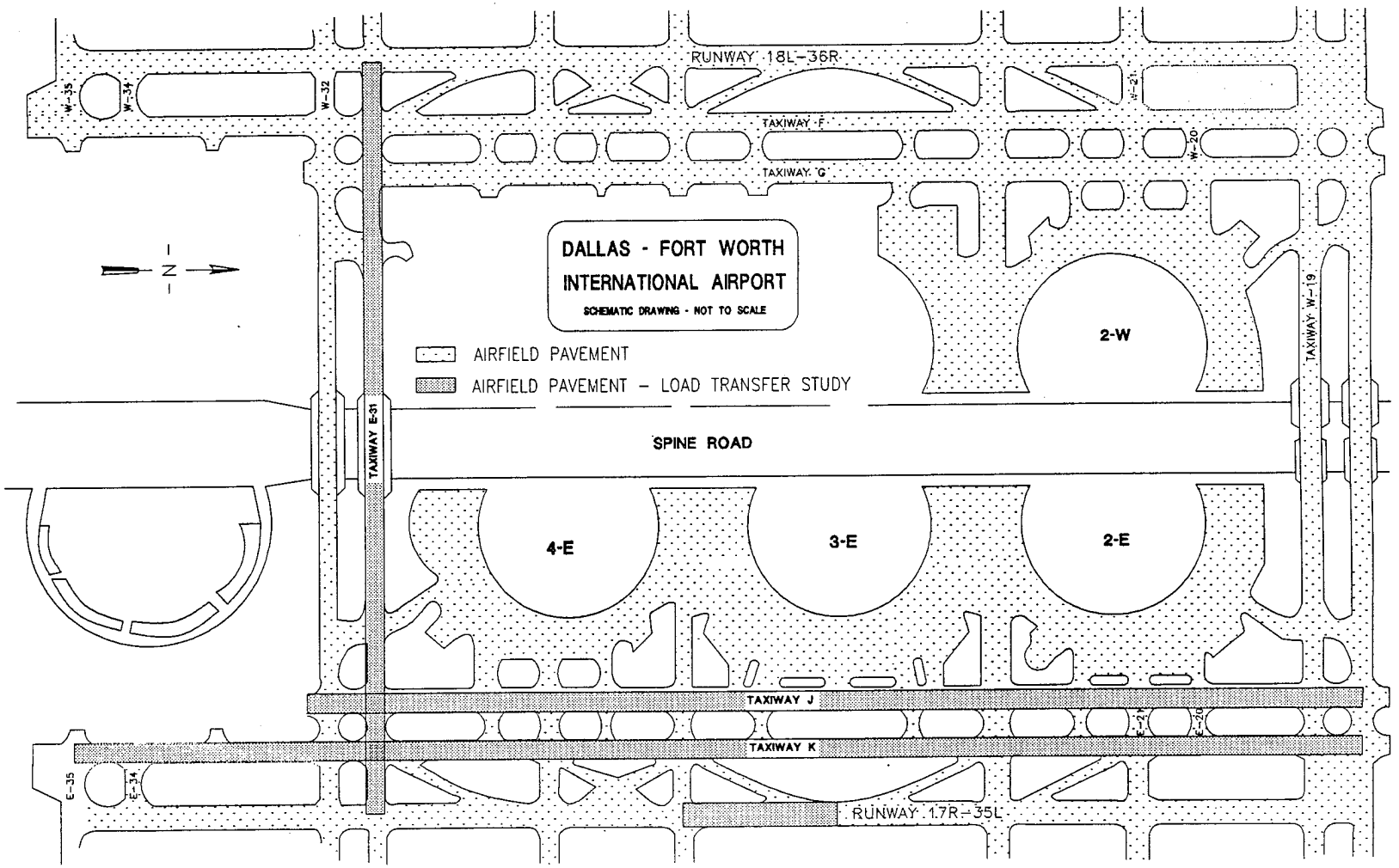

FIGURE 29. PLAN OF DALLAS-FORT WORTH INTERNATIONAL AIRPORT SHOWING FEATURES TESTED

All features tested at Dallas-Fort Worth had the same pavement design (figure 30). The pavement consisted of 16 in. of PCC over a 9-in. cement treated base over 9 in. of lime stabilized base over a compacted subgrade. All transverse joint spacings were 50 ft. The results of the midslab deflection tests for Taxiway K are given table 10. Because the pavement design of all features tests were identical, these midslab results were considered typical for all features.

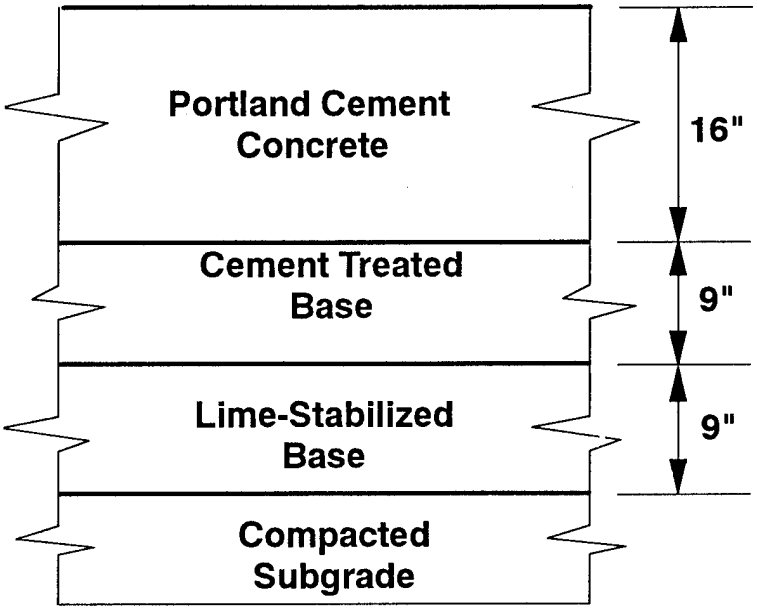

FIGURE 30. TYPICAL PAVEMENT CROSS SECTION, DALLAS-FORT WORTH

TABLE 10. RESULTS OF MIDSLAB TESTS, DALLAS-FORT WORTH INTERNATIONAL AIRPORT

	Area			ℓ			a/ℓ	
	Mean	COV		Mean	COV		Mean	COV
Airport Feature	in.	%		in.	%		in.	%
Taxiway K	30.4	5.0		35.6	17.6		0.171	19.2

The results of field testing at Dallas-Fort Worth International are summarized in table 11. These data are shown graphically in figures 31 and 32, respectively.

TABLE 11. SUMMARY OF RESULTS FROM JOINT EFFICIENCY TESTS, DALLAS-FORT WORTH INTERNATIONAL AIRPORT, 1992 WINTER NIGHT TESTS (1 OF 3)

			Joint Efficiency		Load Transfer, %	
Joint Type	Load	n	Mean	COV	Mean	COV
Runway 31R						
Transverse Contraction Dowel	Low	2	0.67	7.7	14.9	12.8
	High	2	0.70	4.2	15.8	7.2
Transverse Contraction Dowel Corner	Low	2	0.52	3.1	9.7	5.3
	High	2	0.58	4.0	11.7	6.7
Transverse Contraction Reinforced	Low	2	0.83	0.8	22.4	2.0
	High	2	0.84	3.2	22.5	7.9
Transverse Contraction Reinforced Corner	Low	2	0.71	4.3	16.3	7.4
	High	2	0.77	0.9	18.9	1.8
Longitudinal Contraction Reinforced	Low	2	0.78	3.8	19.6	7.8
	High	2	0.77	7.8	19.0	9.5
Longitudinal Construction Keyed	Low	2	0.55	1.7	10.5	2.9
	High	2	0.56	5.6	11.0	9.5
Longitudinal Construction Keyed Corner	Low	1	0.55	*	10.6	*
	High	1	0.52	*	9.7	*
Longitudinal Construction Keyed and Tied	Low	1	0.69	*	15.5*	
	High	1	0.68	*	15.2	*
Longitudinal Construction Keyed and Tied Corner	Low	1	0.84	*	22.8*	
	High	1	0.84	*	23.1	*
Cross-Taxiway 31						
Transverse Contraction Dowel	Low	6	0.69	18.3	16.5	36.4
	High	6	0.68	16.5	15.9	33.1
Transverse Contraction Dowel Corner	Low	6	0.67	12.1	15.0	23.6
	High	6	0.68	10.8	15.1	20.8
Transverse Contraction Reinforced	Low	6	0.75	15.6	19.2	29.5
	High	6	0.76	13.0	19.2	24.4
Transverse Contraction Reinforced Corner	Low	6	0.83	12.0	23.7	22.8
	High	6	0.85	7.9	23.8	16.7
Longitudinal Contraction Reinforced Corner	Low	8	0.79	10.4	20.4	22.5
	High	8	0.77	13.1	19.5	27.4
Longitudinal Construction Keyed and Tied	Low	4	0.81	10.5	21.6	21.9
	High	4	0.81	10.4	21.5	21.2
Longitudinal Construction Keyed and Tied Corner	Low	4	0.80	9.2	21.1	20.7
	High	4	0.81	9.5	21.4	21.3

* Only one measurement was taken on this joint type; therefore, the coefficient of variation has no meaning.

TABLE 11. SUMMARY OF RESULTS FROM JOINT EFFICIENCY TESTS, DALLAS-FORT WORTH INTERNATIONAL AIRPORT, 1992 WINTER NIGHT TESTS (2 OF 3)

			Joint Efficiency		Load Transfer, %	
Joint Type	Load	n	Mean	COV	Mean	COV
Taxiway K						
Transverse Contraction Dowel	Low	14	0.71	15.8	16.7	29.2
	High	14	0.71	13.5	16.8	26.3
Transverse Contraction Dowel Corner	Low	15	0.72	13.1	17.1	26.1
	High	15	0.72	11.6	17.2	23.9
Transverse Contraction Reinforced	Low	5	0.89	2.6	27.0	7.9
	High	5	0.88	3.9	26.2	11.1
Transverse Contraction Reinforced Corner	Low	7	0.91	1.8	28.1	5.6
	High	7	0.89	1.5	26.9	4.4
Longitudinal Contraction Reinforced	Low	35	0.73	21.7	18.2	36.3
	High	35	0.73	20.6	18.0	34.3
Longitudinal Construction Keyed and Tied	Low	19	0.81	14.8	22.1	27.7
	High	19	0.81	13.2	21.8	24.4
Transverse Crack Reinforced	Low	7	0.89	3.1	26.4	9.9
	High	7	0.87	2.3	24.7	6.4
Transverse Crack Reinforced Corner	Low	7	0.88	3.1	26.1	9.2
	High	7	0.86	1.6	23.9	4.3
Taxiway J						
Transverse Contraction Dowel	Low	13	0.69	26.5	17.4	49.1
	High	14	0.66	33.7	16.1	51.4
Transverse Contraction Dowel Corner	Low	14	0.67	36.5	17.0	50.9
	High	14	0.67	36.5	16.9	51.1
Transverse Contraction Reinforced	Low	13	0.67	33.3	16.5	50.9
	High	13	0.68	31.0	16.6	47.8
Transverse Contraction Reinforced Corner	Low	8	0.67	37.3	17.2	54.4
	High	8	0.65	32.8	16.0	52.7
Longitudinal Contraction Reinforced	Low	16	0.70	20.8	16.8	38.9
	High	16	0.68	17.7	15.6	29.6
Longitudinal Contraction Reinforced Corner	Low	14	0.66	24.2	15.1	40.1
	High	14	0.67	22.9	15.4	36.5

TABLE 11. SUMMARY OF RESULTS FROM JOINT EFFICIENCY TESTS, DALLAS-FORT WORTH INTERNATIONAL AIRPORT, 1992 WINTER NIGHT TESTS (3 OF 3)

			Joint Efficiency		Load Transfer, %	
Joint Type	Load	n	Mean	COV	Mean	COV
Taxiway J (Continued)						
Longitudinal Construction Keyed and Tied	Low	10	0.83	12.6	24.0	27.8
	High	10	0.82	11.4	22.5	23.7
Longitudinal Construction Keyed and Tied Corner	Low	10	0.74	27.9	20.1	44.1
	High	10	0.73	25.9	19.3	42.1
Transverse Reinforced Crack	Low	1	0.89	*	26.5	*
	High	1	0.88	*	25.9	*
Transverse Reinforced Crack Corner	Low	5	0.80	22.4	22.5	34.8
	High	5	0.87	1.98	25.3	5.7

* Only one measurement was taken on this joint type; therefore, the coefficient of variation has no meaning.

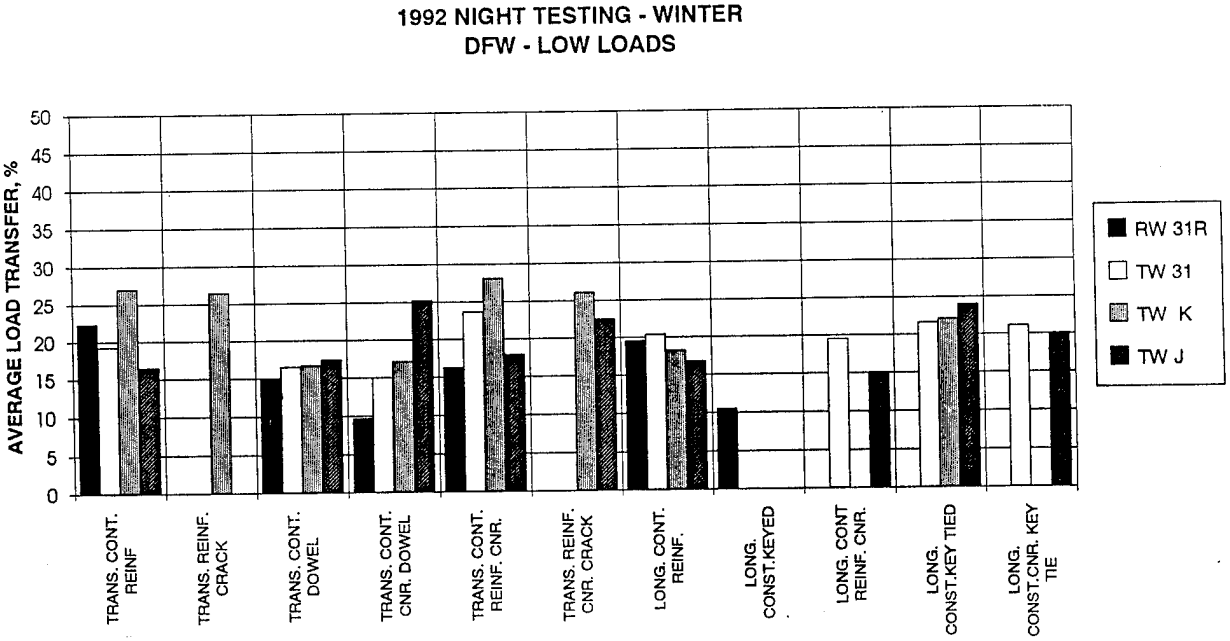

FIGURE 31. SUMMARY OF LOW-LOAD TESTS, DALLAS-FORT WORTH

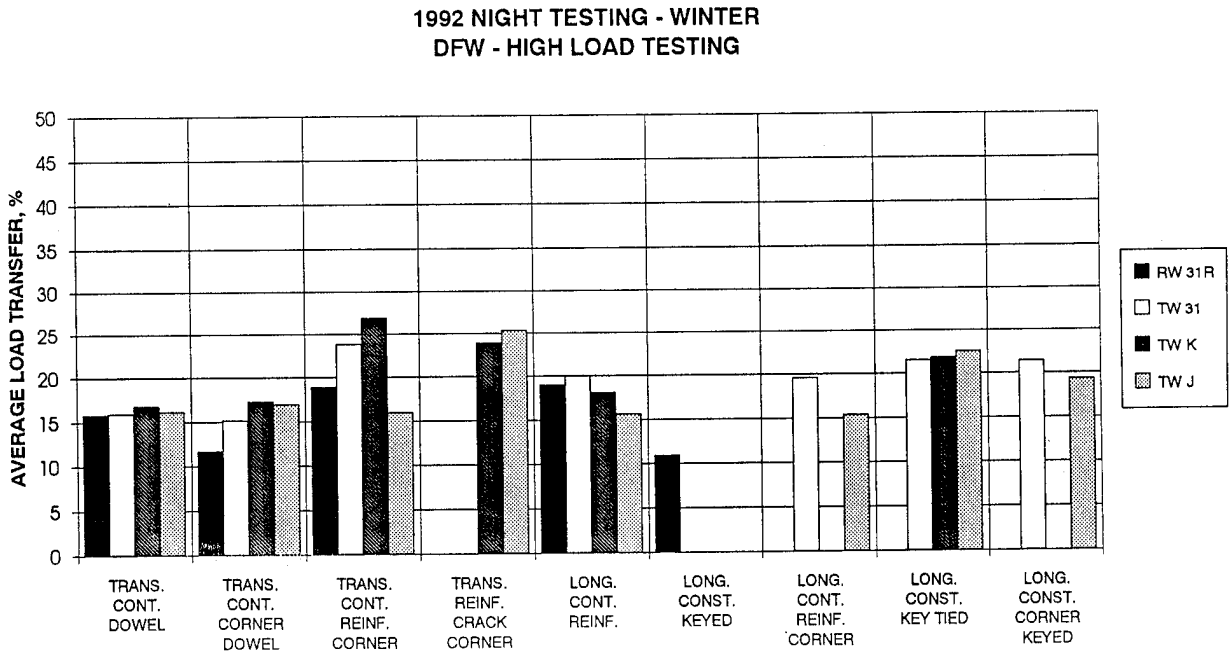

FIGURE 32. SUMMARY OF HIGH-LOAD TESTS, DALLAS-FORT WORTH

DENVER INTERNATIONAL AIRPORT.

Tests were conducted at the Denver International Airport site while construction was still in progress and prior to any aircraft loadings on the pavement. A plan view of the Denver International airport is shown in figure 33. The features tested as a part of this study have been highlighted.

All tests at Denver were conducted during the day in winter conditions. Pavement surface temperatures ranged from 25 to 52°F.

Figure 34 shows a typical cross section of the pavement at Denver International. The PCC pavement at Denver is 17 in. thick over an 8-in.-thick cement treated base and a 12-in.-thick lime-stabilized base. The results of the midslab deflection basins for each feature at Denver are given in table 12.

At the Denver International Airport, the construction method for the doweled construction joints was noted. The construction methods tested included the following: dowels mechanically inserted in the fresh PCC by the paving machine, dowels epoxied in holes drilled in the hardened PCC, and dowels epoxied in holes in the hardened PCC which were formed in the slab by placing "dummy" dowels in the fresh concrete and subsequently removing the "dummy" to leave a hole for dowel insertion.

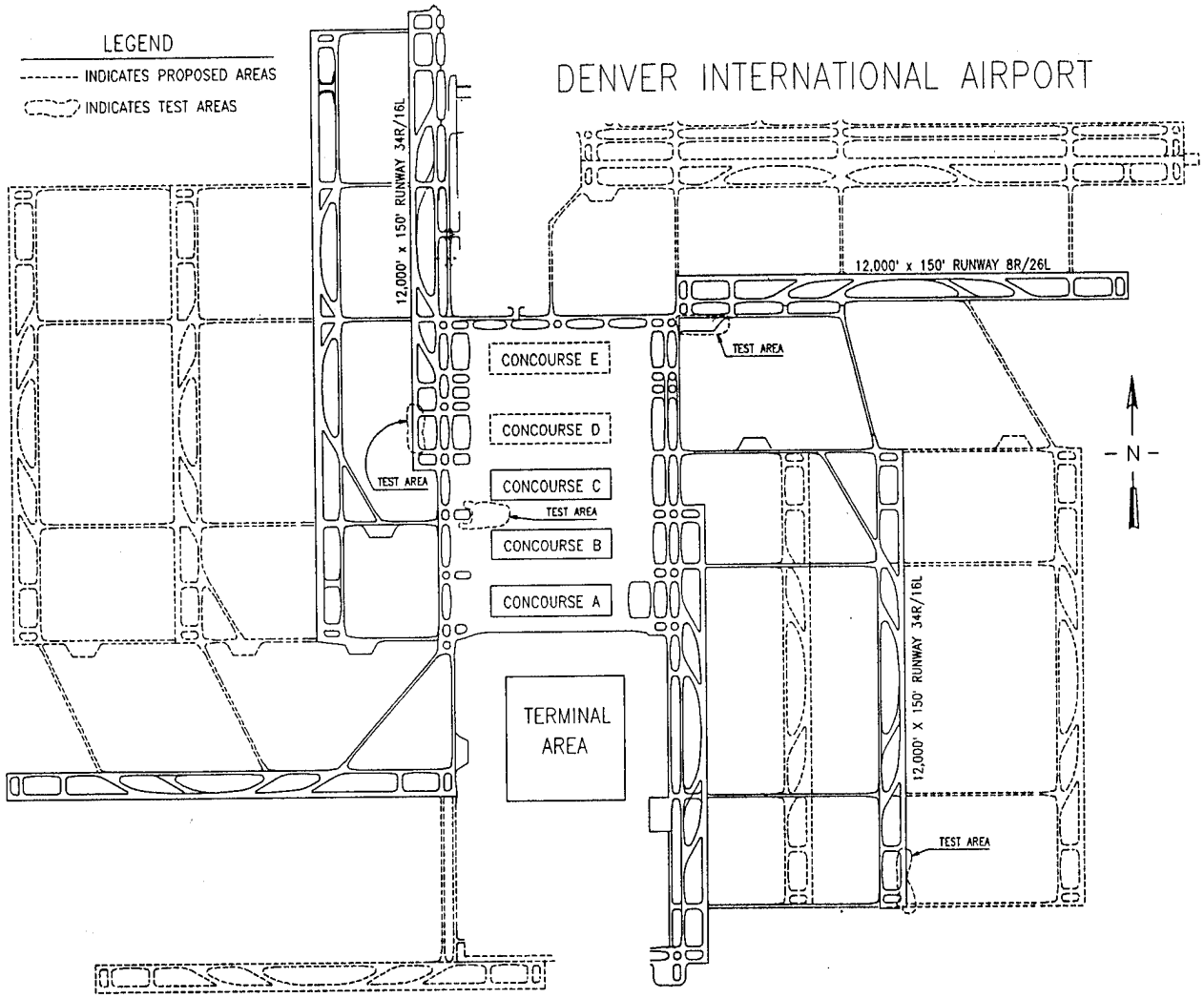

FIGURE 33. PLAN OF DENVER INTERNATIONAL AIRPORT SHOWING FEATURES TESTED

TABLE 12. RESULTS OF MIDSLAB TESTS, DENVER INTERNATIONAL AIRPORT

	Area			ℓ			a/ℓ	
Airport Feature	Mean in.	COV %		Mean in.	COV %		Mean in.	COV %
Runway 16-34	31.5	1.6		40.6	9.1		0.146	8.9
Runway 17-35	31.5	2.6		41.1	14.8		0.746	14.0
Concourse B	31.9	3.6		45.7	21.7		0.135	21.5
Apron 8-26	31.4	1.8		40.1	9.9		0.149	9.6

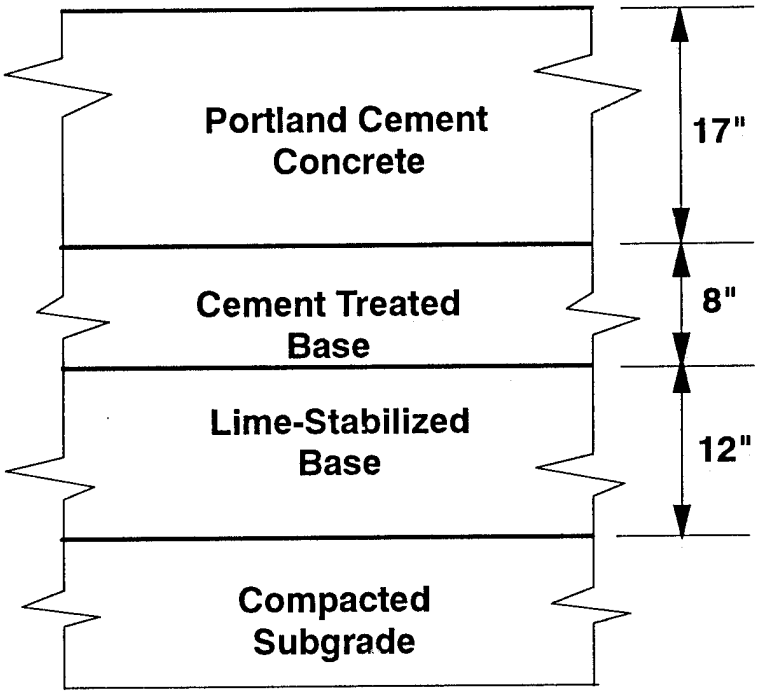

All Transverse Joint Spacings = 20 or 25 ft.

FIGURE 34. TYPICAL PAVEMENT CROSS SECTION, DENVER

The identification of the construction method at the test site was performed by a construction inspector who was present at the site during construction. The data for the doweled construction joints are presented in terms of the construction method in the instances where it could be identified by the inspector. In a couple of features, the construction method was either uncertain or the method employed was a mixture of two or more of the above mentioned techniques. Table 13 summarizes the means and COV's of the various joint types and features. Figures 35 and 36 are bar charts summarizing the mean values of load transfer at the low- and high-load levels, respectively.

TABLE 13. SUMMARY OF RESULTS FROM JOINT EFFICIENCY TESTS, DENVER INTERNATIONAL AIRPORT, 1993 WINTER DAY TESTS

			Joint Efficiency		Load Transfer, %	
Joint Type	Load	n	Mean	COV	Mean	COV
Runway 16-34						
Longitudinal Construction Doweled (Inserted)	Low	11	0.72	11.0	17.1	18.1
	High	11	0.72	12.9	16.3	21.8
Longitudinal Construction Doweled Corner (Inserted)	Low	11	0.61	11.6	12.7	17.8
	High	11	0.58	12.5	11.5	18.5
Longitudinal Construction Doweled (Drilled/Epoxied)	Low	11	0.69	7.3	15.5	14.5
	High	12	0.67	10.2	14.7	17.1
Longitudinal Construction Doweled Corner (Drilled/Epoxied)	Low	11	0.61	11.6	12.7	17.8
	High	11	0.58	12.5	11.5	18.5
Longitudinal Contraction (Tied)	Low	11	0.88	1.9	25.2	4.1
	High	11	0.89	1.3	26.0	3.0
Transverse Construction Doweled (Drilled/Epoxied)	Low	10	0.71	5.5	16.4	11.6
	High	11	0.70	4.5	15.9	9.6
Diamond Blockouts	Low	6	0.72	7.5	16.9	15.2
	High	10	0.69	8.4	15.5	16.0
Apron 8-26						
Longitudinal Construction Doweled	Low	11	0.86	3.1	24.1	6.3
	High	11	0.84	3.2	23.3	6.4
Longitudinal Construction Doweled Corner	Low	12	0.83	5.4	22.9	10.7
	High	12	0.85	3.9	24.0	8.1
Concourse B and C						
Longitudinal Construction Doweled (Dummy/Epoxied)	Low	12	0.87	2.1	24.8	4.2
	High	12	0.86	1.3	24.0	2.5
Longitudinal Construction Doweled (Drilled/Epoxied)	Low	11	0.88	1.8	25.6	4.9
	High	11	0.87	0.9	25.0	1.9
Longitudinal Construction Doweled (Inserted)	Low	12	0.89	1.8	26.0	4.5
	High	12	0.87	1.2	25.0	2.6
Runway 17-35						
Longitudinal Construction Doweled	Low	12	0.73	10.0	17.3	20.3
	High	12	0.70	9.9	16.3	19.8
Transverse Contraction	Low	12	0.71	9.9	16.5	20.2
	High	12	0.71	9.9	16.5	20.0

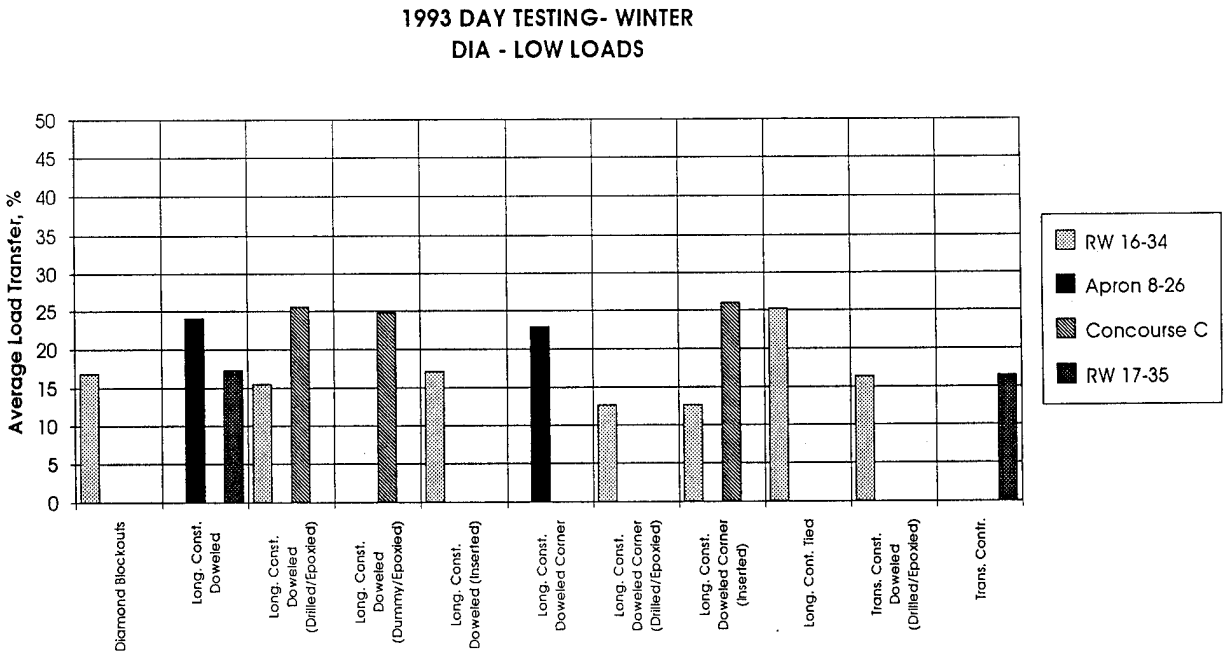

FIGURE 35. SUMMARY OF LOW-LOAD TESTS, DENVER

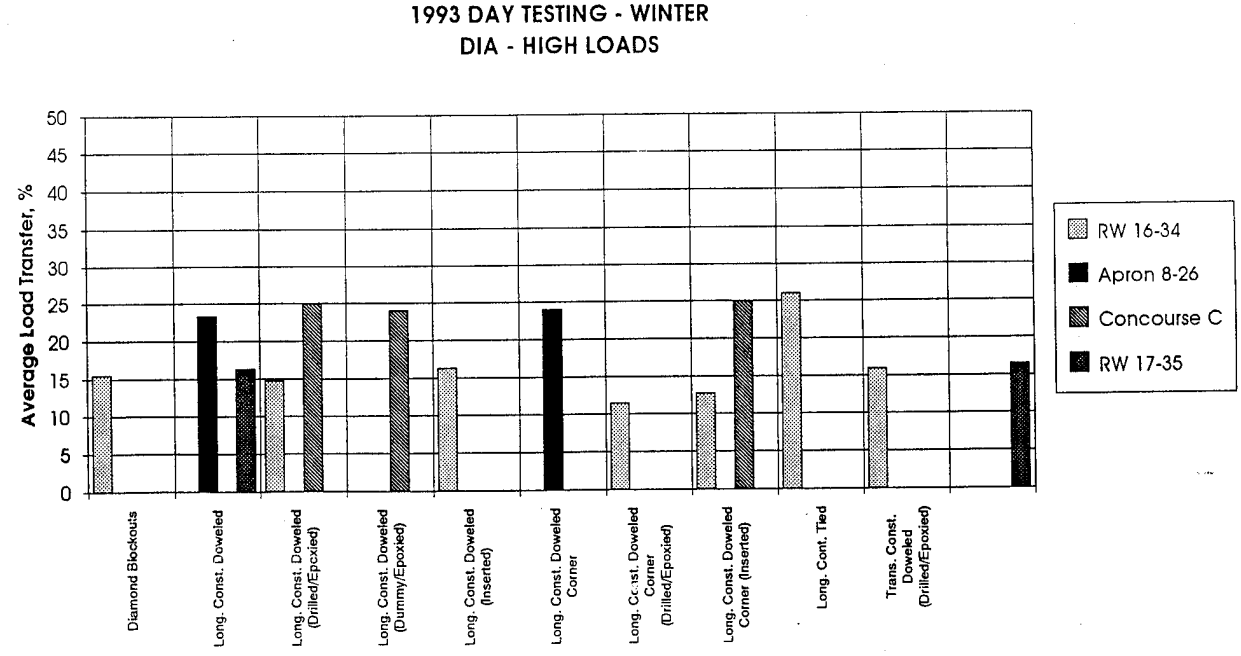

FIGURE 36. SUMMARY OF HIGH-LOAD TESTS, DENVER

DANE COUNTY REGIONAL AIRPORT.

Figure 37 shows a plan view of the Dane County Regional Airport, Madison, Wisconsin, highlighting the features tested. This airport is a former World War II era military airfield which has been modernized to accommodate current commercial and general aviation as well as serve as an Air Force reserve base. Therefore, the pavement cross section of runway 13-31 reflects a number of different renovations through the years (figure 38).

All tests at Madison were conducted during the day under winter conditions. Pavement surface temperatures ranged from 36 to 70°F. Testing was conducted in the early spring just after the subgrade had experienced spring thaw. During the period of testing, the subgrade temperatures were approximately 39°F, as recorded by temperature probes in the subgrade installed and recorded by Airport Operations.

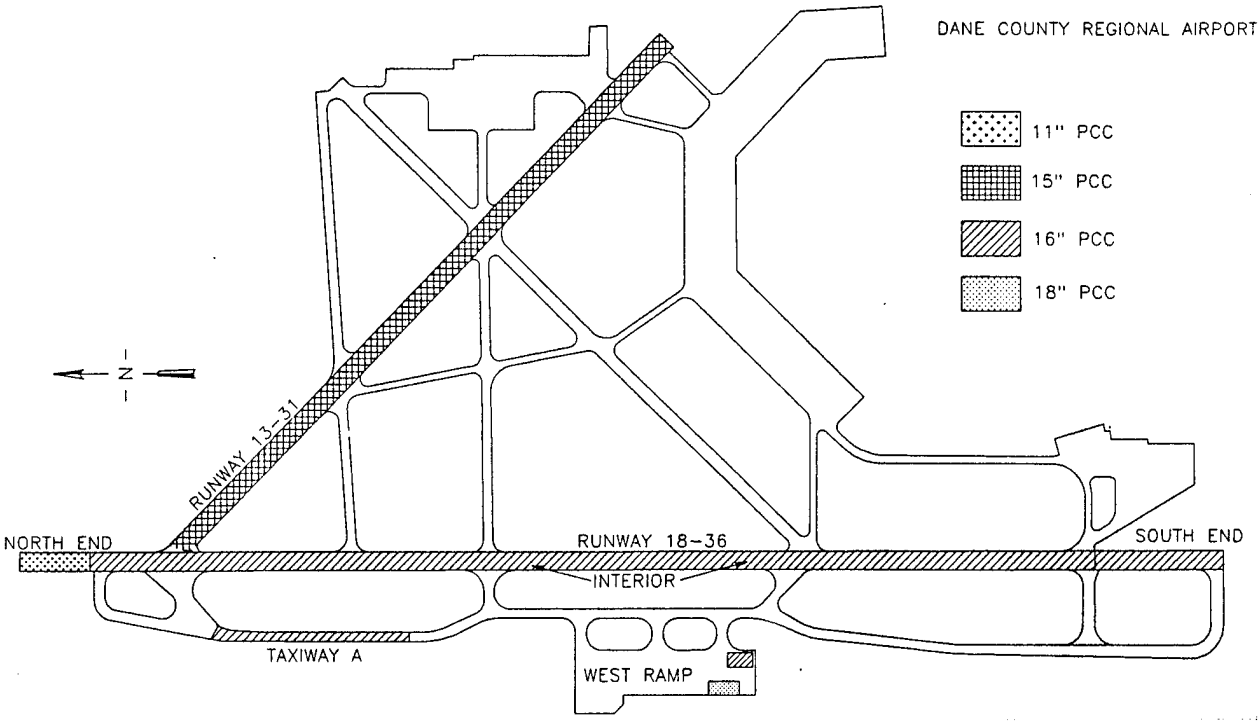

FIGURE 37. PLAN OF DANE COUNTRY REGIONAL AIRPORT SHOWING FEATURES TESTED

Dane County Regional Airport

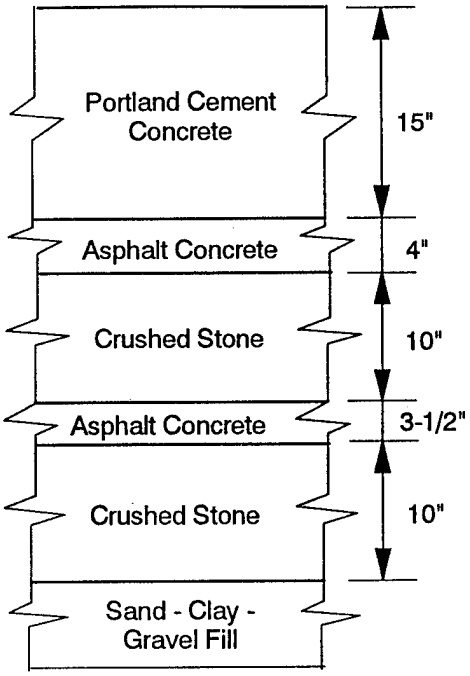

Runway 13-31 (25-ft Joint Spacing)

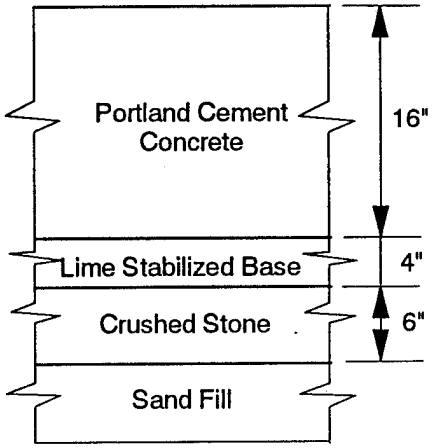

Taxiway A (50-ft Joint Spacing)

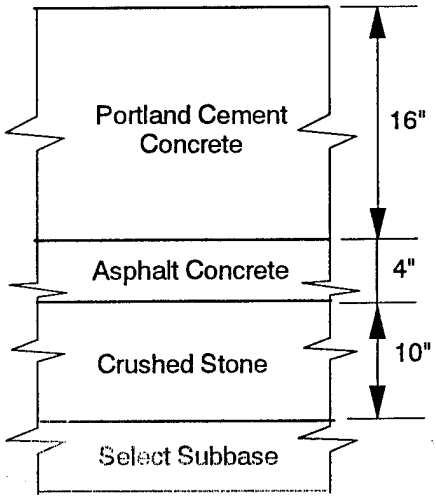

West Ramp 16-in. PCC (20-ft Joint Spacing)

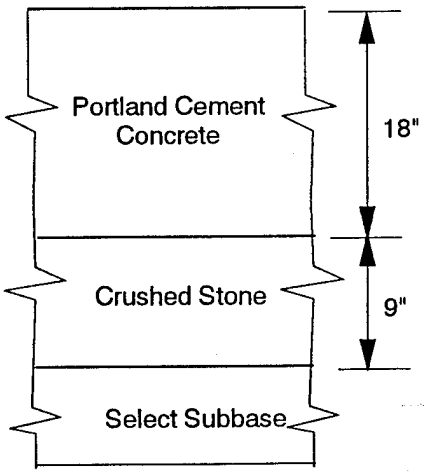

West Ramp 18-in. PCC (20-ft Joint Spacing)

FIGURE 38. CROSS SECTIONS OF PAVEMENT, MADISON (1 OF 2)

Dane County Regional Airport

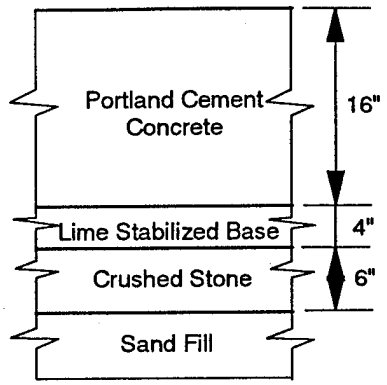

Runway 18-36 South End (25-ft Joint Spacing)

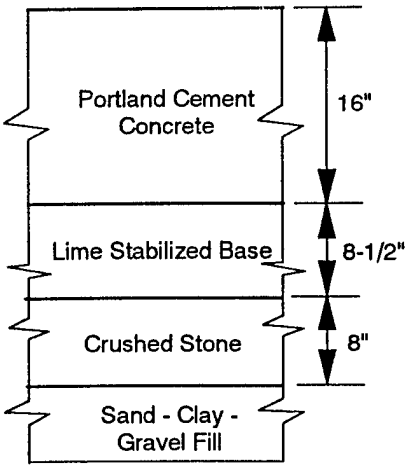

Runway 18-36 Interior (50-ft Joint Spacing)

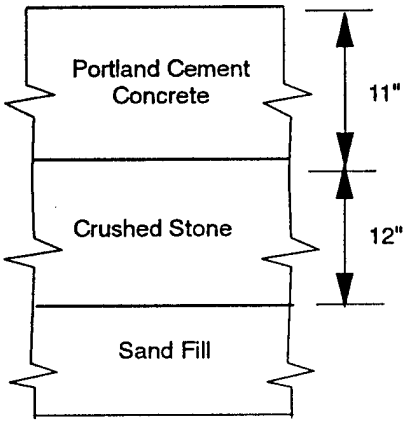

Runway 18-36 South End (25-ft Joint Spacing)

FIGURE 38. CROSS SECTIONS OF PAVEMENT, MADISON (2 OF 2)

The results of mid-slab testing at Madison is summarized in table 14. The means and COV's for the joint types tested from each feature are tabulated in table 15. The means are plotted on the bar charts presented in figures 39 and 40 for the low and high loads, respectively.

TABLE 14. RESULTS OF MIDSLAB TESTS, DANE COUNTY REGIONAL AIRPORT

	Area		ℓ		a/ℓ	
	Mean	COV	Mean	COV	Mean	COV
Airport Feature	in.	%	in.	%	in.	%
Runway 18-36, South End	31.0	1.9	37.8	8.8	0.158	9.0
Runway 18-36, Interior	31.2	3.4	40.0	18.9	0.152	17.1
Runway 18-36, North Overrun	31.2	2.2	39.0	11.3	0.153	11.1
West Ramp (16-inch PCC)	31.4	1.6	40.4	8.9	0.147	8.7
West Ramp (18-inch PCC)	32.3	1.7	47.3	12.3	0.126	11.2
Runway 13-31	31.4	2.0	40.2	11.2	0.148	10.9
Taxiway A	31.5	1.8	41.2	12.0	0.145	10.1

TABLE 15. SUMMARY OF RESULTS FROM JOINT EFFICIENCY TESTS, DANE COUNTY REGIONAL AIRPORT, 1993 WINTER DAY TESTS (1 OF 2)

			Joint Efficiency		Load Transfer, %	
Joint Type	Load	n	Mean	COV	Mean	COV
Runway 18-36, South End (16-in. PCC)						
Longitudinal Construction Hinged	Low	12	0.56	15.8	11.2	25.0
	High	12	0.56	13.9	11.1	22.1
Transverse Contraction Doweled	Low	12	0.75	16.8	18.8	17.2
	High	12	0.76	16.3	18.9	15.5
Transverse Contraction Doweled Corner	Low	12	0.68	4.9	15.1	9.1
	High	12	0.68	4.1	15.1	8.0
Runway 18-36, Interior (16-in. PCC over AC)						
Longitudinal Construction Hinged	Low	12	0.80	3.3	20.9	6.6
	High	12	0.79	6.6	20.6	12.3
Longitudinal Construction Hinged Corner	Low	12	0.80	2.4	21.2	4.7
	High	12	0.80	7.0	21.1	12.7
Transverse Crack (Reinforced)	Low	12	0.87	2.8	24.6	5.9
	High	12	0.88	1.7	25.4	3.6
Transverse Crack Corner (Reinforced)	Low	12	0.87	3.8	24.7	7.7
	High	12	0.87	4.4	25.1	8.6
Transverse Expansion Doweled	Low	6	0.84	3.4	23.0	6.6
	High	6	0.86	4.4	24.3	9.0
Transverse Expansion Doweled Corner	Low	6	0.79	9.9	20.5	19.7
	High	6	0.77	11.5	19.7	22.7
Transverse Contraction Doweled	Low	12	0.81	7.5	21.3	15.0
	High	12	0.81	8.6	20.9	17.9
Transverse Contraction Doweled Corner	Low	12	0.69	14.2	16.0	26.7
	High	12	0.70	12.1	16.5	23.5
Runway 18-36, North Overrun (11-in. PCC)						
Longitudinal Construction Hinged	Low	12	0.72	25.2	18.2	41.3
	High	12	0.75	18.9	19.4	33.4
Longitudinal Construction Hinged Corner	Low	12	0.89	6.2	27.0	16.7
	High	12	0.88	5.6	26.0	13.2
Transverse Contraction Doweled	Low	12	0.78	6.1	19.9	18.9
	High	12	0.75	15.9	18.9	25.1
Transverse Contraction Doweled Corner	Low	12	0.74	6.1	17.7	12.9
	High	12	0.74	6.3	18.0	13.1

TABLE 15. SUMMARY OF RESULTS FROM JOINT EFFICIENCY TESTS, DANE COUNTY REGIONAL AIRPORT, 1993 WINTER DAY TESTS (2 OF 2)

			Joint Efficiency		Load Transfer, %	
Joint Type	Load	n	Mean	COV	Mean	COV
Taxiway A						
Longitudinal Construction Hinged	Low		0.49	9.3	8.9	13.9
	High		0.46	10.3	8.1	16.4
Transverse Contraction Doweled	Low		0.53	6.9	10.2	9.9
	High		0.51	6.8	9.4	9.9
Transverse Expansion Doweled	Low		0.59	13.1	12.1	23.3
	High		0.54	21.9	10.6	34.4
Transverse Expansion Doweled Corner	Low		0.57	25.7	11.8	43.0
	High		0.56	23.3	11.2	37.0
Runway 13-31 (16-in. PCC)						
Longitudinal Construction Hinged	Low		0.39	16.6	6.1	29.0
	High		0.37	18.8	5.7	33.3
Longitudinal Construction Hinged Corner	Low		0.37	18.8	5.8	32.7
	High		0.37	19.7	5.6	34.7
Transverse Contraction Doweled	Low		0.82	2.7	22.0	5.4
	High		0.81	2.6	21.7	5.1
Transverse Contraction Doweled Corner	Low		0.67	11.0	14.8	20.3
	High		0.67	11.6	15.1	22.3
West Ramp (18-in. PCC)						
Longitudinal Construction Hinged	Low	12	0.69	12.7	15.7	25.1
	High	12	0.69	12.3	16.0	23.0
Longitudinal Construction Hinged Corner	Low	6	0.58	9.0	11.6	12.8
	High	6	0.61	11.4	12.7	16.5
Transverse Contraction Doweled	Low	12	0.71	7.2	16.7	14.7
	High	12	0.72	6.7	16.8	13.3
Transverse Contraction Doweled Corner	Low	6	0.65	8.3	13.8	15.0
	High	6	0.66	10.2	14.5	17.8
West Ramp (16-in. PCC)						
Longitudinal Construction Hinged	Low	12	0.85	3.1	23.6	6.3
	High	12	0.84	1.8	23.1	3.4
Transverse Contraction Doweled	Low	12	0.88	2.8	25.3	6.0
	High	12	0.86	1.8	24.3	3.6

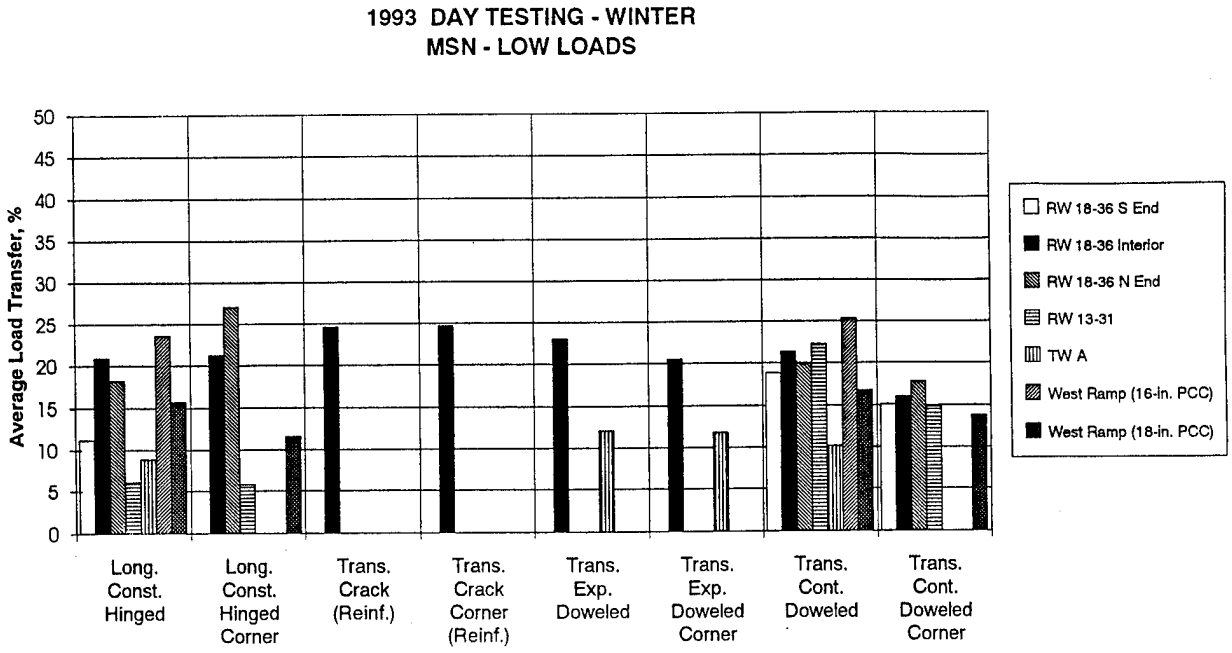

FIGURE 39. SUMMARY OF LOW-LOAD TESTS, MADISON

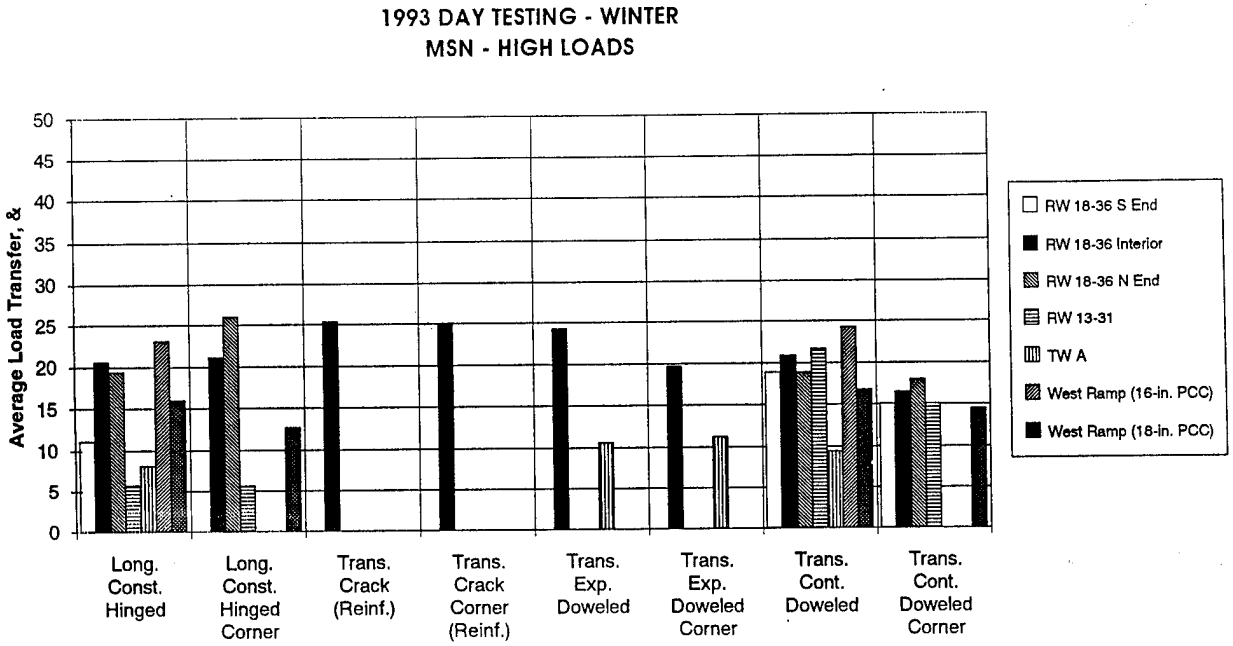

FIGURE 40. SUMMARY OF HIGH-LOAD TESTS, MADISON

ANALYSIS OF DATA

GENERAL.

Hundreds of individual pieces of data were collected at the four airports at which nondestructive field testing was conducted. Figure 41 is a histogram of the global mean values of load transfer considering all joint types, subgrade types, load levels, all types of features, both winter and summer conditions, day and night testing, etc. This histogram presents the frequency of occurrence of all 267 mean values of load transfer estimated in the testing program. It is apparent from the histogram that the global distribution of mean values is multimodal; therefore, a single probability distribution function will not adequately describe the distribution of the means. The range of the mean load transfer values is from 2 to 33 percent. Also, the distribution of the mean values of load transfer is widespread. For example the frequency of occurrence of values load transfer between approximately 10 and 27 percent are, with a few exceptions, greater than or equal to 10 occurrences. This translates to a probability of occurrence of greater than or equal to 0.037 for values of load transfer between 10 and 27 percent. Based upon the literature survey, this type of multimodal, widespread distribution of data was to be expected because of the many parameters that can affect load transfer across joints in a rigid pavement.

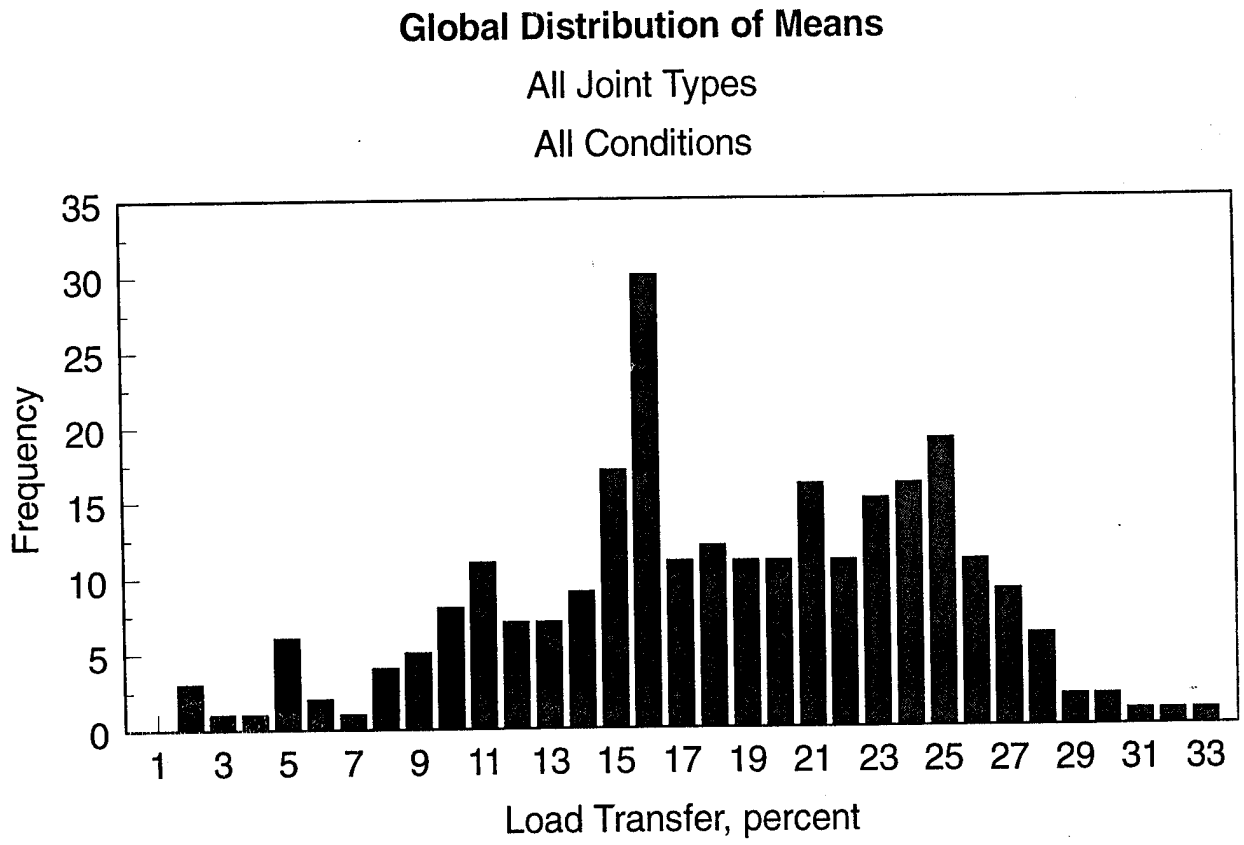

FIGURE 41. HISTOGRAM OF MEAN LOAD TRANSFER VALUES FOR ALL JOINT TYPES AND CONDITIONS

A parametric study was conducted using a paired t-test analysis to determine if there was a significant difference in load transfer values at the low- and high-load levels. Certain major categories of parameters (type of joint, type of subgrade, winter and summer tests) were selected to segregate the data into subsets that allowed a more meaningful analysis of the data. Probability distributions for each subset of data were proposed. These analyses are reported in this chapter.

PAIRED T-TEST ANALYSIS OF LOAD LEVELS.

As explained earlier, two drops of the mass of the HWD were conducted at each test station. The first drop was from the height required to produce a force of approximately 25,000 lb (called the "low-load" level), and the second drop was from the height required to produce a force of approximately 50,000 lb (called the "high-load" level). For both load levels, the joint efficiencies were calculated from the slab deflections in the manner described in chapter 4. The literature survey (Foxworthy 1985) suggested that there was not a significant difference in joint efficiency at load levels between 7,000 and 25,000 lb. Therefore, a fundamental question to be answered in the analysis of the data was the following: Is there a statistically significant difference in the joint efficiency measured at the low- and high-load levels for the data obtained as a part of this research? If so, then the data from the low- and high-load levels must be treated separately in the analysis.

Furthermore, as described in chapter 3, tests were conducted on each side of each joint to mitigate the possible effects of joint face skewing. Thus, another fundamental question to be answered by this research is the following: For the joints tested in this research program, is there a statistically significant difference in the joint efficiencies for tests conducted on either side of the same joint?

To test the statistical significance of the load level and the direction of test, a paired student's t-test analysis for the means was performed for each joint type on each feature at the four airports. This type of analysis tests whether means from two samples (here, low- and high-load levels) are distinct. The type of analysis chosen for this study does not assume that the variances of the two populations are equal.

To simplify the analysis, all joint types and conditions were compiled in a database along with the results of the student's t-test results.

The null hypotheses for these analyses were as follows: Ho_1: [Mean Low Loads East (or South) - Mean Low Loads West (or North)] = 0. That is, the direction of test is not significant at the low (25,000 lb) load level, Ho_2: [Mean Low Loads East (or South) - Mean Low Loads West (or North)] = 0. That is, the direction of test is not significant at the high (50,000 lb) load level, and Ho_3: [Mean Low Loads] - [Mean High Loads] = 0. That is, the load level is not significant.

All testing was conducted at the 0.05 percent significance level. This means that there is only a 5 percent probability of accepting a null hypothesis that is in reality false. For 99 joint types and conditions, there were data available for the high and low tests for t-test analysis. These results are summarized in table 16.

TABLE 16. SUMMARY OF PAIRED T-TEST ANALYSES FOR JOINT TYPES/CONDITIONS

Accept Ho_1?	Accept Ho_2?	Accept Ho_3?	Number of Means	Percentage of Total
Yes	Yes	Yes	63	64
No	Yes	Yes	4	4
Yes	No	Yes	3	3
Yes	Yes	No	4	4
No	No	Yes	15	15
No	Yes	No	4	4
Yes	No	No	4	4
No	No	No	2	2

These analyses clearly show that for 86 percent of the cases, the null hypothesis Ho_3 cannot be rejected at the 0.05 significance level; that is, of the joint types and conditions tested, for approximately 5 out of 6 joints there is no statistically significant difference in joint efficiency between tests conducted at 25,000 and 50,000 lb.

For 75 percent of the cases, the null hypothesis Ho_1 could not be rejected at the 0.05 significance level. This means that for fully 3 out of 4 of the joint types and conditions tested there was no statistically significant difference in tests conducted on each side of the same joint at the low-load level (25,000 lb). Similarly, for 76 percent of the cases, the null hypothesis Ho_2 could not be rejected at the 0.05 significance level. In other words, for over 3 out of 4 of the joint types and conditions tested, there was no significant difference in tests conducted on each side of the same joint at the high-load level (50,000 lb).

PROBABILITY DISTRIBUTION FUNCTIONS.

Because joint load transfer is stochastic, it is desirable to determine probability distributions for each joint type and condition. Due to the large numbers of tests conducted and the rigor of the analysis required to develop probability distributions considering each individual measurement, probability distributions were developed for the mean values where there were at least six means available for developing this distribution.

The probability distributions given in this report are beta distributions. The beta distribution (Harr 1987) is defined over the range $[a, b]$ by the function

$$f(x) = C(x - a)^{\alpha}(b - x)^{\beta} \qquad (7)$$

where a > -1 and b > -1. The constant C is given by the relationship

$$C = \frac{(\alpha + \beta + 1)!}{\alpha!\beta!(b - a)^{\alpha + \beta + 1}} \tag{8}$$

Knowing the mean value, standard deviation, and minimum and maximum values, the beta distribution is uniquely determined for a set of data. Furthermore, it has been shown by Harr (1987) that this distribution satisfies the *principle of maximum entropy* for data in which the mean, standard deviation, and range is known; therefore, the beta distribution results in the least biased assignment of probabilities for the data.

Using the methods set forth by Harr (1987), beta distributions were assigned to each of the sets of means for which there were 6 or more means available. Table 17 gives the parameters for each joint type and condition. In figures 42 through 51 plots of the beta distributions for each joint type and condition are shown. For purposes of comparison, the mean values of the joint types and conditions for which there were less than 6 means are also plotted on the figures.

Of particular interest is the influence of the season on load transfer. This influence can be observed in the doweled transverse contraction joints (figure 42). From this figure, it can be readily observed that the effects of season are twofold: load transfer is significantly reduced during winter conditions as compared to summer conditions, and load transfer is more erratic (more scatter or dispersion of data) in winter months as compared to summer conditions. This difference is likely due to the tighter joints during the warmer summer conditions leading to increased aggregate interlock at the joint. A similar influence may be observed for the mean value for keyed longitudinal construction joints with no tie (figure 50) and for keyed and tied longitudinal construction joints (figure 51). However, due to lack of data, no conclusion can be drawn about the dispersion of the means for the latter two joint types.

It also appears from the data that nonstabilized bases tend to result in high load transfer as compared to identical joints in pavements on stabilized bases under similar conditions (figures 42 and 50). It is generally believed that aggregate interlock forces can be modeled as a spring; therefore, the resistance to motion provided by aggregate interlock is proportional to the deflection of the joint. Nonstabilized bases allow greater deflections than stabilized bases, thus giving rise to more aggregate interlock or dowel resistance effectively increasing the load transfer at the joint.

TABLE 17. BETA DISTRIBUTION PARAMETERS

			Beta Distribution Input Parameters					
Joint Type	Subgrade Type	Season	Mean	Std. Deviation	a	b	α	β
Transverse Contraction Dowel	Stabilized	Winter	14.7	5.3	0.0	34.0	2.85	4.06
Transverse Contraction Dowel	Non-Stabilized	Winter	19.9	5.7	2.8	34.0	2.53	1.91
Transverse Contraction Dowel	Stabilized	Summer	28.1	2.0	15.0	34.0	11.70	4.72
Transverse Contraction Reinforced	Stabilized	Winter	21.6	4.6	7.5	32.0	2.49	1.57
Transverse Crack Reinforced	Stabilized	Winter	23.1	4.3	10.1	32.0	2.09	1.11
Longitudinal Construction Dowel	Stabilized	Winter	18.6	4.6	4.7	34.0	3.26	3.72
Longitudinal Construction Tied	Stabilized	Winter	15.9	4.92	0.0	30.0	3.38	2.88
Longitudinal Construction Keyed - No Tie	Stabilized	Winter	15.5	5.8	2.0	32.9	1.62	2.37
Longitudinal Construction Keyed - No Tie	Non-Stabilized	Winter	23.6	2.3	19.0	30.0	0.88	1.62
Longitudinal Construction Keyed and Tied	Stabilized	Winter	20.2	4.1	7.8	32.6	3.02	3.02
Longitudinal Contraction Reinforced	Stabilized	Winter	18.2	2.0	8.0	30.0	12.72	14.86

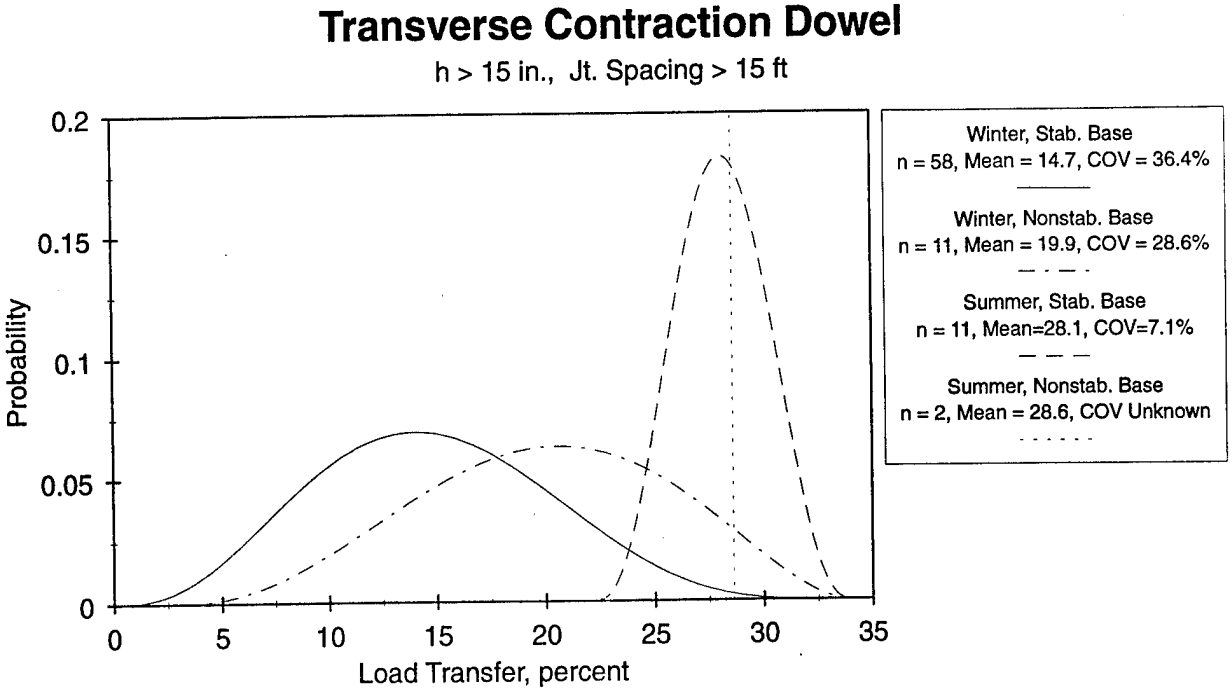

FIGURE 42. PROBABILITY DISTRIBUTION FUNCTIONS, DOWELED TRANSVERSE CONTRACTION JOINTS, H > 15 IN., JOINT SPACING > 15 FT

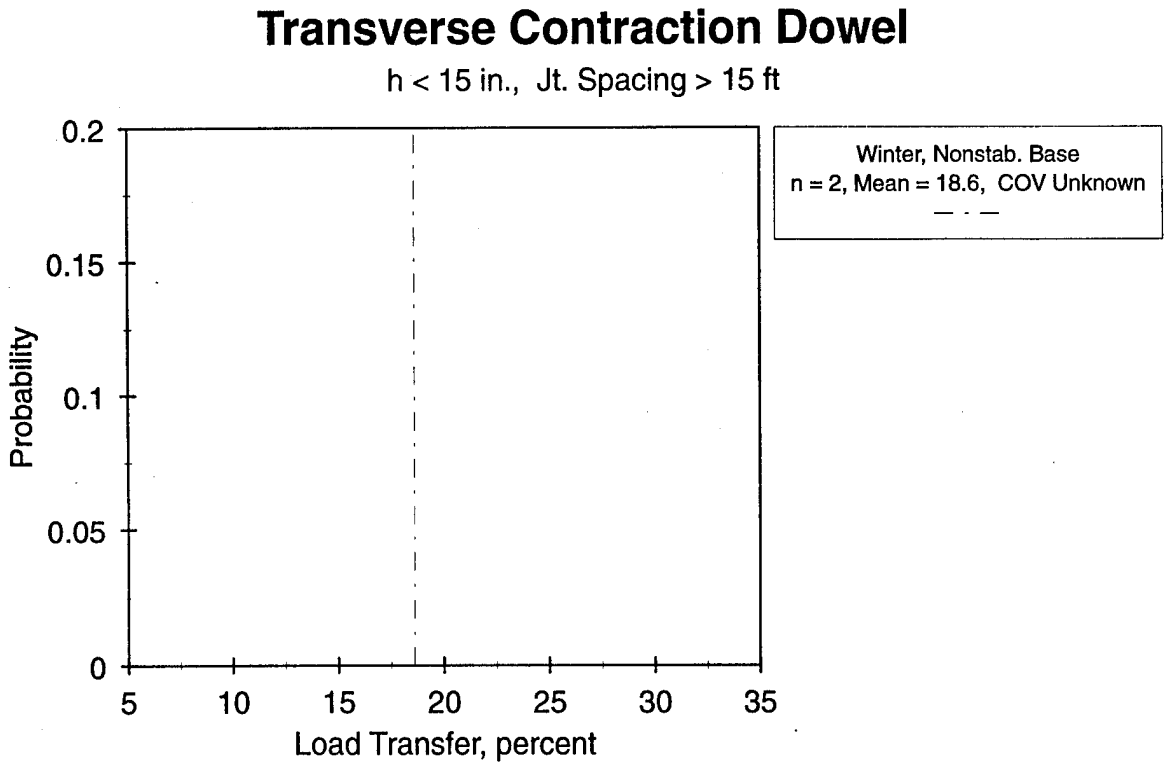

FIGURE 43. PROBABILITY DISTRIBUTION FUNCTIONS, DOWELED TRANSVERSE CONTRACTION JOINTS, H < 15 IN., JOINT SPACING > 15 FT

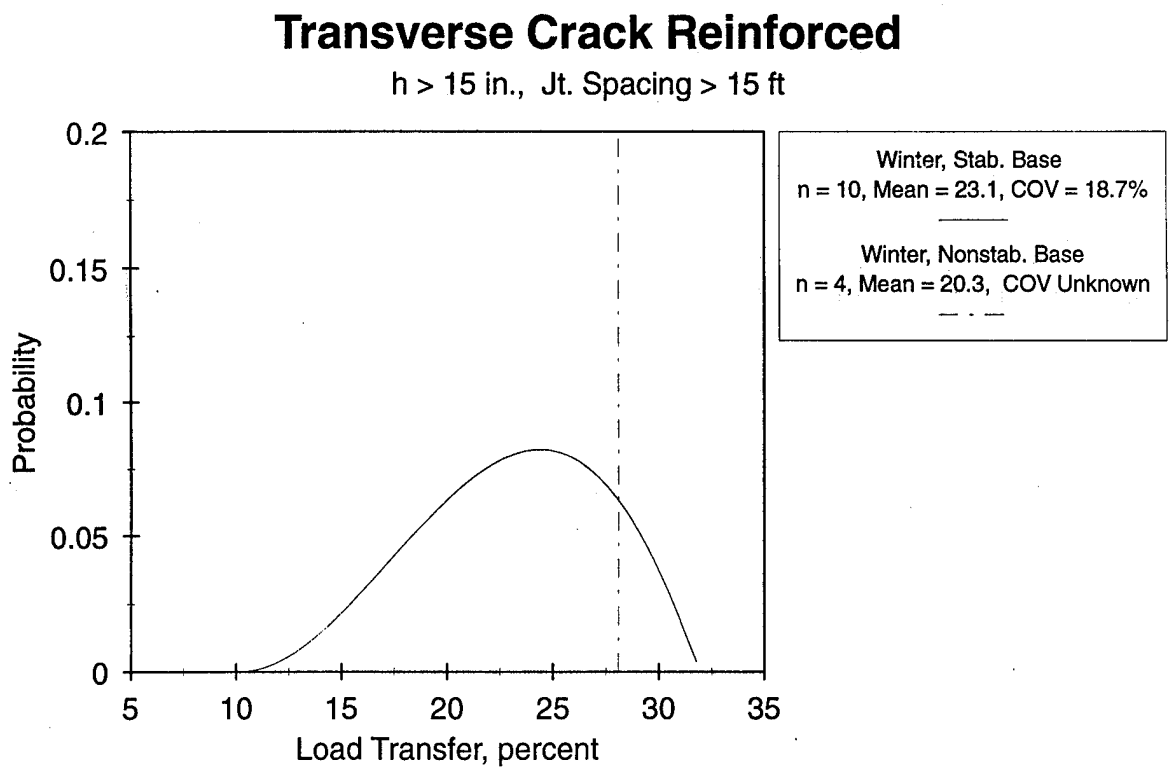

FIGURE 44. PROBABILITY DISTRIBUTION FUNCTIONS, TRANSVERSE CRACKS , H > 15 IN., JOINT SPACING > 15 FT

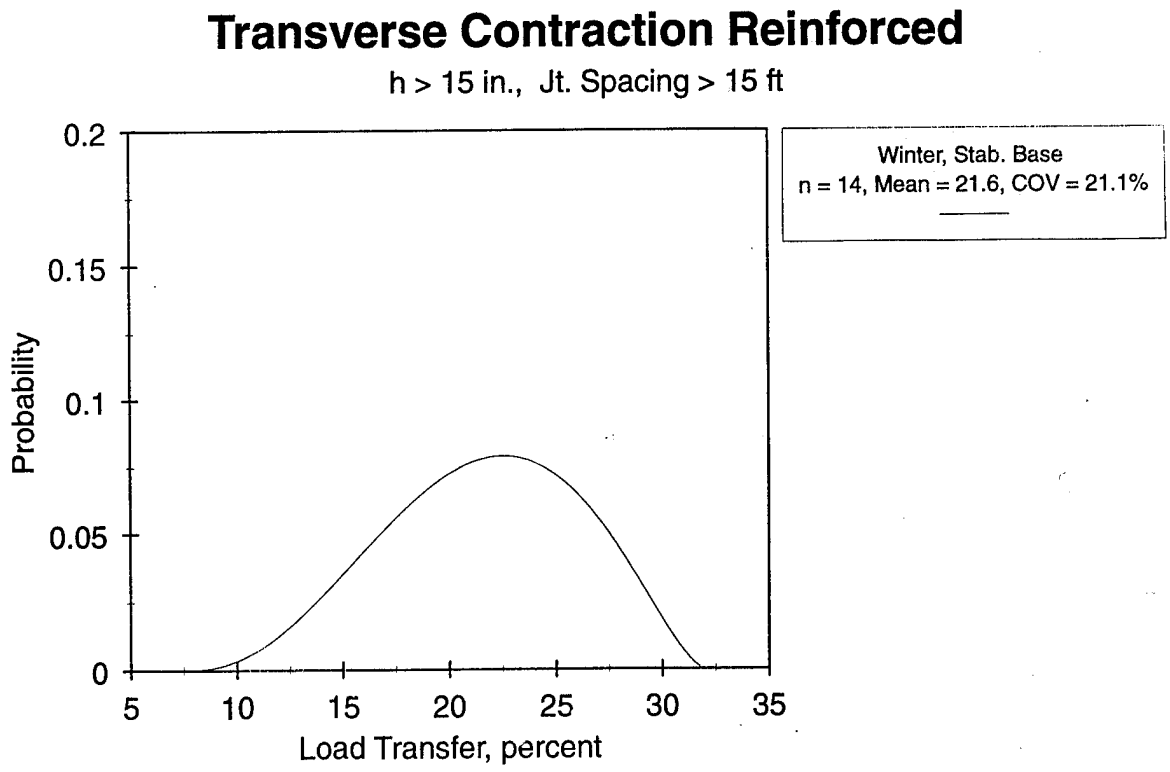

FIGURE 45. PROBABILITY DISTRIBUTION FUNCTIONS, TRANSVERSE CONTRACTION JOINTS, H > 15 IN., JOINT SPACING > 15 FT

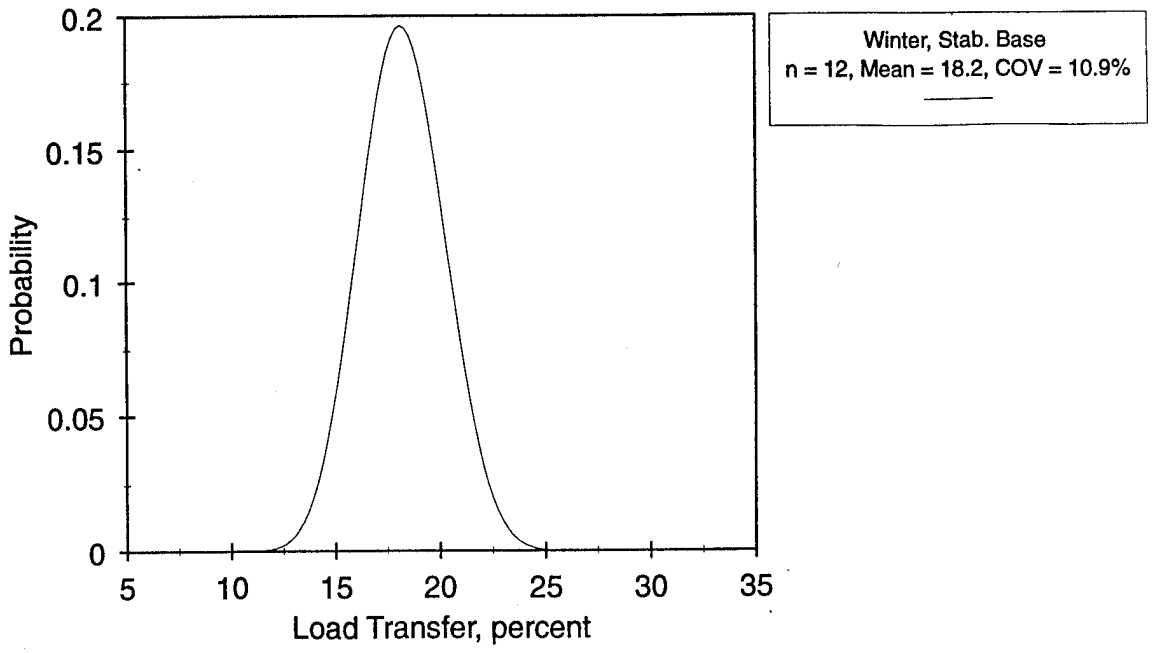

FIGURE 46. PROBABILITY DISTRIBUTION FUNCTIONS, LONGITUDINAL CONTRACTION JOINTS, H > 15 IN., JOINT SPACING > 15 FT

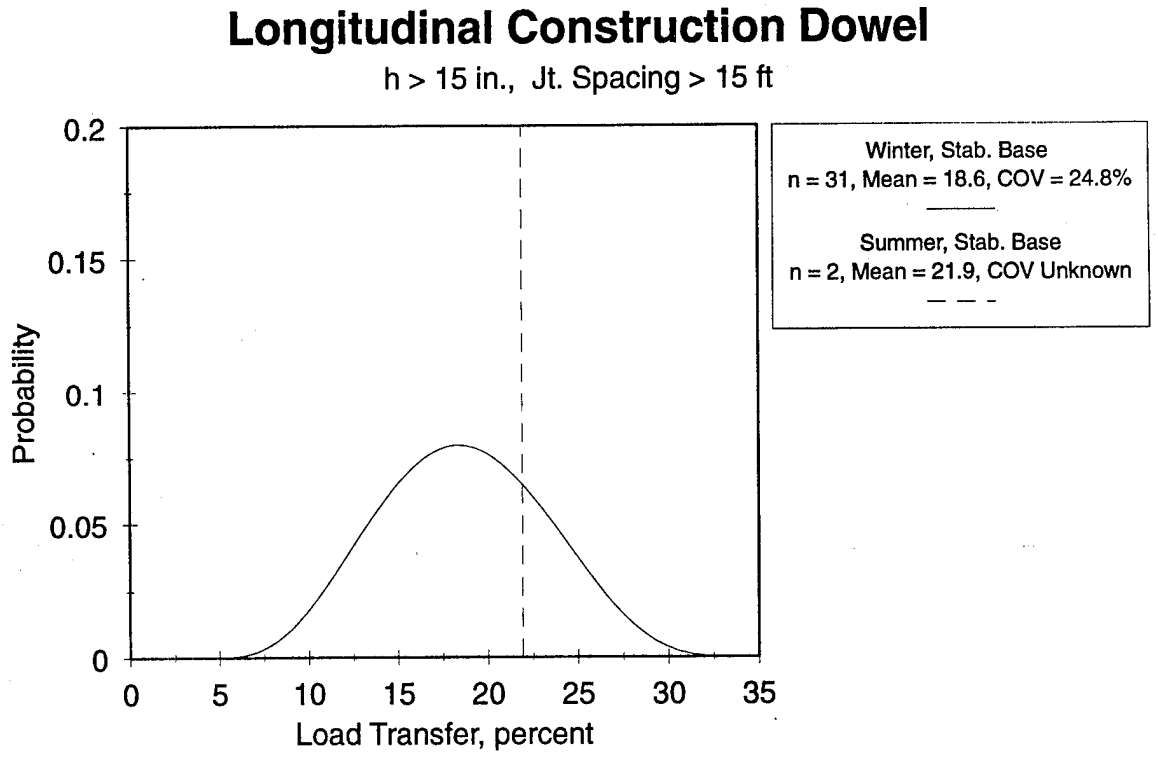

FIGURE 47. PROBABILITY DISTRIBUTION FUNCTIONS, DOWELED LONGITUDINAL CONSTRUCTION JOINTS, H > 15 IN., JOINT SPACING > 15 FT

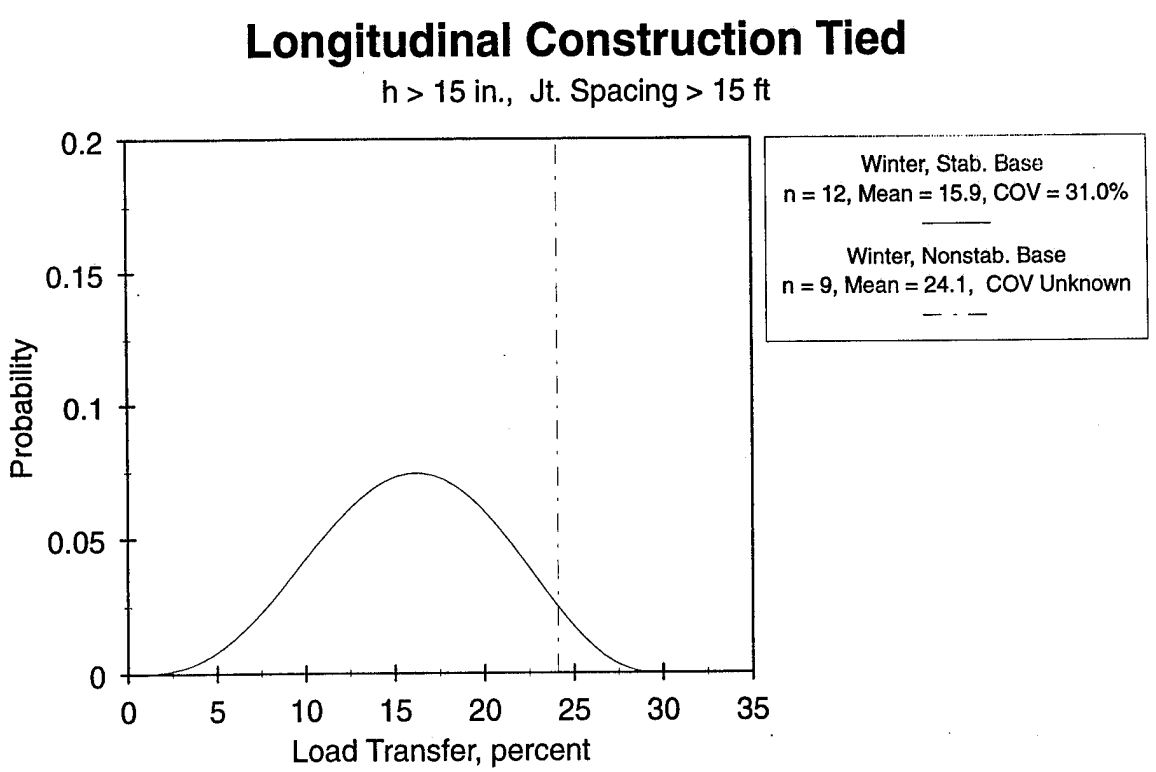

FIGURE 48. PROBABILITY DISTRIBUTION FUNCTIONS, TIED LONGITUDINAL CONSTRUCTION JOINTS, H > 15 IN., JOINT SPACING > 15 FT

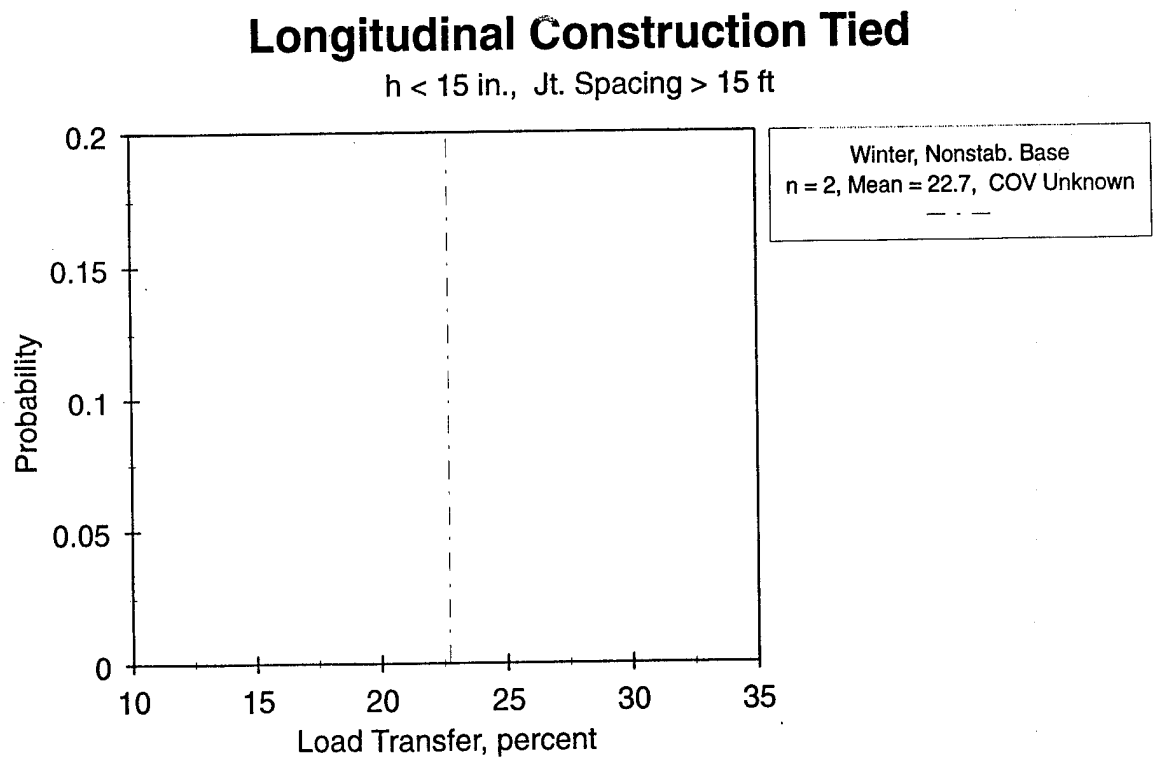

FIGURE 49. PROBABILITY DISTRIBUTION FUNCTIONS, TIED LONGITUDINAL CONSTRUCTION JOINTS, H < 15 IN., JOINT SPACING > 15 FT

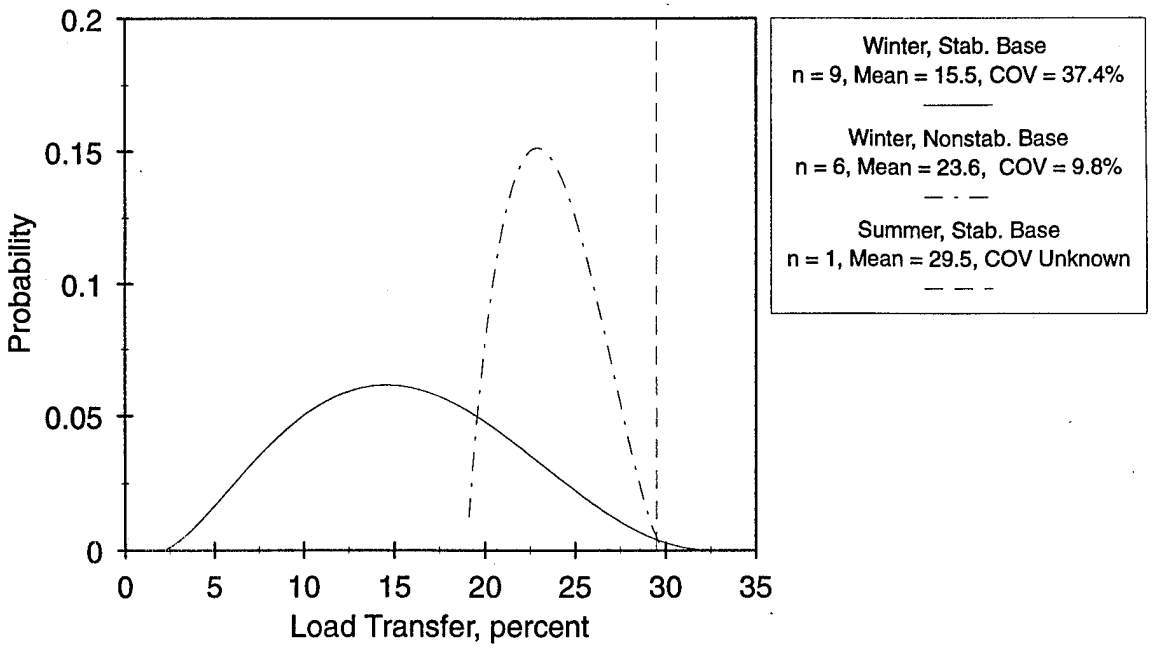

FIGURE 50. PROBABILITY DISTRIBUTION FUNCTIONS, KEYED LONGITUDINAL CONSTRUCTION JOINTS, H > 15 IN., JOINT SPACING > 15 FT

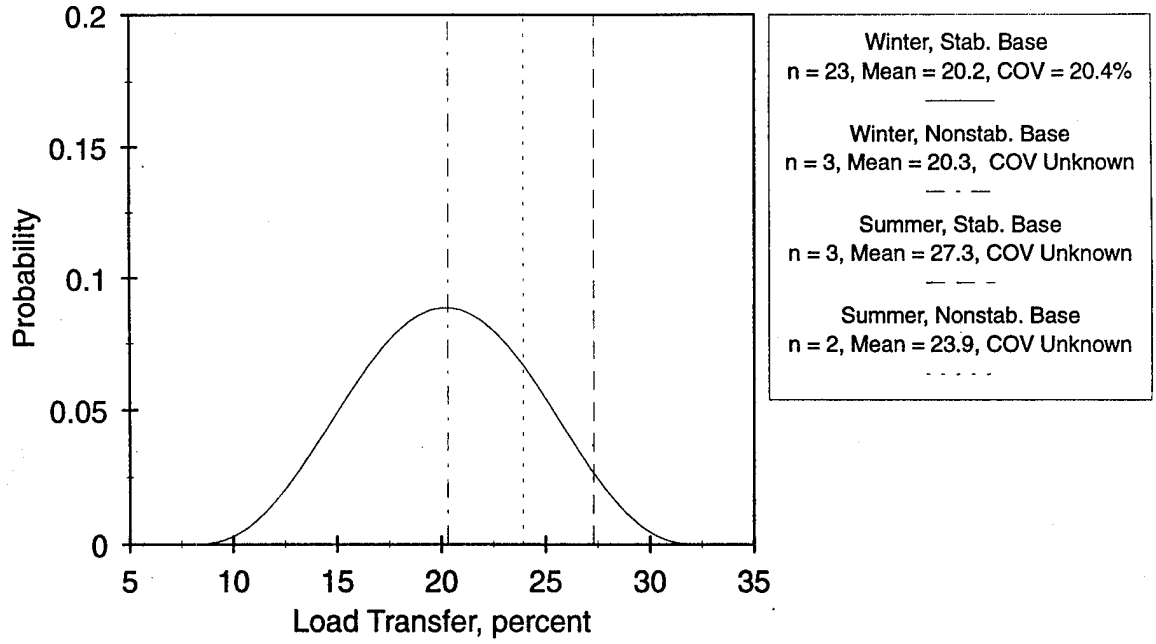

FIGURE 51. PROBABILITY DISTRIBUTION FUNCTIONS, KEYED AND TIED LONGITUDINAL CONSTRUCTION JOINTS, H > 15 IN., JOINT SPACING > 15 FT

To further evaluate the applicability of the beta distribution to represent the distribution of the observed means, the beta distributions were used to predict the frequency of occurrence of load transfer values in intervals of 5 percent. The histograms shown in figures 52 through 62 show the observed frequencies as well as those predicted by the beta distributions for the various joint types and conditions. As can be seen in the figures, the frequencies of occurrence predicted by the selected beta distributions are in good agreement with the frequencies observed in the tests.

Cumulative probability distribution functions for the various joint types and conditions have been plotted in figures 63 through 70. The cumulative probability is the probability that one would observe a mean value x (in this case, load transfer) will be less than or equal to some value X. On these plots, two particular values have been highlighted with dashed lines. The first is the value of load transfer associated with a cumulative probability of 10 percent. Stated differently, there is a 90 percent probability that the mean value of load transfer will exceed the indicated value on the abscissa of the plot. It can be observed from the figures that this value of load transfer is in the range of 10 to 20 percent for most joint types and conditions.

The second indicated value on the cumulative probability distribution function is the probability associated with 25 percent load transfer. The ordinate associated with this value is the probability of observing a mean value of load transfer less than or equal to 25 percent. It can also be readily seen from figures 63 through 70 that the likelihood of observing mean values of load transfer less than or equal to 25 percent ranges from 60 to 100 percent.

INFLUENCE OF LOAD TRANSFER ON PAVEMENT LIFE AND DESIGN.

The reduction of Westergaard's edge stress by the percentage load transfer is fundamental to the FAA rigid pavement design procedure. The calculated influence of load transfer on pavement life in the FAA design procedure is graphically illustrated in figure 71 for one particular case. Figure 71 is not intended as a design chart, but rather as a tool to discuss the role load transfer plays in life of the pavement. For the pavement design parameters listed in figure 71, 25 percent load transfer results in 100 percent of the design coverages until failure. Using these assumptions, it can be readily seen that the coverages to failure drop off rapidly with decreasing load transfer. For example at 10 percent load transfer the coverages to failure have decreased to 10 percent of their value at 25 percent load transfer. Therefore, it can be concluded that load transfer has a profound influence on pavement life.

Figure 72 illustrates the influence of load transfer on pavement thickness in a design calculation. This plot was developed by calculating the thickness required to achieve a design factor equivalent to 100 percent design coverages until failure in figure 71. (Note that at 25 percent load transfer, the required pavement thickness is 12 in.) If one assumes the load transfer to be 10 percent, the pavement thickness required to achieve an equivalent design factor is approximately 13.25 in.

Figures 71 and 72 illustrate the tradeoffs between pavement thickness and coverages until failure. If one designs a pavement assuming 25 percent load transfer and the actual value of load transfer is somewhat less, the pavement life will be significantly reduced. However, if one assumes a more realistic value of load transfer based upon the results of these analyses, the pavement thickness to achieve the required design factor will increase.

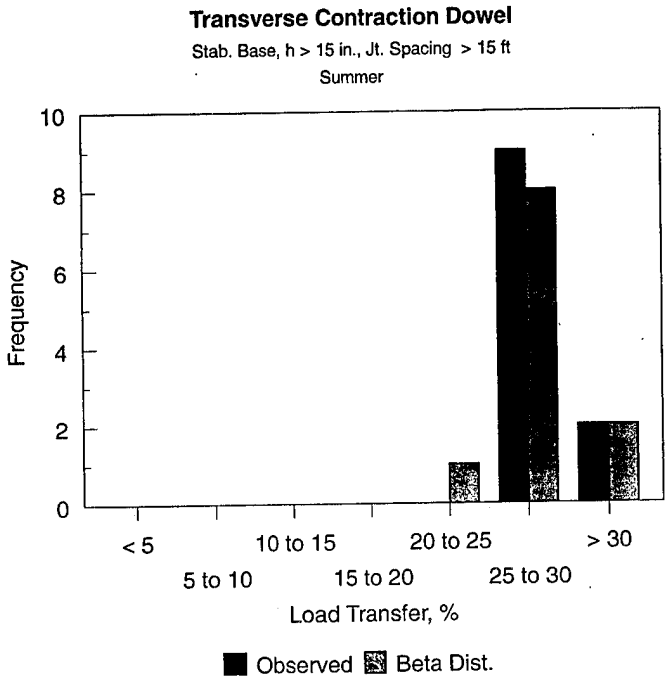

FIGURE 52. HISTOGRAM OF OBSERVED AND PREDICTED MEAN VALUES, DOWELED TRANSVERSE CONTRACTION JOINTS, STABILIZED BASE, SUMMER CONDITIONS, H > 15 IN., JOINT SPACING > 15 FT

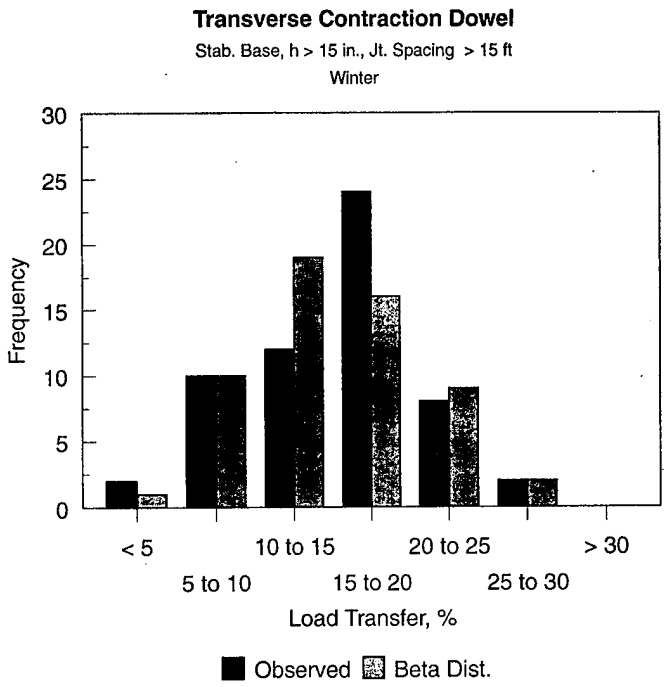

FIGURE 53. HISTOGRAM OF OBSERVED AND PREDICTED MEAN VALUES, DOWELED TRANSVERSE CONTRACTION JOINTS, STABILIZED BASE, WINTER CONDITIONS, H > 15 IN., JOINT SPACING > 15 FT

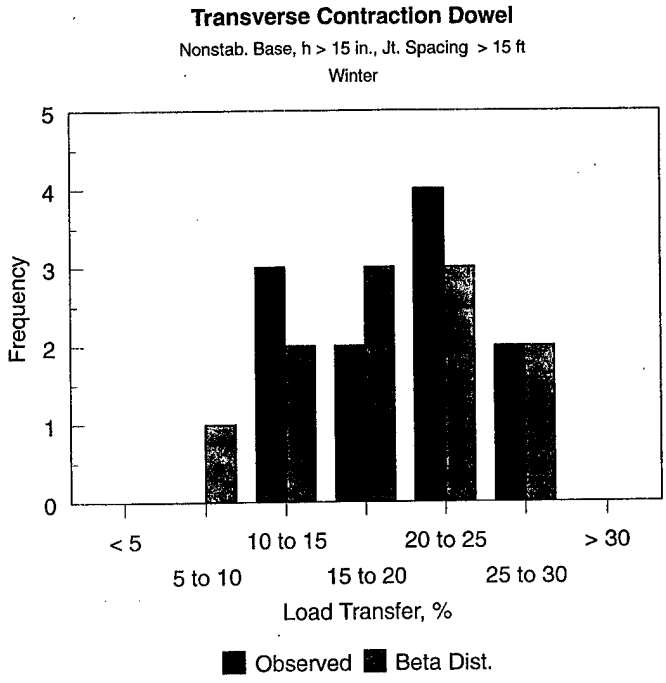

FIGURE 54. HISTOGRAM OF OBSERVED AND PREDICTED MEAN VALUES, DOWELED TRANSVERSE CONTRACTION JOINTS, NONSTABILIZED BASE, WINTER CONDITIONS, H > 15 IN., JOINT SPACING > 15 FT

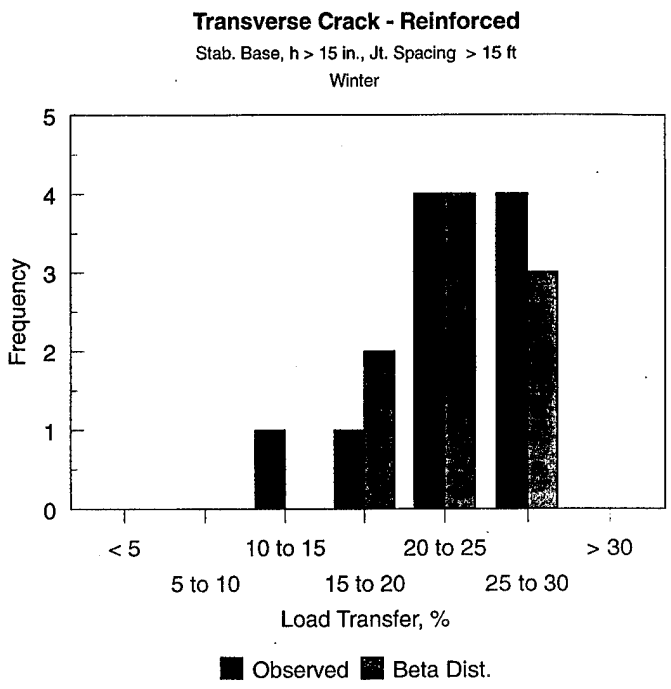

FIGURE 55. HISTOGRAM OF OBSERVED AND PREDICTED MEAN VALUES, TRANSVERSE CRACKS, STABILIZED BASE, WINTER CONDITIONS, H > 15 IN., JOINT SPACING > 15 FT

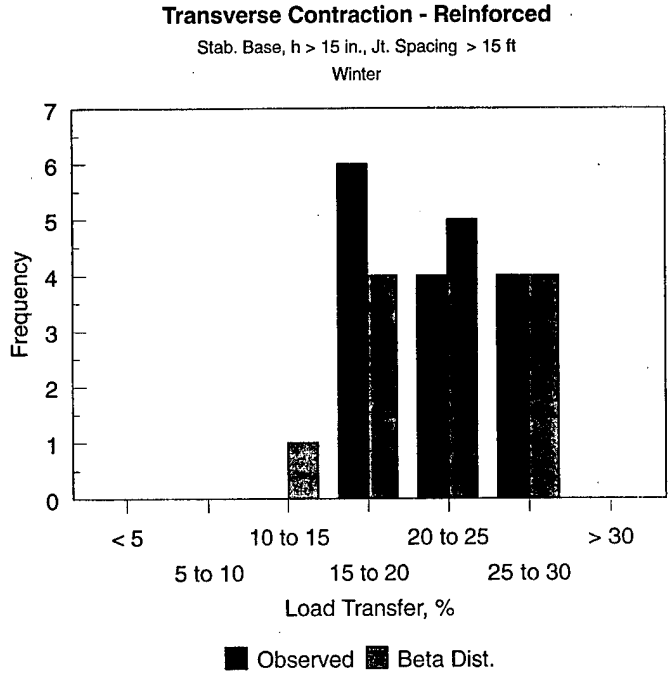

FIGURE 56. HISTOGRAM OF OBSERVED AND PREDICTED MEAN VALUES, TRANSVERSE CONTRACTION JOINTS, STABILIZED BASE, WINTER CONDITIONS, H > 15 IN., JOINT SPACING > 15 FT

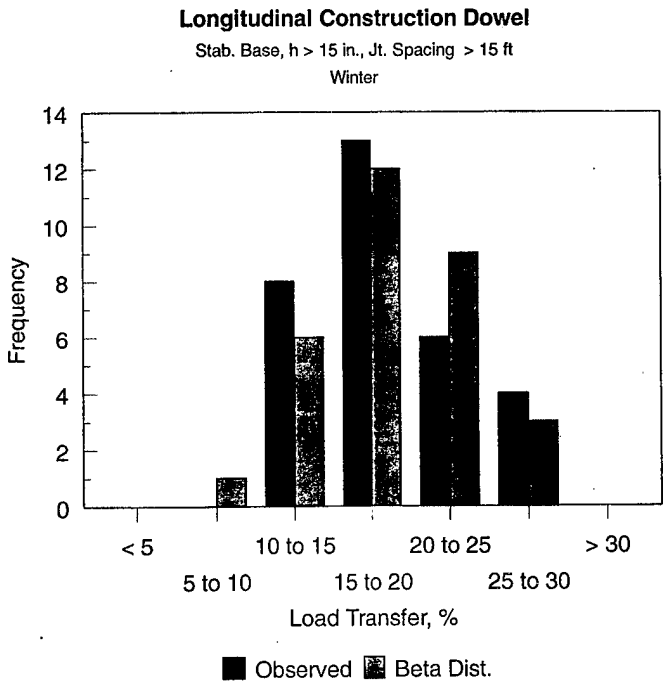

FIGURE 57. HISTOGRAM OF OBSERVED AND PREDICTED MEAN VALUES, DOWELED LONGITUDINAL CONSTRUCTION JOINTS, STABILIZED BASE, WINTER CONDITIONS, H > 15 IN., JOINT SPACING > 15 FT

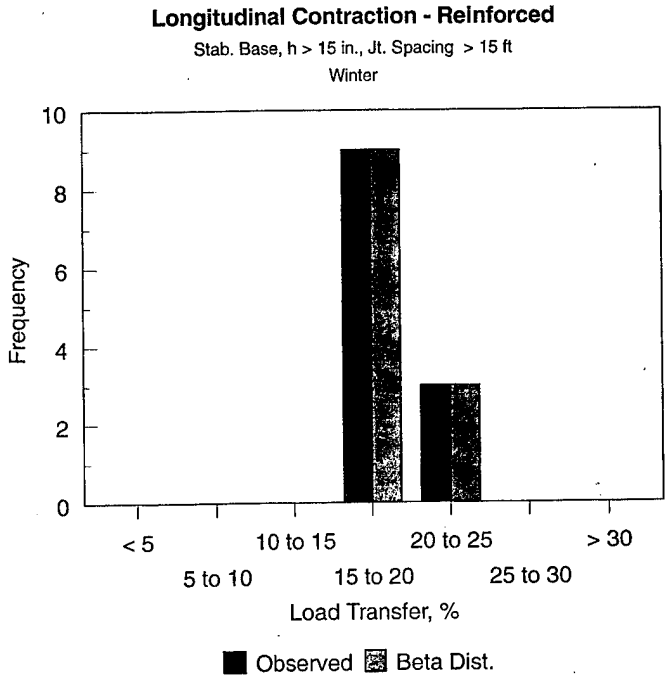

FIGURE 58. HISTOGRAM OF OBSERVED AND PREDICTED MEAN VALUES, LONGITUDINAL CONTRACTION JOINTS, STABILIZED BASE, WINTER CONDITIONS, H > 15 IN., JOINT SPACING > 15 FT

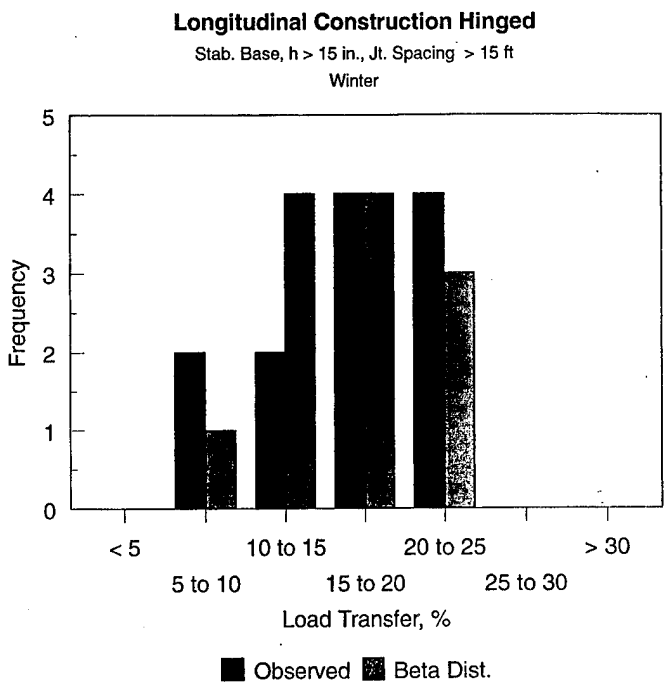

FIGURE 59. HISTOGRAM OF OBSERVED AND PREDICTED MEAN VALUES, HINGED LONGITUDINAL CONSTRUCTION JOINTS, STABILIZED BASE, WINTER CONDITIONS, H > 15 IN., JOINT SPACING > 15 FT

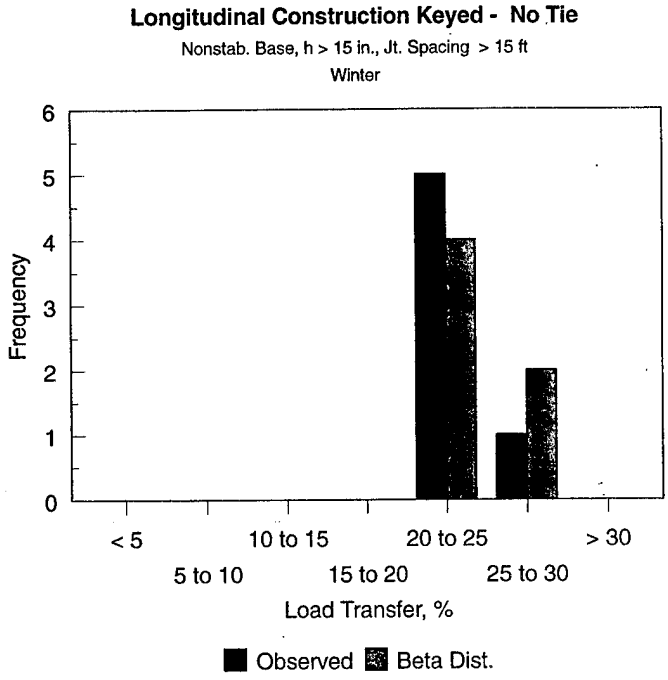

FIGURE 60. HISTOGRAM OF OBSERVED AND PREDICTED MEAN VALUES, KEYED LONGITUDINAL CONSTRUCTION JOINTS, NONSTABILIZED BASE, WINTER CONDITIONS, H > 15 IN., JOINT SPACING > 15 FT

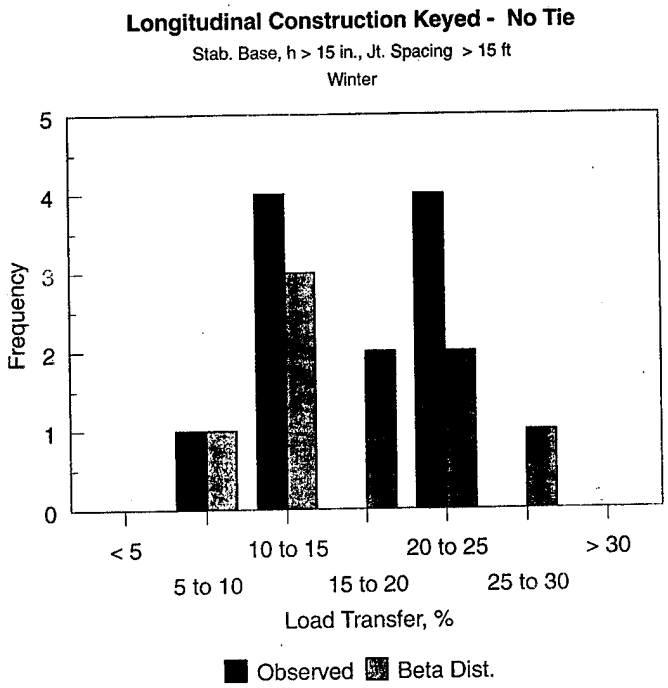

FIGURE 61. HISTOGRAM OF OBSERVED AND PREDICTED MEAN VALUES, KEYED LONGITUDINAL CONSTRUCTION JOINTS, STABILIZED BASE, WINTER CONDITIONS, H > 15 IN., JOINT SPACING > 15 FT

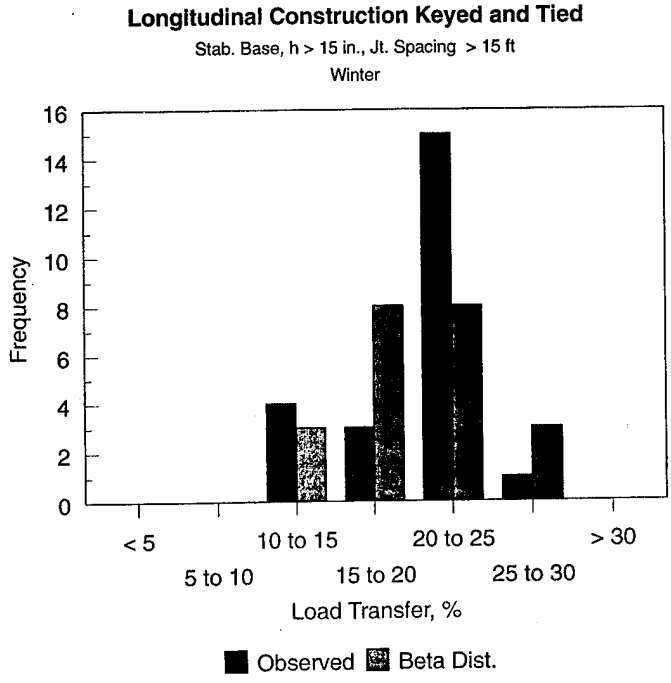

FIGURE 62. HISTOGRAM OF OBSERVED AND PREDICTED MEAN VALUES, KEYED AND TIED LONGITUDINAL CONSTRUCTION JOINTS, STABILIZED BASE, WINTER CONDITIONS, H > 15 IN., JOINT SPACING > 15 FT

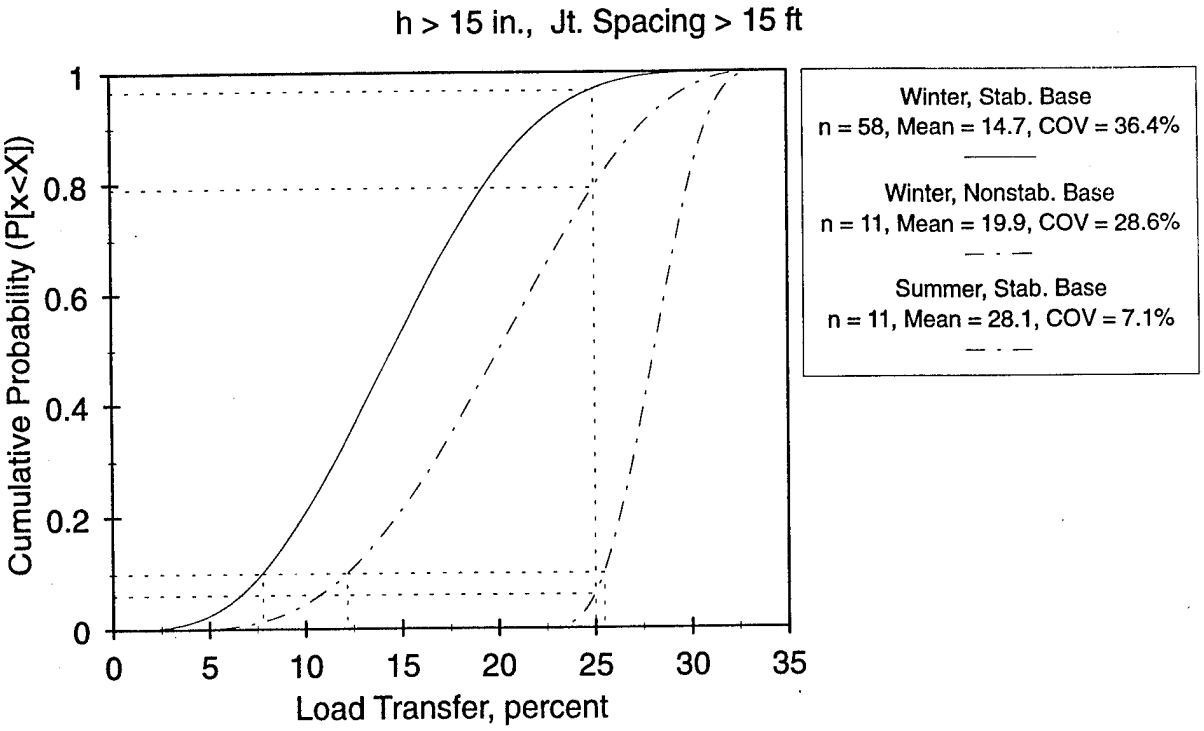

FIGURE 63. CUMULATIVE PROBABILITY DISTRIBUTION FUNCTIONS, DOWELED TRANSVERSE CONTRACTION JOINTS, H > 15 IN., JOINT SPACING > 15 FT

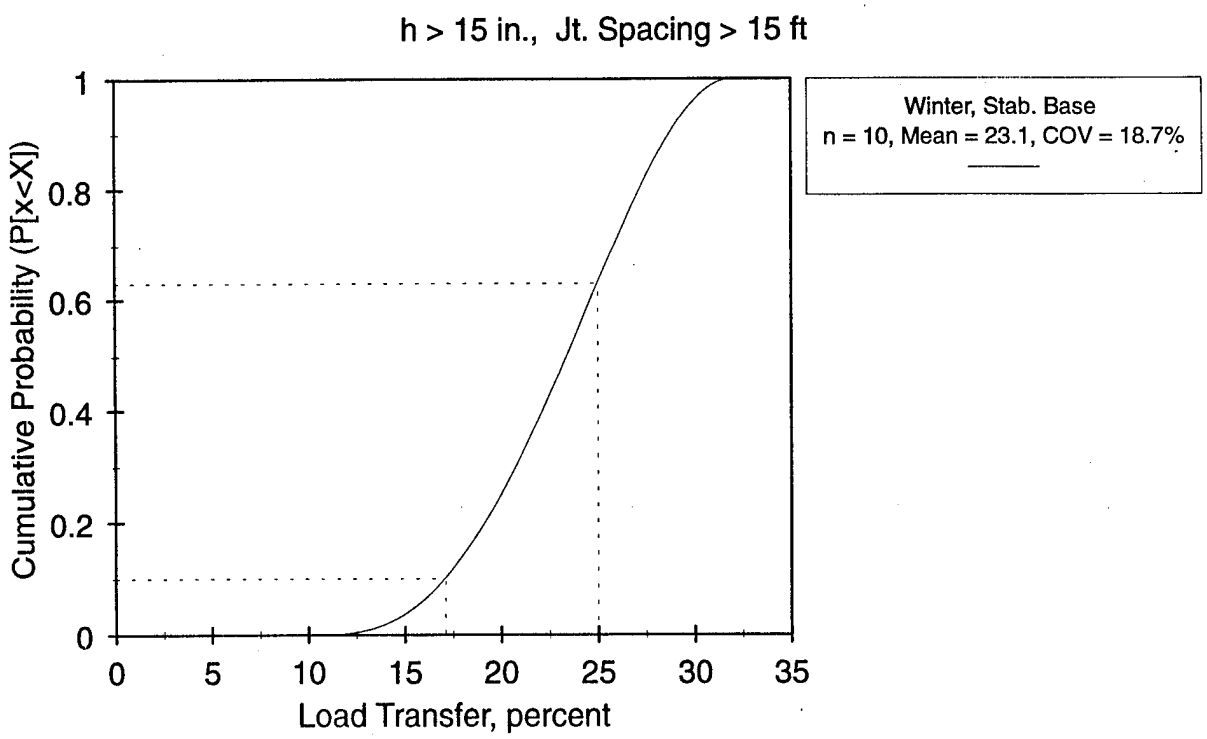

FIGURE 64. CUMULATIVE PROBABILITY DISTRIBUTION FUNCTIONS, TRANSVERSE CRACKS, H > 15 IN., JOINT SPACING > 15 FT

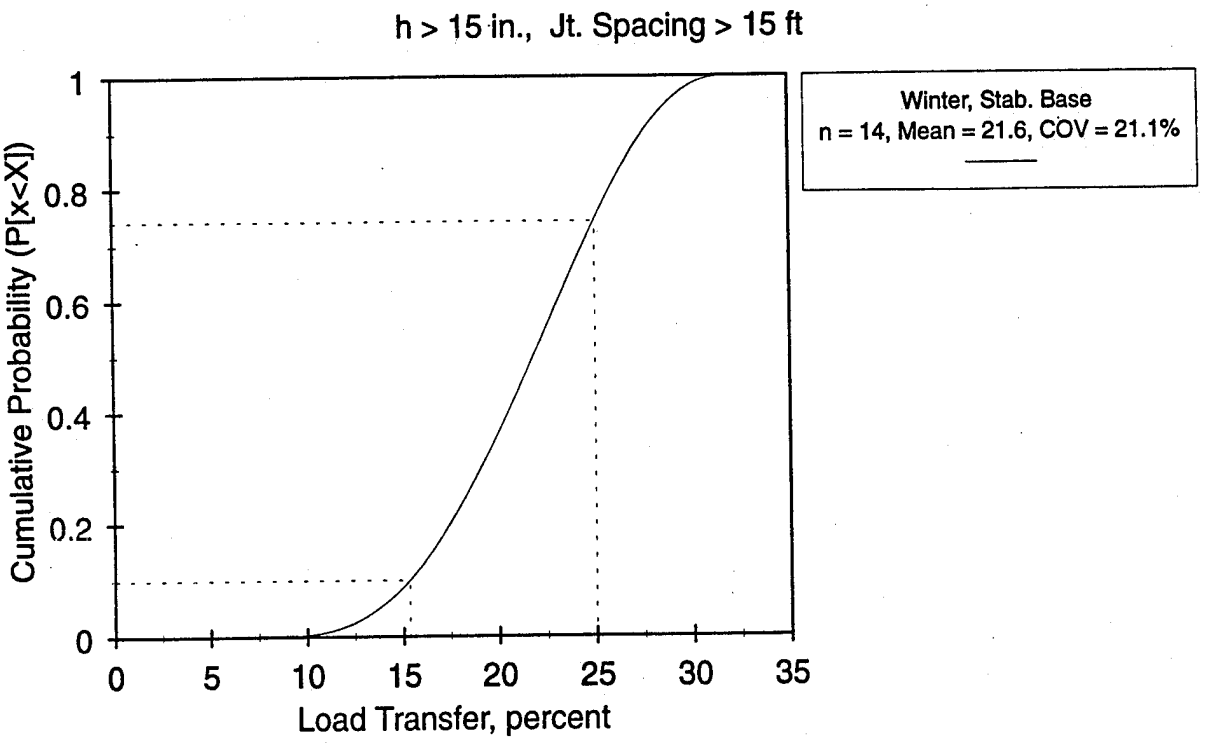

FIGURE 65. CUMULATIVE PROBABILITY DISTRIBUTION FUNCTIONS, TRANSVERSE CONTRACTION JOINTS, H > 15 IN., JOINT SPACING > 15 FT

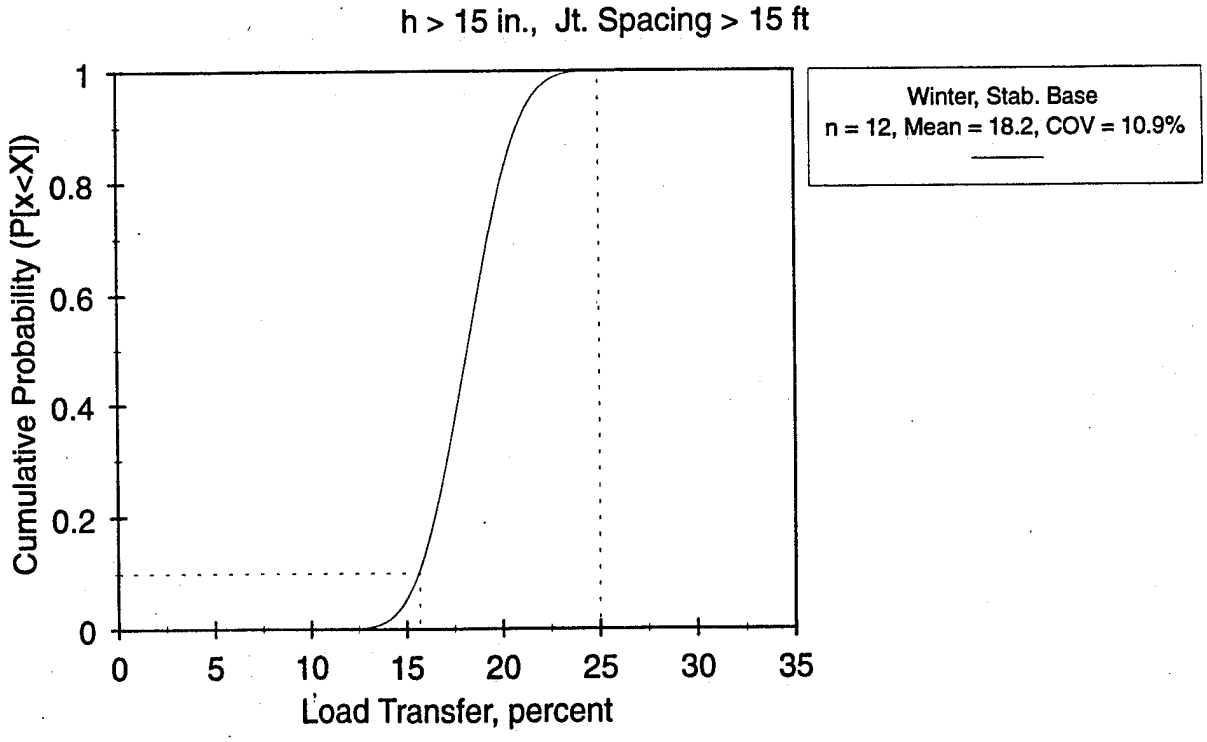

FIGURE 66. CUMULATIVE PROBABILITY DISTRIBUTION FUNCTIONS, LONGITUDINAL CONSTRUCTION JOINTS, H > 15 IN., JOINT SPACING > 15 FT

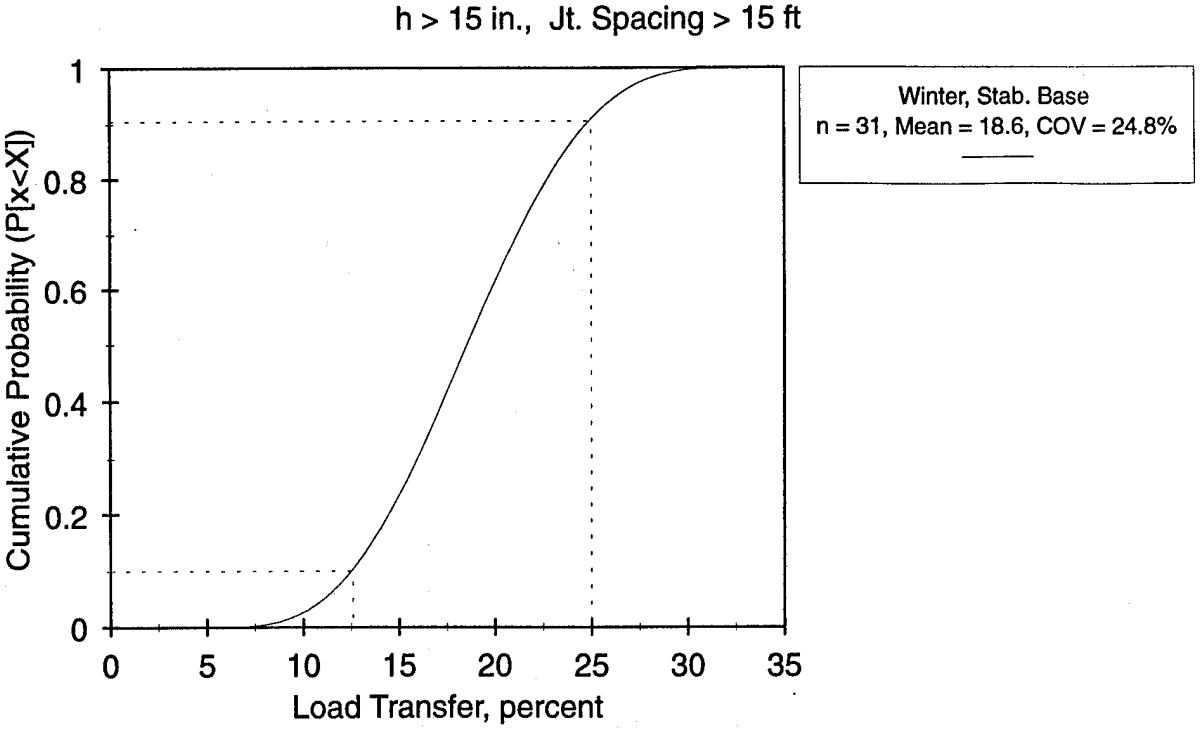

FIGURE 67. CUMULATIVE PROBABILITY DISTRIBUTION FUNCTIONS, DOWELED LONGITUDINAL CONSTRUCTION JOINTS, H > 15 IN., JOINT SPACING > 15 FT

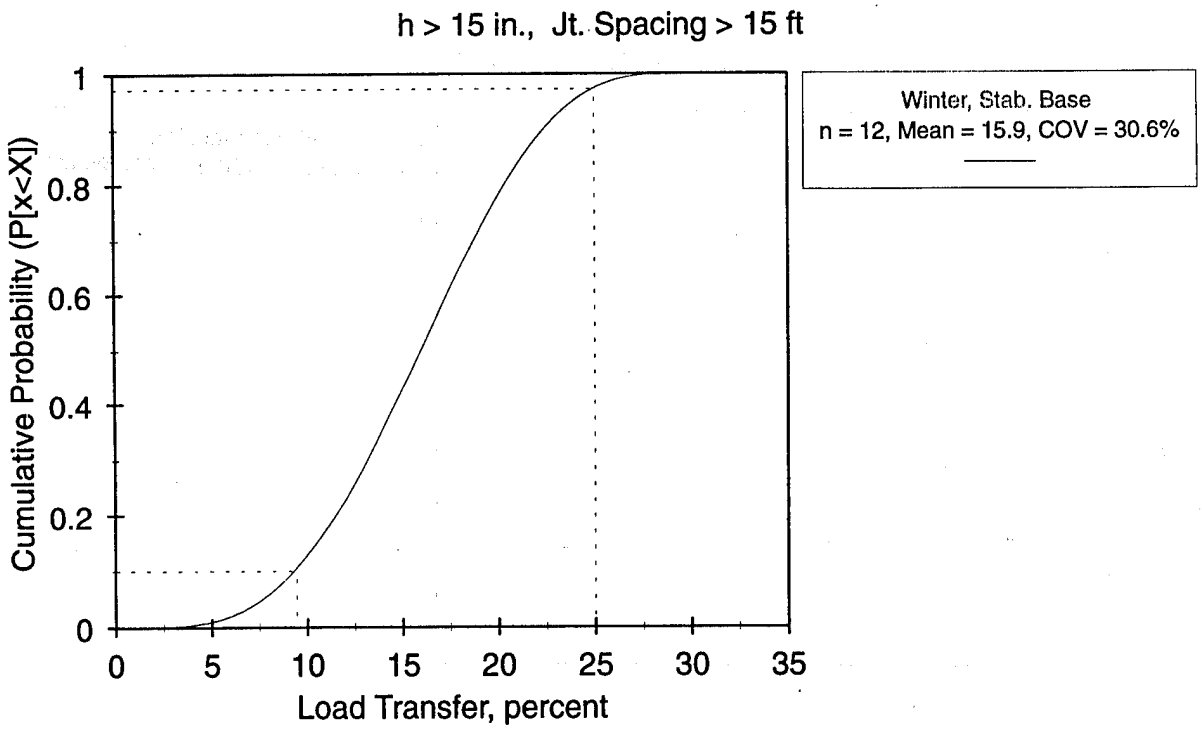

FIGURE 68. CUMULATIVE PROBABILITY DISTRIBUTION FUNCTIONS, TIED LONGITUDINAL CONSTRUCTION JOINTS, H > 15 IN., JOINT SPACING > 15 FT

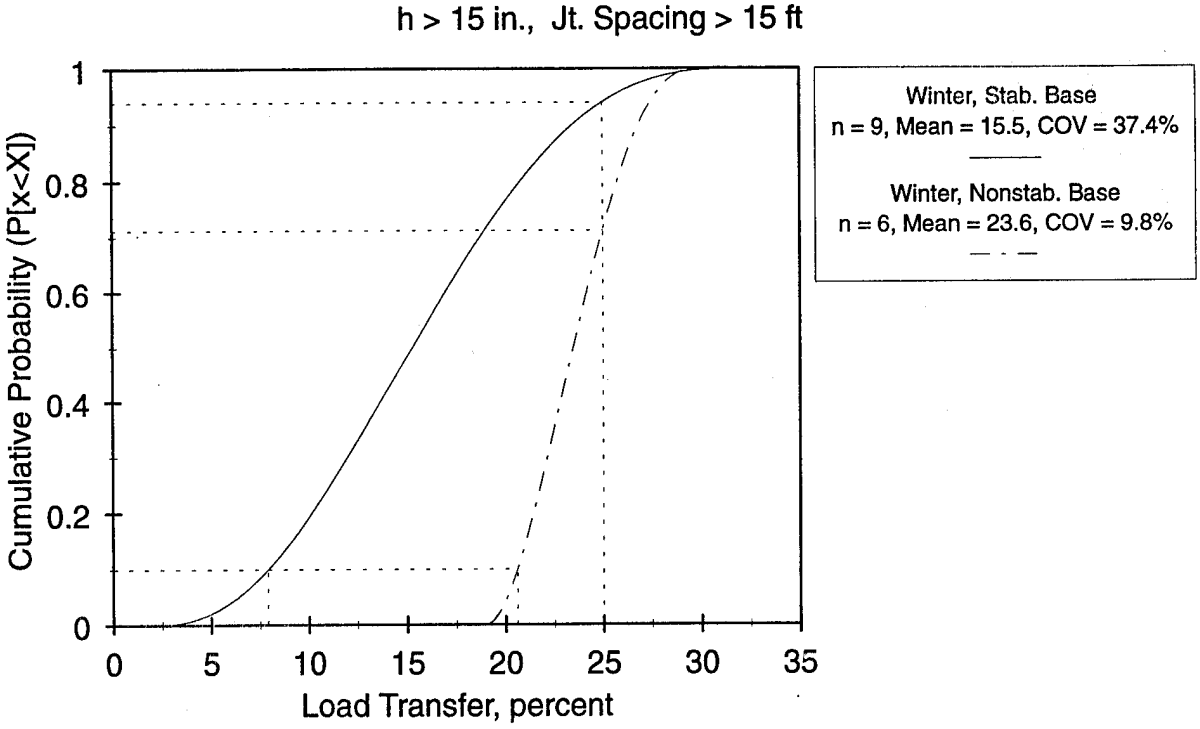

FIGURE 69. CUMULATIVE PROBABILITY DISTRIBUTION FUNCTIONS, KEYED LONGITUDINAL CONSTRUCTION JOINTS, H > 15 IN., JOINT SPACING > 15 FT

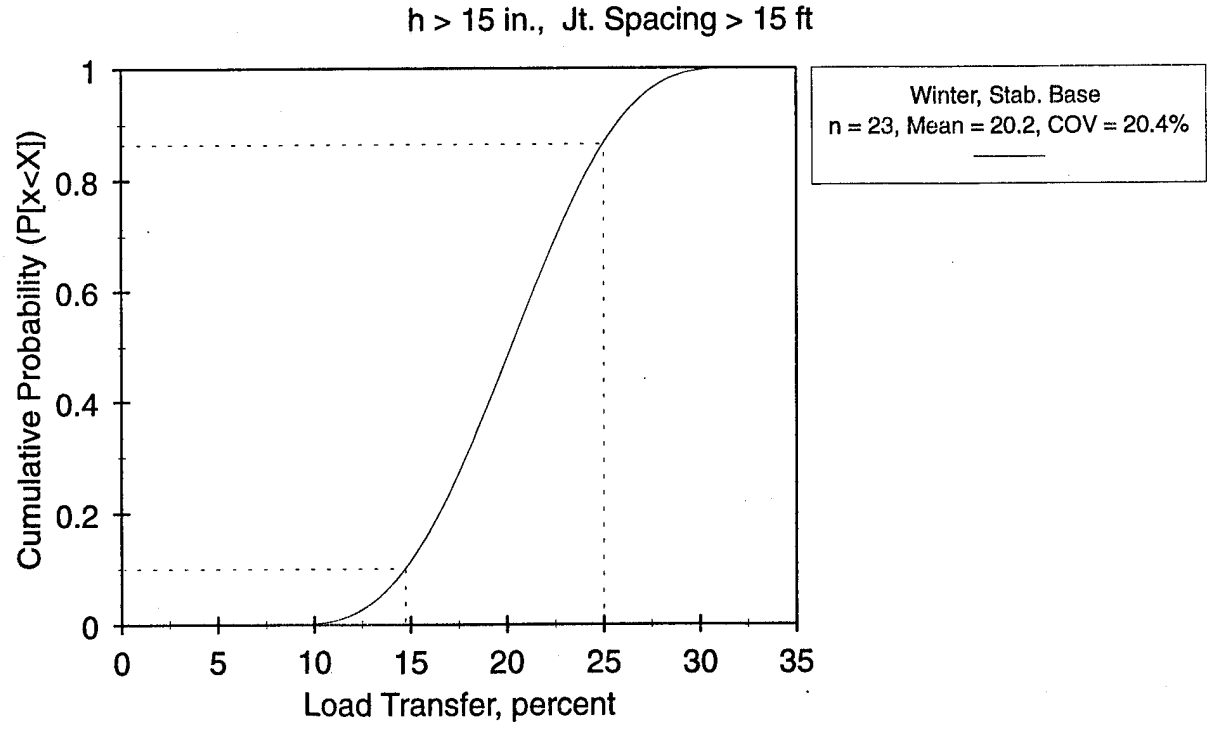

FIGURE 70. CUMULATIVE PROBABILITY DISTRIBUTION FUNCTIONS, KEYED AND TIED LONGITUDINAL CONSTRUCTION JOINTS, H > 15 IN., JOINT SPACING > 15 FT

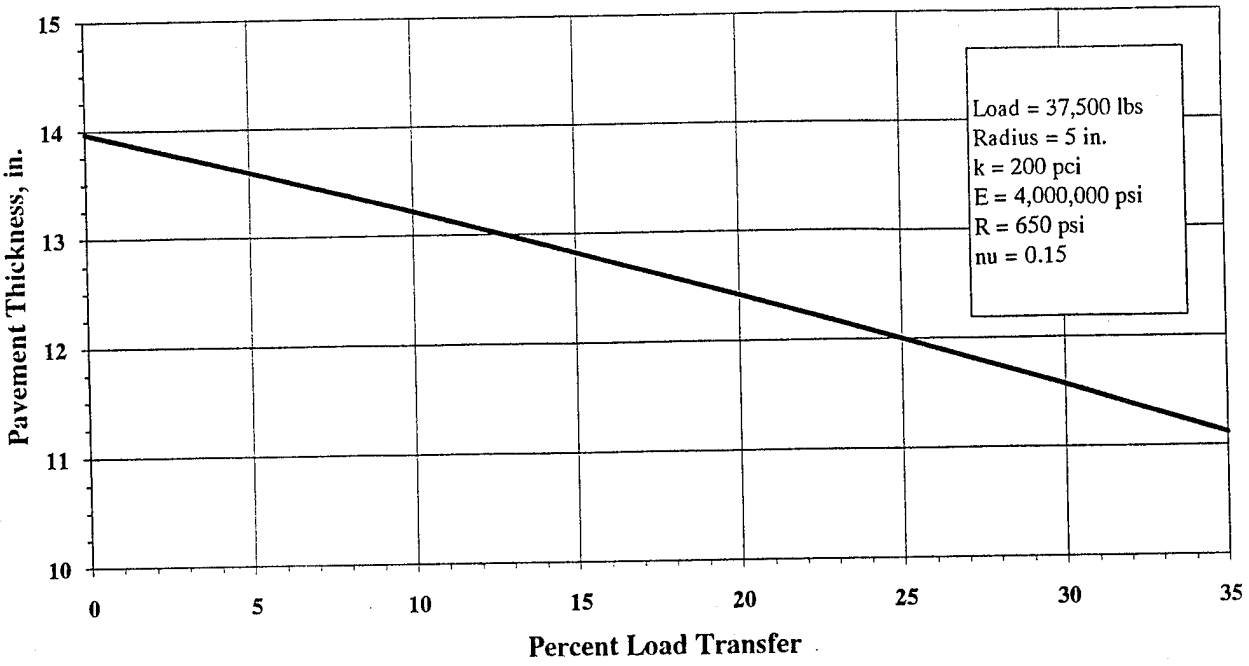

FIGURE 71. INFLUENCE OF LOAD TRANSFER ON PAVEMENT LIFE

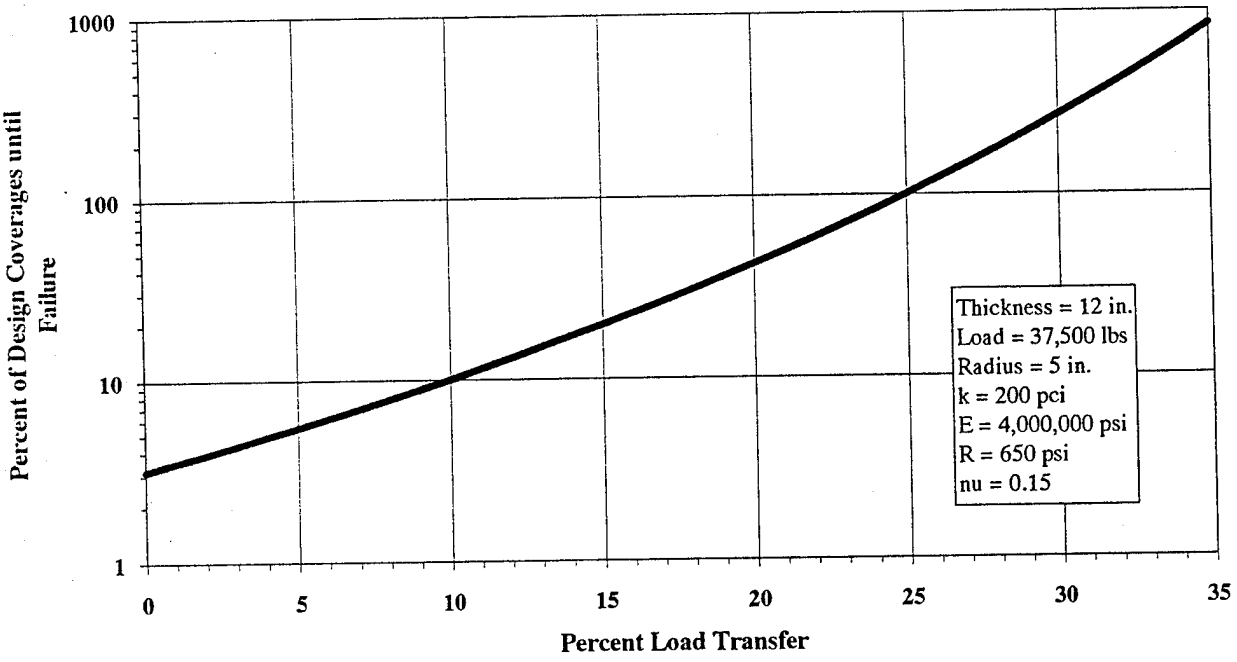

FIGURE 72. INFLUENCE OF LOAD TRANSFER ON REQUIRED PAVEMENT THICKNESS

CONCLUSIONS AND RECOMMENDATIONS

CONCLUSIONS.

Joint efficiency tests were nondestructively conducted with an HWD device at four U.S. airports representing a wide geographic and climatic range. Virtually every commonly used joint type was tested. Within the funding and time constraints of the project, it was attempted to obtain joint efficiency data under winter and summer conditions, day and night conditions, stabilized and nonstabilized bases, and thick and thin pavements. From the joint efficiency data, joint load transfer values were estimated based upon the radius of relative stiffness of the pavement. The following conclusions can be drawn from the data obtained: The assumption of load transfer as a constant value of 25 percent may be nonconservative, especially during the winter months. Joint load transfer is stochastic and cannot be completely described by a single deterministic value. Furthermore, load transfer is greatly influenced by temperature, stiffness of the subgrade, pavement thickness, joint spacing (or joint opening), type of joint, and thickness of pavement. No single probability distribution function was found to describe the load transfer for all joint types and conditions; for the joint types and conditions tested, the value of joint efficiency was found to be independent of load level for over 5/6 of the cases; for approximately 3/4 of the joint types and conditions tested, joint efficiency was not affected by the direction of test across the joint for both low and high loads; and load transfer is significantly reduced in winter conditions as compared to summer conditions. Also, the load transfer is more erratic with more widespread scatter of observed load transfer in winter conditions than in summer conditions. It appears that nonstabilized bases tend to increase load transfer as compared to identical joints in pavements on stabilized bases. In general, nonstabilized bases allow greater deflections for the same load than stabilized bases. Therefore, the effect of the aggregate interlock mechanism as well as dowel action (when dowels are present) is likely greater for nonstabilized bases than for stabilized bases. Probability distribution functions were proposed for the mean values of load transfer for the various joint types and conditions. The form of the distribution functions chosen was the beta distribution, which requires that the mean, standard deviation, and range of the data be known. However, under these conditions, the beta distribution provides the least biased assignment of probabilities of load transfer. The resulting probability distributions of the mean values gave good agreement with observed experimental data. Based upon the proposed probability distribution functions, it can be shown that the likelihood of observing mean values of load transfer less than 25 percent ranges from 60 to 100 percent, depending on the joint type and conditions. The reduction of Westergaard's edge stress is fundamental to the FAA rigid pavement design procedure. A small reduction in load transfer will likely result in a large decrease in pavement life. Conversely, using a more realistic value of load transfer in pavement design will likely result in only small increases in pavement thickness. The life-cycle benefits of increasing the pavement thickness may be significant, and the values of load transfer obtained in this study are for the HWD device and its value the loaded area (a = 11.9 in.). For other values of a for a particular aircraft, the load transfer obtained would be different from the value obtained for the HWD. The influence of the a/ℓ ratio for various aircraft has not be included in this study.

RECOMMENDATIONS.

The mechanism of load transfer at joints is not well understood. The results of these tests are based upon an assumed analytical model derived from finite element analyses in which the joint is not explicitly modeled. The state-of-the-art in computational techniques and computing power has advanced to the point that explicit, three-dimensional modeling of the joint-slab-foundation system is now practical. These types of analyses, along with experimental verification, can be used to develop a more fundamental, mechanistic understanding of the mechanism of load transfer. Therefore, it is recommended that additional research of this type be conducted before changes in design guidance are implemented.

REFERENCES

Ball, C. G. and Childs, L. D. 1975. "Tests of Joints for Concrete Pavements," Portland Cement Association Research and Development Bulletin, Skokie, IL.

Brown, D. N. and Rice, J. L. 1971. "Airfield Pavement Requirements for Multiple-Wheel Heavy Gear Loads," Miscellaneous Paper S-71-5, U.S. Army Engineer Waterways Experiment Station, CE, Vicksburg, MS.

Colley, B. E. and Humphrey, H. A. 1967. "Aggregate Interlock at Joints in Concrete Pavements," Highway Research Record No. 189, Highway Research Board, Washington, D.C.

Federal Aviation Administration. 1978. "Airport Pavement Design and Evaluation," Advisory Circular AC 150/5320-6C, Washington, D.C.

Foxworthy, Paul T. 1985. "Concepts for the Development of a Nondestructive Testing and Evaluation System for Rigid Airfield Pavements," Ph.D. Dissertation, University of Illinois, Urbana, IL.

Harr, Milton E. 1987. Reliability-Based Design in Civil Engineering, McGraw-Hill Book Company, New York.

Hoffman, M. S. and Thompson, M. R. 1981. "Mechanistic Interpretation of Nondestructive Pavement Testing Deflections," Civil Engineering Studies, Transportation Engineering Series Number 32, Illinois Cooperative Highway and Transportation Research Program Series Number 190, University of Illinois, Urbana, IL.

Ioannides, Anastasios M. 1990. "Extension of Westergaard Solutions Using Dimensional Analysis," Presented at the Second International Workshop on the Design and Analysis of Concrete Pavements, October 4 and 5, 1990, Siguenza, Spain.

Ioannides, Anastasios M. and Korovesis, George T. 1990. "Aggregate Interlock: A Pure-Shear Load Transfer Mechanism," Transportation Research Record, No. 1286, Transportation Research Board, Washington, DC.

Owusu-Antwi, Emmanuel B.; Meyer, Alvin H.; and Hudson, W. R. 1989. "Preliminary Evaluation of Procedures for the Assessment of Load Transfer Across Joints and Cracks in Rigid Pavements using the Falling Weight Deflectometer," Proceedings of the 4th International Conference on Concrete Pavement Design and Rehabilitation, Purdue University, West Lafayette, IN.

Poblette, M.; Valenzuela, R.; and Salsilli, R. 1989. "Load Transfer in Undoweled Transverse Joints in PCC Pavements," Transportation Research Record 1207, Transportation Research Board, Washington, D.C.

Rollings, Raymond S. 1987. "Design of Rigid Airfield Pavement Overlays," Federal Aviation Administration, Washington, D.C.

Tabatabaie, A. M.; Barenberg, E. J.; and Smith, Roger. 1979. "Longitudinal Joint Systems in Slip-Formed Rigid Pavements," Federal Aviation Administration Report No. FAA-R9-79-4, Parts 1-3, Washington, D.C.

☆U.S. GOVERNMENT PRINTING OFFICE: 1995 - 704-066/20156